

The Sun's Supergranulation

Michel Rieutord

Laboratoire d'Astrophysique de Toulouse-Tarbes,
Université de Toulouse, CNRS
14 Avenue Edouard Belin,
31400 Toulouse, France
email: rieutord@ast.obs-mip.fr
<http://www.ast.obs-mip.fr/article121.html>

François Rincon

Laboratoire d'Astrophysique de Toulouse-Tarbes,
Université de Toulouse, CNRS
14 Avenue Edouard Belin,
31400 Toulouse, France
email: rincon@ast.obs-mip.fr
<http://www.ast.obs-mip.fr/article643.html>

Accepted on 28 May 2010
Published on 15 June 2010

Abstract

The Sun's supergranulation refers to a physical pattern covering the surface of the quiet Sun with a typical horizontal scale of approximately 30,000 km and a lifetime of around 1.8 d. Its most noticeable observable signature is as a fluctuating velocity field of 360 m s^{-1} rms whose components are mostly horizontal. Supergranulation was discovered more than fifty years ago, however explaining why and how it originates still represents one of the main challenges of modern solar physics.

A lot of work has been devoted to the subject over the years, but observational constraints, conceptual difficulties and numerical limitations have all concurred to prevent a detailed understanding of the supergranulation phenomenon so far. With the advent of 21st century supercomputing resources and the availability of unprecedented high-resolution observations of the Sun, a stage at which key progress can be made has now been reached. A unifying strategy between observations and modelling is more than ever required for this to be possible.

The primary aim of this review is therefore to provide readers with a detailed interdisciplinary description of past and current research on the problem, from the most elaborate observational strategies to recent theoretical and numerical modelling efforts that have all taken up the challenge of uncovering the origins of supergranulation. Throughout the text, we attempt to pick up the most robust findings so far, but we also outline the difficulties, limitations and open questions that the community has been confronted with over the years.

In the light of the current understanding of the multiscale dynamics of the quiet photosphere, we finally suggest a tentative picture of supergranulation as a dynamical feature of turbulent magnetohydrodynamic convection in an extended spatial domain, with the aim of stimulating future research and discussions.

Imprint / Terms of Use

Living Reviews in Solar Physics is a peer reviewed open access journal published by the Max Planck Institute for Solar System Research, Max-Planck-Str. 2, 37191 Katlenburg-Lindau, Germany. ISSN 1614-4961.

This review is licensed under a Creative Commons Attribution-Non-Commercial-NoDerivs 3.0 Germany License: <http://creativecommons.org/licenses/by-nc-nd/3.0/de/>

Because a *Living Reviews* article can evolve over time, we recommend to cite the article as follows:

Michel Rieutord and François Rincon,
“The Sun’s Supergranulation”,
Living Rev. Solar Phys., **7**, (2010), 2. [Online Article]: cited [<date>],
<http://www.livingreviews.org/lrsp-2010-2>

The date given as <date> then uniquely identifies the version of the article you are referring to.

Article Revisions

Living Reviews supports two ways of keeping its articles up-to-date:

Fast-track revision A fast-track revision provides the author with the opportunity to add short notices of current research results, trends and developments, or important publications to the article. A fast-track revision is refereed by the responsible subject editor. If an article has undergone a fast-track revision, a summary of changes will be listed here.

Major update A major update will include substantial changes and additions and is subject to full external refereeing. It is published with a new publication number.

For detailed documentation of an article’s evolution, please refer to the history document of the article’s online version at <http://www.livingreviews.org/lrsp-2010-2>.

Contents

1	Introduction	5
2	General Considerations	7
2.1	Solar convection	7
2.2	Scales in turbulent convection	7
2.3	The supergranulation puzzle	9
3	Flows at Scales Smaller than the Supergranulation	11
3.1	Granulation	11
3.2	Mesogranulation	11
4	Observational Results on Supergranulation	13
4.1	Methods	13
4.1.1	Dopplergrams	13
4.1.2	Tracking	13
4.1.3	Local helioseismology	16
4.2	The scales of supergranulation	16
4.2.1	Length scales	16
4.2.2	Time scales	17
4.2.3	Velocity scales	18
4.3	Intensity variations in supergranules	18
4.4	Supergranulation depth	20
4.5	Rotational properties of supergranules	21
4.6	Multiscale convection and magnetic fields	22
4.6.1	Supergranulation and the magnetic network	23
4.6.2	Internetwork fields	25
4.6.3	The magnetic power spectrum of the quiet photosphere	26
4.6.4	Supergranulation and flows in active regions	26
4.6.5	Supergranulation variations over the solar cycle	27
4.7	Conclusions	28
5	Theoretical Models of Supergranulation	30
5.1	The rotating MHD Rayleigh–Bénard convection problem	30
5.1.1	Formulation	30
5.1.2	Linear instability and the solar regime	32
5.2	Convective origin of supergranulation	32
5.2.1	Multiple mode convection	32
5.2.2	Effects of temperature boundary conditions	33
5.2.3	Oscillatory convection and the role of dissipative processes	34
5.2.4	Oscillatory convection, rotation, and shear	34
5.2.5	Oscillatory convection and magnetic fields	35
5.2.6	Other effects	35
5.2.7	Shortcomings of simple convection models	35
5.3	Large-scale instabilities and collective interactions	36
5.3.1	Rip currents and large-scale instabilities	36
5.3.2	Plume interactions	36
5.4	Conclusions	37

6	Numerical Modelling	38
6.1	Numerical simulations of turbulent Rayleigh–Bénard convection	38
6.1.1	Rayleigh–Bénard and Navier–Stokes	38
6.1.2	State-of-the-art modelling	38
6.2	Numerical simulations of solar convection	40
6.2.1	Idealised simulations	40
6.2.2	Realistic simulations	40
6.2.3	Current limitations	41
6.3	Simulations at granulation scales	41
6.3.1	Stratified convection and flows	41
6.3.2	Main successes and caveats	42
6.4	Large-scale simulations	42
6.4.1	Introduction	42
6.4.2	Global spherical simulations	43
6.4.3	Local hydrodynamic Cartesian simulations: mesoscale dynamics	45
6.4.4	State-of-the-art local hydrodynamic Cartesian simulations	47
6.4.5	Local hydrodynamic Cartesian simulations with rotation	48
6.4.6	Local MHD Cartesian simulations	48
6.5	Conclusions	49
7	Summary of Current Knowledge and Issues	51
7.1	Observations	51
7.2	Theory	53
7.3	Numerical simulations	53
8	Discussion and Outlook	55
8.1	Preliminary comments	55
8.1.1	The large-scale tail of the kinetic power spectrum	55
8.1.2	Supergranulation, network and internetwork fields	55
8.2	Nonlinear MHD at large scales	56
8.2.1	Comparing energy spectra	56
8.2.2	Breaking the large-scale similarity of solar surface flows	56
8.2.3	Dynamical magnetic feedback: a tricky question	58
8.2.4	Comments on the equipartition argument	58
8.3	Suggestions for future research	59
9	Acknowledgements	61
	References	62

List of Tables

1	List of numerical simulations of mesogranulation to supergranulation-scale dynamics.	50
---	--	----

1 Introduction

The story of supergranulation really started in Oxford when Avril B. Hart reported in 1953 the existence of a “noisy” fluctuating velocity field on top of the mean rotation speed of the solar equator that she was measuring (Hart, 1954). Actually, it is most probable that this “noise” was already detected as early as 1915 by Plaskett (1916). Two years after her first detailed report, Hart (1956) confirmed the discovery and was able to give the first estimate¹ of 26 Mm for the typical horizontal length scale of these “velocity fluctuations” (sic). Supergranulation was further recognised as a characteristic feature of the whole surface of the quiet Sun (the regions of weak magnetic fields, which represent the most important part of the solar surface) after the seminal work of Leighton *et al.* (1962), who published the first Doppler images of the Sun (and also the first detection of the five minutes oscillations). This work was soon after completed by another important paper by Simon and Leighton (1964) who showed, amongst other results, the intimate relation between supergranulation and the magnetic network of the quiet Sun.

It is remarkable that all the fundamentals of supergranulation have basically been uncovered over that 1954–1964 decade. Since then, progresses have been much less spectacular, especially on the theoretical side. This is certainly why supergranulation is still a fascinating subject. We are still wondering where it comes from, what its exact relation with magnetic fields is, if it is a universal feature of solar type stars, or of stellar surface convection, if it plays a role in the solar dynamo(s), etc. All these questions are pending fifty years after the discovery. There are many reasons why the solar physics community has not yet managed to answer them, several of which are not actually specific to the supergranulation problem. Most of these reasons are described in detail in this review, but it is worth pointing out a few important issues here as an introduction.

For a long time only a limited set of observables and restricted time-records of the evolution of the supergranulation pattern have been available, may it be on short (24 consecutive hours) or long timescales (a solar cycle). This has somewhat hindered the study of the detailed spatial structure of supergranulation and the identification of the physical factors that affect it (buoyancy, stratification, magnetic fields, rotation). From the theoretical and numerical perspectives, on the other hand, the strongly nonlinear physical nature of magnetised thermal convection in the outer layers of the Sun makes it extremely difficult to come up with a simple, unique, verifiable physical model of the process (a similar problem arises in many subfields of solar physics, if not of astrophysics). Overall, these observational uncertainties and theoretical or numerical limitations have somewhat negatively interfered to prevent a rigorous solution to the supergranulation problem. The currently fairly obfuscated state of affairs may nevertheless get clarified in a near future, as the solar physics community is now armed with both high-resolution solar observatories such as Hinode² and large supercomputers that allow for increasingly realistic numerical simulations of the complex solar surface flows. However, it is clear that stronger connections between theory, numerics, and observations need to be established for the problem to be resolved.

In this review, we would like to introduce readers to this subject by first describing the full range of past and current research activities pertaining to the solar supergranulation, from the breadth of historical and modern observational results to the most elaborate numerical models of supergranulation convection. We particularly wish to provide a useful guide to the abundant literature related to that theme, to point out the important findings in the field, but also to stress the limitations and difficulties that have been encountered over the years in order to help overcome them. To this end, we attempt to discuss the already existing or possible connections between

¹ In solar physics, an appropriate length unit is the megametre (Mm), also 1000 km.

² Hinode is led by the Japanese Aerospace Exploration Agency (JAXA) in collaboration with NASA, the Science and Technology Facilities Council (STFC), and the European Space Agency (ESA). Hinode is a Japanese mission developed, launched, and operated by ISAS/JAXA, in partnership with NAOJ, NASA, and STFC (UK). Additional operational support is provided by ESA and NSC (Norway). The project website can be found at <http://solarb.msfc.nasa.gov/>

various pieces of research and try to identify some important questions whose answer may be crucial to understand how and why supergranulation originates.

The review is divided into eight parts, including this introduction. The next two sections offer some introductory material on the physics of deep and surface convection in the Sun (Section 2) and a brief recap on small-scale flows, namely granulation and mesogranulation (Section 3.1). Section 4 is dedicated to a presentation of observational facts that have been collected on supergranulation. We then carry on with the discussion of existing theoretical models to explain the origin of supergranulation in Section 5. In Section 6, we discuss related numerical experiments. Our current knowledge on supergranulation is summarised and commented in Section 7 for the convenience of hurried readers. In the light of the present understanding of multiscale dynamics of the quiet photosphere, we finally suggest a tentative picture of supergranulation as a dynamical feature of turbulent magnetohydrodynamic (MHD) convection in an extended spatial domain, with the aim of stimulating future research and discussions. We notably propose several numerical and observational diagnostics that could help make important progress on the problem in the near future (Section 8).

We tried to make the paper readable by all astrophysicists, assuming only little background in that field and trying to avoid as much as possible the solar physicists jargon, or to explain it when necessary.

2 General Considerations

2.1 Solar convection

To better appreciate the following discussions, we find it useful to start this section with a brief, non-exhaustive recap of the general properties of solar convection. Readers interested in various specific aspects of solar convection such as deep convection or the fine structure of granulation will find much more exhaustive accounts on these matters in the reviews by Miesch (2005) and Nordlund *et al.* (2009).

The outer layers of the Sun, 30% in radius, 2% in mass, are strongly stratified: the density ratio between the visible surface and the $0.3R_{\odot}$ depth is close to 10^6 (see Stix, 2004). This region is unstable with respect to thermal convection and is hence referred to as the solar convection zone (SCZ). The solar luminosity is mostly transported by fluid motions driven by thermal buoyancy in the SCZ: physically, the strongly non-adiabatic cooling of the surface layers, like the top cold plate of a convection experiment, imposes a strong negative entropy gradient below the surface, where the heat flux coming from the solar interior cannot be evacuated by microscopic heat diffusion alone. This entropy gradient gets smaller at larger depth as a consequence of the efficiency of convective mixing, but remains negative down to $\sim 0.3R_{\odot}$, where it changes sign and becomes stable against convection.

2.2 Scales in turbulent convection

Solar convection is in a highly turbulent state. Global Reynolds numbers $Re = LV/\nu$, based on the (large) vertical extent of the convective layer and typical convective velocities, range from 10^{10} to 10^{13} in the SCZ. To fix ideas, laboratory experiments on turbulent convection are currently limited to rms $Re < 10^7$ (e.g., Niemela *et al.*, 2000). As the general topic of this review is the origin and structure of the supergranulation pattern, what we are mostly interested in here are the remarkable length scales of such a turbulent flow. For this purpose, we assume that solar convection is simply thermal convection of an electrically conducting fluid and that the flow is incompressible (which it is not, as a consequence of the important stratification of the SCZ). Hydrodynamic, incompressible turbulent flows in the laboratory are characterised by two length scales: the injection scale and the viscous dissipation scale.

- The injection range is the typical range of scales at which kinetic energy is injected into turbulent motions. In turbulent convection, injection of kinetic energy is due to the work of the buoyancy force. The scale most representative of the injection range under these conditions is called the Bolgiano scale L_B (Bolgiano, 1959; L'vov, 1991; Chillá *et al.*, 1993; Rincon, 2006). It can be shown, based on purely dimensional arguments and scaling considerations for heat transport in turbulent convection, to be almost always of the same order (up to some order one prefactor) as the local typical scale height (Rincon, 2007). In an incompressible thermal convection experiment, this corresponds to the distance between the hot and cold plates, but in the strongly stratified SCZ, a more sensible estimate is the local pressure scale height. Close to the surface, the Bolgiano scale is therefore comparable to or slightly larger than the granulation scale $L_G \sim 1$ Mm (Section 3.1 below). As one goes to deeper layers, the pressure scale height gets larger and larger as a consequence of the strong stratification, and so does the Bolgiano scale. So, in the SCZ, the injection scale basically increases with depth and ranges from 1 Mm close to the surface to 100 Mm close to the bottom of the SCZ.

A perhaps more intuitive physical picture of the previous argument is given by cold downflows diving from the Sun's surface. Such flows can cross a significant fraction of the convective zone because of the nearly isentropic state of the fluid (Rieutord and Zahn, 1995). This underlines the

fact that the driving of turbulence spans a wide range of scales in a continuous way as one looks deeper in the SCZ. Note that the expanding thermal plumes undergo secondary instabilities along their descending trajectories, producing a intricate mixture of vorticity filaments (see, e.g., Rast, 1998; Clyne *et al.*, 2007). Figure 1 provides a simple sketch of this process. As we shall see in Section 6.3, numerical simulations of solar convection have provided a very neat confirmation of this phenomenology.

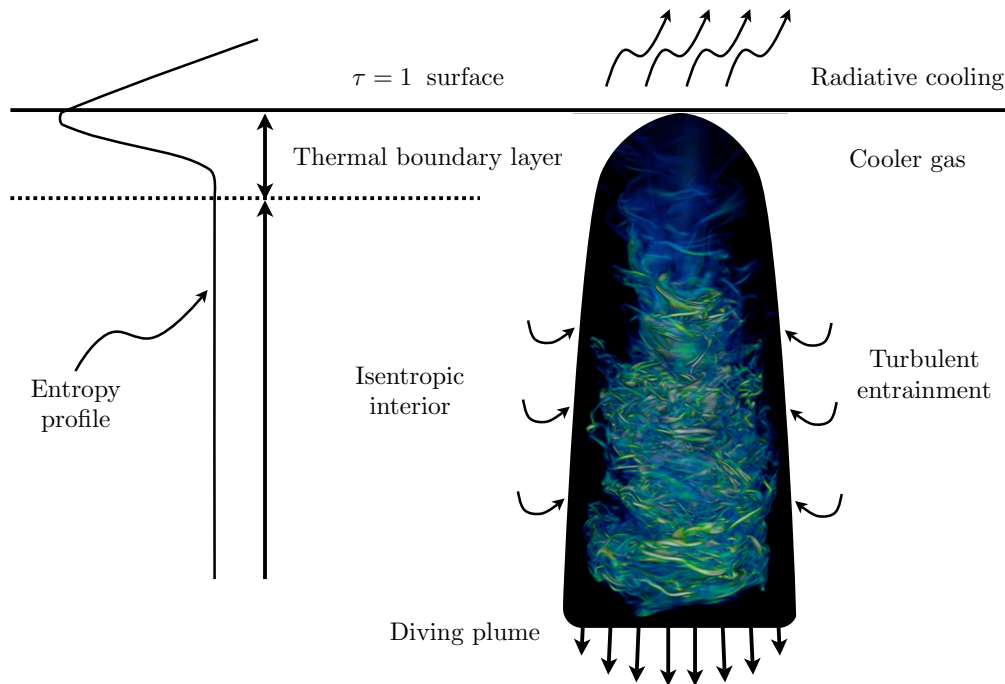


Figure 1: Left: the entropy profile as a function of depth, as estimated by numerical simulations or crude mean-field models like the mixing length theory. Right: section of a cool plume diving from the surface. As it penetrates into the isentropic background, the plume increases both its mass and momentum flux by turbulent mass entrainment (represented by curly arrows). Its horizontal scale grows proportionally to depth, the aperture angle of the cone being around 0.1. At a given depth, the typical size of energetic eddies is like the width of the plume while a mean flow at the scale of the depth is also generated. From this model, we see that the length scale characterising the buoyant flow at a given depth increases monotonically with depth (image by Mark Rast, see <http://www.vapor.ucar.edu/images/gallery/RastPlume.png> and Clyne *et al.*, 2007).

Let us now discuss the ordering of dissipation scales in the SCZ. The most important one is obviously the viscous dissipation scale l_ν but, as we are considering thermal convection in an electrically and thermally conducting fluid, we also need to consider two other dissipative scales: the magnetic dissipation scale l_η and the thermal dissipation scale l_κ . Note that all these scales are local and change with depth in the inhomogeneous SCZ.

- A rough estimate for the viscous dissipation scale l_ν can be obtained from the Kolmogorov phenomenology of turbulence (Frisch, 1995) via the expression $l_\nu \sim Re^{-3/4}L$, where L stands

for the injection scale and $Re = LV/\nu$, V being the typical velocity at the injection scale³. In the SCZ, where $\nu \sim 10^{-3} \text{ m}^2 \text{ s}^{-1}$ (Rieutord, 2008), we find $\ell_\nu \sim 10^{-3} \text{ m}$ at the surface, assuming $L \sim L_G \sim 1 \text{ Mm}$ and $V \sim 1 \text{ km s}^{-1}$ (the typical granulation scale and velocity). At the bottom of the SCZ, where the injection scale is much larger, one can estimate similarly that $\ell_\nu \sim 0.1 \text{ m}$. Hence, ℓ_ν is everywhere extremely small and not available to observations.

- In MHD, the relative value of the magnetic dissipation scale ℓ_η with respect to the viscous cut-off scale ℓ_ν depends on the ordering of dissipative processes (see, e.g., Schekochihin *et al.*, 2007) in the fluid. When the magnetic diffusivity η is much larger than the kinematic viscosity ν , as is the case in the Sun, one may use $\ell_\eta/\ell_\nu \sim Pm^{-3/4}$ (Moffatt, 1961), where $Pm = \nu/\eta$ is called the magnetic Prandtl number⁴ and we have assumed a Kolmogorov scaling for the velocity field. The magnetic diffusivity in the subsurface layers of the Sun is $\eta \sim 10^2 \text{ m}^2 \text{ s}^{-1}$ (Spruit, 1974; Rieutord, 2008), so $Pm \sim 10^{-5}$. Consequently, $\ell_\eta \sim 100 \text{ m}$ close to the surface (see also Pietarila Graham *et al.*, 2009). This is also very small in comparison to the resolution of current observations, but is much larger than ℓ_ν . Close to the bottom of the SCZ, $Pm \sim 10^{-1} - 10^{-2}$, so $\ell_\eta \sim 1 \text{ m}$.
- The thermal dissipation scale ℓ_κ is very important in the solar context, as it is the largest of all dissipation scales in the problem. In the SCZ, the thermal diffusivity κ is everywhere much larger than the kinematic viscosity ν , so the thermal Prandtl number $Pr = \nu/\kappa$ is very small. Under these conditions, we may estimate ℓ_κ from the expression⁵ $\ell_\kappa/\ell_\nu \sim Pr^{-3/4}$, once again assuming a Kolmogorov scaling for the velocity field. Thermal diffusion in the Sun is insured by photons, and thus depends strongly on the opacity of the fluid. In the deep SCZ, $Pr \sim 10^{-4} - 10^{-6}$, so $\ell_\kappa \sim 500 \text{ m}$. In the very surface layers, ℓ_κ is comparable to the scale of granulation $L_G \sim 1 \text{ Mm}$, at which heat advection and radiation are comparable (see Section 3.1 below). This is not small anymore in terms of solar observations, but remains nevertheless smaller than the typical scale of supergranulation L_{SG} .

To summarise, the ordering of scales close to the solar surface is as follows:

$$\ell_\nu \ll \ell_\eta \ll \ell_\kappa \sim L_B \sim L_G \ll L_{SG} .$$

2.3 The supergranulation puzzle

From the previous discussion, the scales that can be constructed from standard arguments on turbulence and convection all appear to be much smaller than the supergranulation scale in the surface layers. Besides, as one goes deeper into the stratified SCZ, the injection scale increases smoothly and monotonically with depth, so the supergranulation scale does not show up as a special scale in deep layers either in this simple scenario. Overall, we may therefore conclude that understanding supergranulation from simple arguments based on available theories of turbulent convection is not possible. In this respect, it is worth pointing out that supergranulation lies at the large-scale edge of the injection range of turbulence at the solar surface, and might therefore not be directly correlated with hydrodynamic turbulent processes.

Uncovering the origin of supergranulation probably requires invoking physical processes that are not present in the most simple descriptions of turbulence. These processes may be specific to the solar context (e.g., surface radiation, chemical composition, ionisation states) or may have

³ ℓ_ν can be understood physically as the scale at which viscous effects start to dominate over inertial effects, so that the Reynolds number at this scale $Re_{\ell_\nu} = \ell_\nu V_{\ell_\nu}/\nu = 1$, where $V_{\ell_\nu} \sim Re^{-1/4}V$ is the typical velocity at scale ℓ_ν in the framework of the Kolmogorov theory.

⁴ ℓ_η is the scale at which resistive effects take over magnetic field stretching, corresponding to a scale-defined magnetic Reynolds number $Rm_{\ell_\eta} = \ell_\eta V_{\ell_\eta}/\eta = 1$.

⁵ Similarly to ℓ_ν and ℓ_η , this scale corresponds to the scale-defined Péclet number $Pe_{\ell_\kappa} = V_{\ell_\kappa} \ell_\kappa/\kappa = 1$.

a more general dynamical origin (instabilities related to the interaction with rotation, magnetic fields, shear, non-local scale interactions in a turbulent flow). As we shall see in Sections 5, 6, and 8, a variety of qualitative physical scenarios based on one or several such processes has been proposed in the past but, as yet, they have not provided a fully comprehensive, predictive, and verifiable theoretical model for supergranulation.

If we succeed one day in explaining the origin of the solar supergranulation, we may very well gain some new insight into turbulent convection or discover completely new physical effects at the same time. Attempting to solve the supergranulation problem therefore represents a very exciting challenge not only from the astrophysics point of view, but also from a fundamental physics perspective.

3 Flows at Scales Smaller than the Supergranulation

Before we head into the specific topic of supergranulation, a brief overview of smaller-scale flows at the Sun's surface, the well-known granulation and the more controversial mesogranulation, is required to set the stage completely.

3.1 Granulation

The solar granulation is an intensity pattern with a contrast around 15%, which displays cellular convective motions with length scales ranging from ~ 0.5 Mm to 2 Mm. From recent observations with the Solar Optical Telescope on board the Hinode satellite (Ichimoto *et al.*, 2004; Suematsu *et al.*, 2008), Rieutord *et al.* (2010) showed that power spectra of both intensity fluctuations and vertical velocities have a maximum amplitude at a scale around 1.7 Mm, with a weak dependence on photospheric height for V_z . Previous work had shown that the typical lifetime of granules is 10 min and that the associated velocities range from 0.5 to 1.5 km s⁻¹ (Title *et al.*, 1989). Hundreds of observations of the solar granulation have been done, and several reviews are dedicated to this subject. We notably refer the reader to Spruit *et al.* (1990) and Nordlund *et al.* (2009).

The granulation pattern is certainly the best understood feature of solar convection. Most notably, it is well reproduced by numerical simulations (Section 6). A remarkable property is that the advection of heat by the velocity field and the radiation of heat proceed on comparable timescales in a granule, so the corresponding Péclet number is order unity. As already discussed in Section 2.2, this means that the scale of granulation is comparable to the thermal dissipation scale. Physically, the granulation pattern corresponds to a thermal boundary layer formed in the strongly non-adiabatic surface region of the SCZ where the solar plasma becomes optically thin (see Figure 1).

3.2 Mesogranulation

Mesogranulation refers to flows at scales between the granulation and the supergranulation scales. It was first reported by November *et al.* (1981), who identified a pattern of prominent vertical motions at scales of the order of 8 Mm by time-averaging Doppler images. This was thought as a significant finding because it seemed to provide the missing piece in the theory of multiscale convection at the solar surface (see Section 5) formulated by Simon and Leighton (1964): granulation was associated with the ionisation of Hydrogen, while mesogranulation and supergranulation were associated to the first and second ionisation of Helium, respectively (viz. November *et al.*, 1981). Subsequent ground-based observations (November and Simon, 1988) and space-based observations using the SOUP instrument on SpaceLab 2 (Title *et al.*, 1989) gave some extra weight to this result.

However, the very existence of mesogranulation as a specific distinguishable convection scale at the solar surface remains a source of debate in the solar community. Wang (1989), Chou *et al.* (1991), and Straus *et al.* (1992) did not find any local maximum in the power spectrum (the scale-by-scale distribution of energy) of solar convection that would correspond to mesogranulation. Ginet and Simon (1992) and Chou *et al.* (1992) came to an opposite conclusion. Power spectra computed from MDI observations by Hathaway *et al.* (2000) only revealed two peaks at granulation and supergranulation scales.

November (1994) wrote that the term “mesogranulation” was misleading and instead suggested to interpret this feature as “the vertical component of the supergranular convection”. Then, Straus and Bonaccini (1997) argued that mesogranulation was a mere powerful extension of granulation at large scales and Roudier *et al.* (1999b) and Rieutord *et al.* (2000) suggested that mesogranulation was likely an artefact produced by the correlation tracking algorithm. This view was disputed by

Shine *et al.* (2000) because they found mesogranules in the range of 4–7 Mm, with a lifetime of 3 to 6 h (they used local correlation tracking on a 45 h MDI record of wide field images). Soon after, Lawrence *et al.* (2001), using a new technique based on wavelets applied to MDI images, found what they called a mesogranulation peak, but at 4 Mm, somewhat shorter compared to previous values.

The very recent work of Matloch *et al.* (2009) and Rieutord *et al.* (2010) may finally bring this debate to a conclusion. Indeed, Matloch *et al.* (2009) devised a simple model of granulation which mimics very well the fusion and splitting of granules. A conclusion of this work is that *the statistical properties and behaviour of mesogranulation structures are consistent with the results of spatial and temporal averaging of random data*. This conclusion underlines the fact that previous detection of mesogranulation were very likely misled by the weird consequences of averaging procedures. On the other hand, using Doppler measurements of vertical velocities from Hinode/SOT, Rieutord *et al.* (2010) did not find any spectral signature of a distinguishable scale in between granulation and supergranulation.

To conclude, it is very likely that mesogranulation is a ghost feature of surface convection generated by averaging procedures. In our opinion, the most recent observational results strongly argue against the existence of a genuine surface feature similar to granulation or supergranulation. To avoid any misunderstanding, we shall hereafter refer to the scales in the range of 4 to 12 Mm as *the mesoscales*. These length scales are between the smallest scale of supergranulation (12 Mm, see Section 4.2 below) and the largest scale of granulation (4 Mm).

4 Observational Results on Supergranulation

We shall now review the current observational knowledge on solar surface convection from granulation to supergranulation scales. We first introduce the main detection methods of solar surface flows (Section 4.1), which are central to the identification and characterisation of the supergranulation pattern and expose the main observational results. We then review the numerous observational findings on the scales of supergranulation (Section 4.2), the measurements of supergranulation-scale intensity variations (Section 4.3), the inferred depth of the pattern (Section 4.4), and its interactions with rotation (Section 4.5) and magnetic fields (Section 4.6). Some words of conclusion follow.

4.1 Methods

Let us recall that supergranulation is first of all a feature of the surface velocity field at the surface of the quiet Sun. Three methods are currently able to detect the associated signal. These are Doppler imaging, granule tracking, and local helioseismology.

4.1.1 Dopplergrams

Doppler imaging is the oldest technique used to monitor supergranulation (the first detection by Hart (1954) was on a Doppler signal). A SOHO/MDI view of supergranulation is shown in Figure 2. An inconvenience of Doppler imaging is that it only provides the line-of-sight component of the velocity field, which except at the disc centre or at the solar limb is a mixture of the horizontal and vertical velocity field components. In this figure, one clearly notices that the supergranulation velocity field is mainly horizontal, as the signal almost disappears near the disc centre.

4.1.2 Tracking

Another way to infer the velocity fields of the solar plasma in the photosphere is to track various structures visible at the surface. The idea is that small-scale structures like granules (see Section 3.1 below) are simply advected by large-scale flows. This technique is used in three different algorithms: the local correlation tracking (LCT), the coherent structure tracking (CST), and the ball-tracking (BT). The first one determines the motion of features on an image by maximising the correlation between small sub-images (November and Simon, 1988). The second method identifies coherent structures in the image by a segmentation process and then measures their displacement (e.g., Roudier *et al.*, 1999a; Rieutord *et al.*, 2007; Tkaczuk *et al.*, 2007). The third algorithm (BT) follows the displacement of floating balls over the intensity surface of images. The motion of the floating balls traces the mean motion of granules; this is presumably more effective computationally speaking than LCT and CST (Potts *et al.*, 2004).

The principles and accuracy of granule tracking with LCT or CST were tested by Rieutord *et al.* (2001) using synthetic data extracted from numerical simulations. They showed that flows at scales larger than 2.5 Mm are well reproduced by the displacements of granules. At shorter scales, the random motion of granules (which are dynamical structures) generates a noise that blurs the signal. The 2.5 Mm lower limit was recently confirmed by Rieutord *et al.* (2010) with observations using the Hinode/SOT data.

Since the spatial resolution of the granule tracking technique is well above the one needed for supergranulation, this method is well adapted to derive the horizontal components of the supergranulation flow, and it does not suffer from a projection effect, unlike Doppler imaging. An example of the flow fields obtained by Rieutord *et al.* (2008) using this technique is shown in Figure 3.

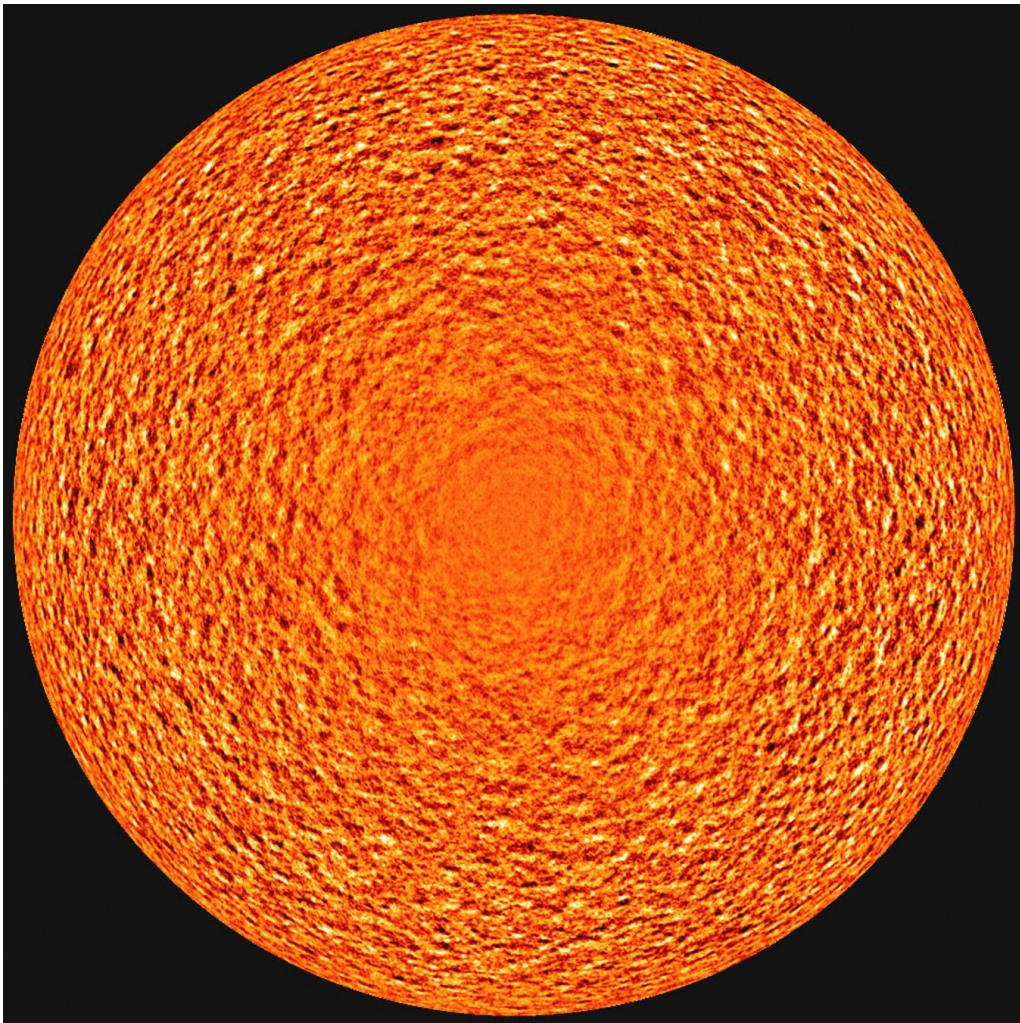


Figure 2: A Dopplergram revealing the supergranulation pattern (credits SOHO/MDI/ESA).

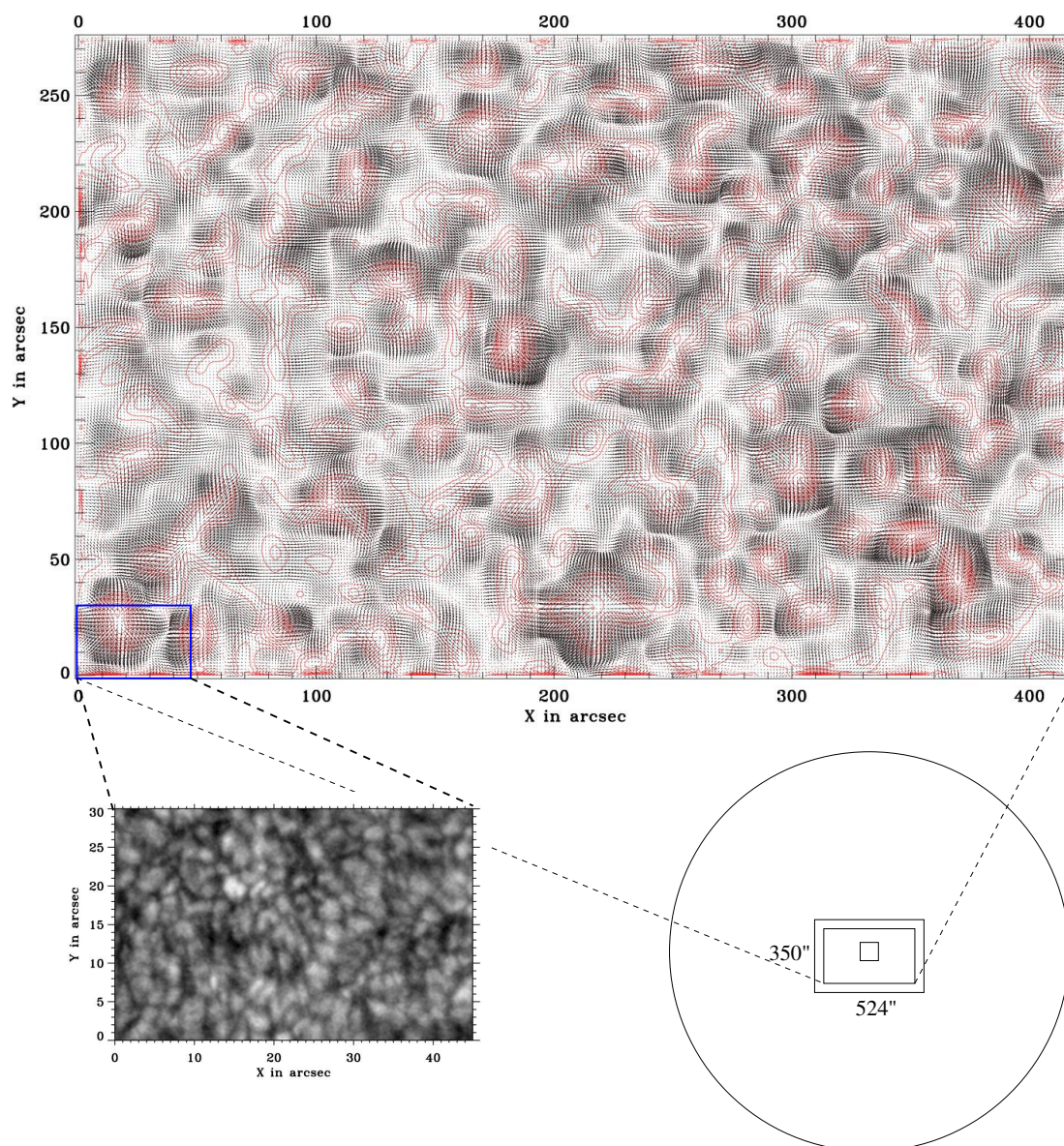


Figure 3: The supergranulation horizontal velocity field as obtained by granule tracking (from Rieutord *et al.*, 2008).

4.1.3 Local helioseismology

This method uses the propagation of acoustic or surface gravity waves (f -modes) to determine the velocity of the medium over which they propagate. Basically, if the wave velocity is c and that of the fluid is V , a plane wave travelling downstream shows a velocity $V + c$ whereas the one travelling upstream moves with a velocity $V - c$. The sum of the two measured velocities gives that of the fluid. However, the phase velocity of the waves is not directly measurable: the observable quantity is the local oscillation of the fluid which results from the superposition of many travelling waves. A proper filtering is thus needed to select the desired wave; this operation requires a true machinery. We refer the reader to the review of [Gizon and Birch \(2005\)](#) for a detailed introduction to this subject. Here, we just want to recall some basic information about the output of this technique: the spatial resolution at which velocity fields can be measured is around 5 Mm, and the time resolution for time-distance helioseismology is around 8 h. This is lower than what can be achieved with other methods but, in exchange, this technique is the only one that can probe the vertical profiles of the velocities and image the subphotospheric dynamics. Typically, vertical variations can be evaluated down to 10–15 Mm below the surface, but the accuracy of measurements deeper than 10 Mm is still debated. A comparison between the tracking and helioseismic reconstructions of large-scale solar surface flows was done by [Švanda *et al.* \(2007\)](#), who found very good agreement between the two.

4.2 The scales of supergranulation

4.2.1 Length scales

The horizontal scale of the supergranulation velocity field was the very first physical characteristic of the pattern to be measured. Using correlation of the signal, [Hart \(1956\)](#) found a typical length of 26 Mm. Since this pioneering work, this value has oscillated around 30 Mm. To appreciate correctly the values that are given in the literature, one should have in mind that supergranulation is a fluctuating, disordered pattern, hence only its statistical properties make sense. We should also remember that each technique has its own biases and gives values according to these biases.

A first technique to determine the typical length scale of the supergranulation is to measure the position of the maximum of spectral power or the correlation length of the horizontal velocity fields. The auto-correlation of Dopplergrams was first used in the seminal work of [Leighton *et al.* \(1962\)](#) and [Simon and Leighton \(1964\)](#), who gave the value of 32 Mm for the supergranulation length scale. The following major step was realized with the data from the SOHO/MDI instrument. The major progress made with this instrument has been the tremendous increase of the size (and quality) of the data set leading to very good statistics. Using data collected in May–June 1996, i.e., at solar minimum, [Hathaway *et al.* \(2000, 2002\)](#) determined the power spectrum of the line-of-sight velocity, finding a peak at 36 Mm (spherical harmonic $\ell = 120$). This peak extends from 20 Mm up to 63 Mm as given by the width at half-maximum.

Using the granule tracking method, [Rieutord *et al.* \(2008\)](#) also determined the characteristics of the spectral peak of supergranulation. They found a similar length scale of 36 Mm and an extension between 20 Mm and 75 Mm (the epoch is March 2007, also at solar minimum). The data set in this case was much smaller (7.5 h and a field of view of $300 \times 200 \text{ Mm}^2$), but still a hundred of supergranules were captured, giving good statistics. A similar measurement by [Rieutord *et al.* \(2010\)](#) using the small field of view of Hinode ($76 \times 76 \text{ Mm}^2$) encompassing only four supergranules, gave a peak at 30 Mm.

Other authors, like [DeRosa *et al.* \(2000\)](#) and [DeRosa and Toomre \(2004\)](#), used local correlation tracking to determine the horizontal flows from the Doppler signal of SOHO/MDI and identified supergranules with horizontal divergences. From these data, they derived a rather small “diameter” in the 12–20 Mm range. Using a similar technique, [Meunier *et al.* \(2007c\)](#) found a mean value for

supergranule diameters around 30 Mm. As underlined in these papers, the size of supergranules very much depends on the smoothing procedure used in the data processing.

Another set of independent measurements was performed by [Del Moro *et al.* \(2004\)](#) using data from local helioseismology. The technique is based on the fact that local helioseismology gives (more easily than the velocity itself) the local horizontal divergence of the flows, as this quantity appears as a difference between wave travel times. Thus, using a similar data set as [DeRosa and Toomre \(2004\)](#), [Del Moro *et al.* \(2004\)](#) extracted the horizontal divergence from the local propagation of waves and could also determine the statistics of supergranule sizes. They found a mean diameter at 27 Mm with a peak in the distribution at 30 Mm. These latter results have been confirmed by [Hirzberger *et al.* \(2008\)](#) using an even larger set of data (collecting more than 10^5 supergranules).

Alternatively, several authors used tessellation algorithms or threshold-based identification techniques to capture individual supergranulation cells and subsequently study their geometrical properties and spatial arrangement. Such techniques have mostly been applied to maps of the chromospheric network (e.g., [Hagenaar *et al.*, 1997](#); [Schrijver *et al.*, 1997](#); [Berrilli *et al.*, 1998](#)), whose relationship to supergranulation is further described in Section 4.6.1. Following this approach, [Schrijver *et al.* \(1997\)](#) notably found that the patterns of granulation and supergranulation are very similar when properly rescaled. Their results are “nearly compatible with an essentially random distribution of upflow centers”. Comparisons between the spatial arrangement of supergranulation cells and granulation cells were also performed by [Berrilli *et al.* \(2004\)](#), who found that the supergranules distribution is well represented by a “hard sphere random close packing model” and by [Hirzberger *et al.* \(2008\)](#), whose result differ markedly from those of [Berrilli *et al.* \(2004\)](#) and are compatible with a field of “non-overlapping circles with variable diameters”.

To conclude this paragraph, we would like to stress an important difference between the various techniques used to characterize the scale and spatial distribution of supergranules. The first technique consists in determining the scale at which the kinetic energy spectral density or correlation length of horizontal motions is maximal, while the second technique relies on identifying coherent structures using tessellation algorithms and threshold conditions (such as the FWHM of autocorrelation functions) to study the size statistics of the resulting distribution. Unsurprisingly, the two methods provide slightly different values for the supergranulation “length scale”. As noticed by [Leighton *et al.* \(1962\)](#), threshold-based detection gives an estimate of the size of supergranules, whereas the location of the kinetic energy spectrum is an indication of the average distance between supergranules (assumed as to be the energy-containing structures).

4.2.2 Time scales

After supergranulation was discovered, one of the first questions was that of the lifetime of the structures. Here too, we would have to distinguish the lifetime of the coherent structures and the spectral power in a given time scale. However, this latter quantity, being too difficult to derive, is not available. Thus, the time scales discussed below are based on coherent cellular structures.

[Worden and Simon \(1976\)](#) suggested a lifetime of 36 h for the lifetime of supergranulation and reported a detection of vertical velocity fields only at the edge of supergranulation cells, confirming earlier work by [Frazier \(1970\)](#). Later, [Wang and Zirin \(1989\)](#) showed that supergranulation lifetime estimates depended strongly on the choice of tracer or proxy. They obtained 20 h using Dopplergrams, two days using direct counting techniques of supergranulation cells and 10 h using the tracking of magnetic structures (see also Section 4.6). Here again, SOHO/MDI data have dramatically increased the statistics and thus quality of the determinations. The latest results of [Hirzberger *et al.* \(2008\)](#) lead to a lifetime around 1.6 ± 0.7 or 1.8 ± 0.9 d, depending on the technique used. These values are somewhat longer than the previous ones, but the length of the time series associated with the size of the sample enable a better representation of long-living supergranules.

4.2.3 Velocity scales

A typical velocity associated with supergranules can be derived from the ratio between the previously discussed typical length and time scales. Taking 30 Mm for the former and 1.7 d for the latter, we find 205 m s^{-1} as the typical horizontal velocity. This estimate is in reasonable agreement with more direct inferences of the supergranulation velocity field from observations: the original work of Hart (1954) inferred 170 m s^{-1} , Simon and Leighton (1964) mentioned 300 m s^{-1} and more recently Hathaway *et al.* (2002) evaluated this amplitude at $\sim 360 \text{ m s}^{-1}$.

The preceding values are obtained from Doppler shifts. They are quite imprecise because they always mix the horizontal and vertical components of the flow. Granule tracking does not suffer from such a problem, however we here face the remaining problem of the scale dependence of the velocity. The obtained values depend on the way data are filtered.

Possibly, the best way to describe the velocity field amplitude of supergranulation is the spectral density of horizontal kinetic energy $E_h(k)$, which describes the relation between the scale and amplitude of the flow. It is defined as

$$\frac{1}{2} \langle v_h^2 \rangle = \int_0^\infty E_h(k) dk. \quad (1)$$

Figure 4 provides an example of such a power spectrum. The dimensional value of $E_h(k)$ was derived very recently from Hinode/SOT data by Rieutord *et al.* (2010). The spectral power density at supergranulation scales is $500 \text{ km}^3 \text{ s}^{-2}$, which is larger than that at granulation scales⁶. This energy density is related (dimensionally) to the velocity at scale $\lambda = 2\pi/k$ by the relation $V_\lambda = \sqrt{k E_h(k)}$. Here, $V_{\lambda=36 \text{ Mm}} \simeq 300 \text{ m s}^{-1}$, which is quite consistent with the direct Doppler measurements of the velocity field at supergranulation scales.

The horizontal velocity needs to be completed by the vertical velocity. This latter quantity is unfortunately much harder to extract, because the signal is noised by the 5 min oscillations and by the presence of magnetic field concentrations at supergranule boundaries, where up and downflows tend to be localised (see Section 4.6 below). November (1989, 1994) advocated that this vertical component was in fact the mesogranulation that he detected some years before on radial velocities at disc centre (November *et al.*, 1981). The rms value of this quantity was then estimated to be 60 m s^{-1} . More recently this quantity was evaluated using the SOHO/MDI data by Hathaway *et al.* (2002). They derived an estimate of 30 m s^{-1} . This value is in line with the results of Rieutord *et al.* (2010) obtained from Hinode/SOT data using power spectra of line-of-sight velocities.

4.3 Intensity variations in supergranules

Next, one may wonder if supergranulation-scale motions are associated with any temperature or intensity fluctuations, as this information may give an important clue to understand the origin of supergranulation.

As shown by Worden (1975), the thermal signature of supergranulation, if any, must be very faint. The intensity contrast between the border and the centre of supergranules probably does not exceed a few percents, at least in the infrared. For comparison, rms intensity variations at the granulation scale have been shown to be up to 27% by Wedemeyer-Böhm and Rouppe van der Voort (2009) using the recent data of Hinode. Several studies (Beckers, 1968; Frazier, 1970; Foukal and Fowler, 1984; Lin and Kuhn, 1992) found an increase of intensity at the edge of supergranulation cells, corresponding to a negative correlation between the supergranulation horizontal divergence maps and intensity maps. These results, which tend to rule out a convective origin for supergranulation, are however subject to caution because supergranulation vertices are strongly correlated

⁶ At granulation scales, the spectral power density is less than $300 \text{ km}^3 \text{ s}^{-2}$. We recall that granules have a much larger typical velocity than supergranules though, of the order $1-2 \text{ km s}^{-1}$ (Section 3.1). The difference comes from the definition of the spectral power density at wavenumber k , $E(k) \sim k^{-1} V_k^2$, which introduces an extra k factor.

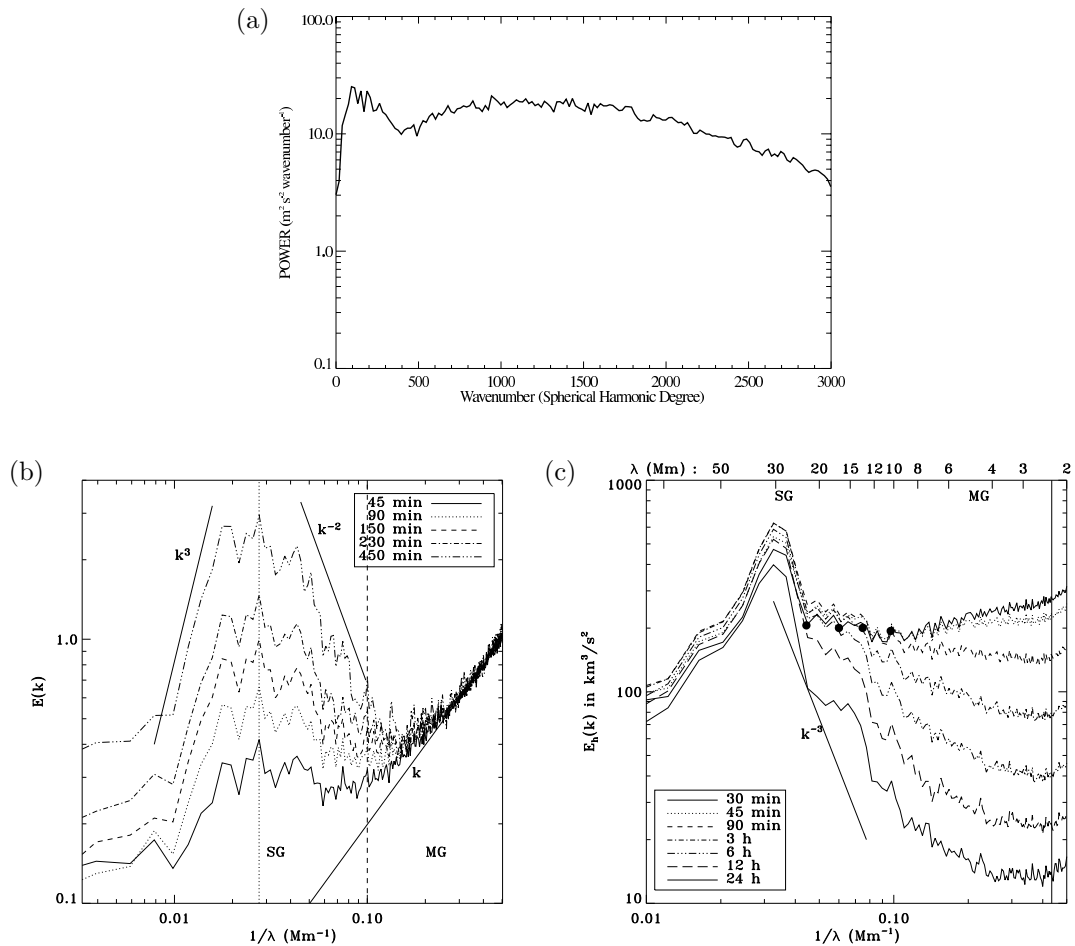


Figure 4: Kinetic energy spectra of solar surface flows. (a) The power spectrum of the line-of-sight velocity using SOHO/MDI Doppler data (Hathaway *et al.*, 2000). The supergranulation peak near $\ell = 120$ is clearly visible, while the granulation peak expected around $\ell = 3000$ is eroded and effectively shifted to larger scales ($\ell \sim 1500$) due to time-averaging. (b) From the CALAS camera at Pic du Midi. Power spectrum (in relative units) of the horizontal velocity obtained from granule tracking for different time averages (Rieutord *et al.*, 2008). (c) Absolute spectral density in $\text{km}^3 \text{s}^{-2}$ also derived from granule tracking, but applied to Hinode/SOT data (Rieutord *et al.*, 2010). In (b) and (c) the power spectra are those defined in Equation (1).

with magnetic bright points (see Section 4.6 below). To circumvent this difficulty, Rast (2003a) considered only areas with low magnetic fields and found a small decrease of intensity at the edge of supergranules. The problem was reconsidered in detail by Meunier *et al.* (2007b, 2008) using MDI intensity maps. There too, the influence of the magnetic network was carefully eliminated. In contrast to most previous studies, they report a very small but significant intensity decrease from the centre to the edge of supergranulation cells (in the range 0.8–2.8 K). Goldbaum *et al.* (2009) recently came to the same conclusion using a different methodology. In addition, Meunier *et al.* (2008) noticed that the radial temperature profile at the surface of a supergranule is very similar to that of a simulated granule. These observations are consistent with a driving of supergranulation by buoyancy.

4.4 Supergranulation depth

The aforementioned supergranulation properties were all inferred from observations at the surface level (optical depth $\tau = 1$). But one may also learn something about the origin of supergranulation by trying to infer its vertical extent.

Without the help of local helioseismology, we can only measure the derivative of the vertical variations at the surface levels. Early studies used lines that form at various heights to get an impression of the vertical variations. Proceeding this way, Deubner (1971) concluded on a slight decrease of the horizontal component of the supergranulation flow with photospheric height and on a slight increase of the vertical component. Worden and Simon (1976) also argued that the Doppler signal of the vertical component of the flow at supergranulation scales was smaller at deeper photospheric levels. Another way to proceed is to use the equation of mass conservation of mean flows. When high-frequency acoustic waves are filtered out, one may use the anelastic approximation and write

$$\partial_z v_z = -v_z \partial_z \ln \rho - \vec{\nabla}_h \cdot \vec{v}_h,$$

where the index h refers to the horizontal quantities and z to the vertical ones. From this equation, we see that a measure of the horizontal divergence and the vertical velocity together with a value of the density scale height (given by a model), allow for an estimation of the vertical velocity scale height.

Combining Dopplergrams and correlation tracking inferences with the above considerations on the continuity equation, November (1994) made the noteworthy prediction that the supergranulation flow should disappear at depths larger than 2.4 Mm below the visible surface. Note that his suggestion that the mesogranulation signal detected in power spectra at a horizontal scale of 7 Mm corresponded to the vertical flow component of convective supergranulation cells was part of the same argument. More recently, Rieutord *et al.* (2010) did the same exercise with divergences and velocity fields derived from Hinode data and found a vertical velocity scale height of ~ 1 Mm, indicating a very shallow structure.

The advent of local helioseismology in the late 1990s made it possible to probe the supergranulation flow at optically-thick levels. Duvall Jr *et al.* (1997), using preliminary MDI data, only detected flows at supergranulation scales in the first few Mm below the surface. Duvall Jr (1998) further estimated that the depth of supergranulation was 8 Mm. Zhao and Kosovichev (2003) reported evidence for converging flows at 10 Mm and estimated the supergranulation depth to be 15 Mm. Woodard (2007) reported a detection of the flow pattern down to 5 Mm corresponding to the deepest layers accessible with their data set. Using new Hinode data, Sekii *et al.* (2007) recently found that a supergranulation pattern, monitored for 12 h in a small field of 80×40 Mm², does not persist at depths larger than 5 Mm. The existence of a return flow at depths larger than 5 Mm has also been suggested but remains unclear (Duvall Jr, 1998; Zhao and Kosovichev, 2003). Note that imaging deep convection using helioseismic techniques is not an easy task. Braun and

Lindsey (2003) and Lindsey and Braun (2004) provide a detailed description of the shortcomings and artefacts of helioseismic inversions in this context (see also Gizon and Birch, 2005).

To summarise, the determination of the vertical extent of the supergranulation below the surface is still in a preliminary phase. The few results mentioned above point to a shallow structure but they are affected by large uncertainties associated with both the intrinsic difficulty to perform such measurements and with their weak statistical significance. It is clear that a decisive step forward regarding this problem requires a careful study of the systematics and the processing of a very large amount of data to reduce the impact of the fluctuating nature of the flows.

4.5 Rotational properties of supergranules

A good measure of the influence of the global rotation Ω of the Sun on the dynamics of a structure of size L and typical velocity V is given by the Rossby number:

$$Ro = \frac{V}{2\Omega L} = (2\Omega\tau)^{-1}.$$

The second expression uses the lifetime of the structure $\tau = L/V$. In numbers, taking $\tau_{\text{SG}} = 1.7$ d and a rotation period of 25–30 d leads to $Ro_{\text{SG}} \sim 2-3$. This is not a large value, indicating that the Coriolis acceleration should have an effect on the dynamics of supergranules. This effect has been observed by Gizon and Duvall Jr (2003), who showed (Figure 5a) that the correlation between vertical vorticity and horizontal divergence of supergranules changes sign at the equator: it is negative in the northern hemisphere and positive in the southern one. Hence, supergranules, which may be seen as outflowing cells, behave like anticyclones in the Earth's atmosphere (the vertical vorticity of anticyclones changes sign at the equator, see Figure 5b). These anticyclones are surrounded by cyclonic vorticity associated with downward flows; because these downdrafts have a somewhat smaller scale, this cyclonic vorticity is less conspicuous in measurements than the anticyclonic contribution of supergranules, but it has actually been singled out in the work of Komm *et al.* (2007).

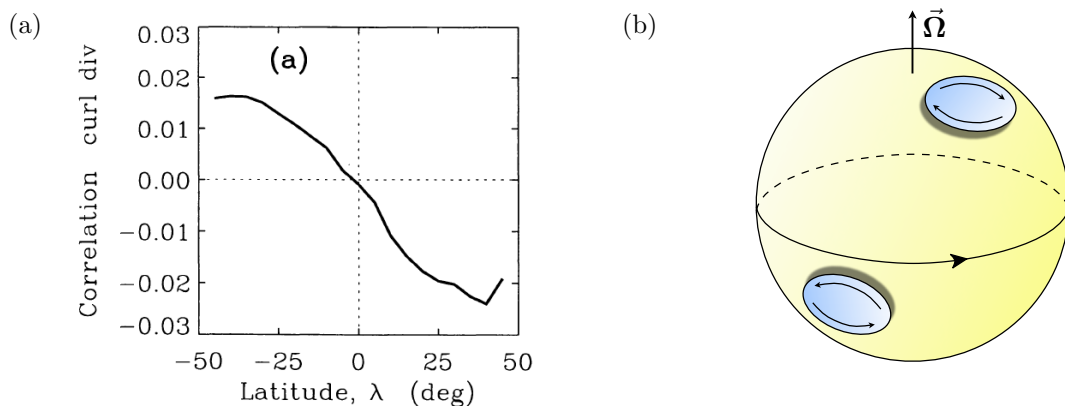


Figure 5: (a) Correlation between the horizontal divergence and vertical vorticity of the supergranulation flow as a function of latitude (from Gizon and Duvall Jr, 2003). (b) Schematic view of anticyclones at the surface of the rotating Sun.

The first reports on the rotational properties of supergranulation focused on the rotation rate of the supergranulation pattern (Duvall Jr, 1980; Snodgrass and Ulrich, 1990). Using Dopplergrams, they found, surprisingly, that supergranulation is rotating 4% faster than the plasma. This is now referred to as the *superrotation* of supergranules. In recent years, local helioseismology

has proven extremely useful to study the rotational properties of supergranules. Their superrotation was confirmed by [Duvall Jr and Gizon \(2000\)](#) using the time-distance technique applied to f -modes. [Beck and Schou \(2000\)](#) estimated that the supergranulation rotation rate is larger than the solar rotation rate at any depth probed by helioseismology. Analysing time series of divergence maps inferred from time-distance helioseismology applied to MDI data, [Gizon *et al.* \(2003\)](#) found that the supergranulation pattern had wave-like properties with a typical period of 6–9 d, fairly longer than the lifetime of individual supergranules. They showed that the power spectrum of the supergranulation signal close to the equator presented a power excess in the prograde direction (with a slight equatorwards deviation in both hemispheres), thus explaining the anomalous superrotation rate of the pattern. The dispersion relation for the wave appears to be only weakly dependent on the latitude ([Gizon and Duvall Jr, 2004](#)). [Schou \(2003\)](#) confirmed these findings with direct Doppler shift measurements and found that wave motions were mostly aligned with the direction of propagation of the pattern. These results brought some extremely interesting new light on the supergranulation phenomenon and led to the conjecture that supergranulation could be a manifestation of oscillatory convection, a typical property of convection in the presence of rotation and/or magnetic fields (see Section 5).

However, [Rast *et al.* \(2004\)](#) and [Lisle *et al.* \(2004\)](#) questioned the interpretation of the observed power spectrum in terms of oscillations and suggested an alternative explanation in terms of two superimposed steady flow components identified as mesogranulation and supergranulation advected by giant cell circulations. According to [Gizon and Birch \(2005\)](#), this interpretation is not supported by observations. They argue that the finding of [Lisle *et al.* \(2004\)](#) that supergranules tend to align in the direction of the Sun’s rotation axis under the influence of giant cells can be explained naturally in terms of wave dynamics. Even more recently, [Hathaway *et al.* \(2006\)](#) argued that the supergranulation pattern superrotation inferred from Doppler shifts was due to projection effects on the line-of-sight signal. Using correlation tracking of divergence maps derived from intensity maps ([Meunier *et al.*, 2007c](#)) and comparing it with direct Doppler tracking, [Meunier and Roudier \(2007\)](#) confirmed the existence of projection effects with the latter method, but found that the supergranulation pattern inferred from divergence maps was still superrotating, albeit at smaller angular velocities than those inferred by [Duvall Jr \(1980\)](#) and [Snodgrass and Ulrich \(1990\)](#). For a detailed discussion on the identification of supergranulation rotational properties with helioseismology, we refer the reader to the review article by [Gizon and Birch \(2005\)](#) on local helioseismology.

For the sake of completeness on the topic of rotation, we finally mention the observations by [Kuhn *et al.* \(2000\)](#) of small-scale 100 m high “hills” at the solar surface, which they interpreted as Rossby waves. Recently, [Williams *et al.* \(2007\)](#) argued that these structures actually resulted from the vertical convective motions associated with supergranules.

4.6 Multiscale convection and magnetic fields

As shown in Section 2.2, the magnetic dissipation scale at the solar surface is $\ell_\eta \sim 100$ m or slightly less. Hence, convection at the solar surface is strongly coupled to the Sun’s magnetic dynamics at all observable scales, including that of supergranulation. The particular role played by magnetic fields in the supergranulation problem and the large amount of observational information available on this topic justify a dedicated subsection. In the following, we first look at the correlations between supergranulation and the magnetic network and then describe the properties of internetwork fields, whose dynamics can hardly be dissociated from the formation of the magnetic network. After a short detour to the observations of the interactions between supergranulation and active regions, we finally review several studies of the dependence of supergranulation on the global solar magnetic activity.

4.6.1 Supergranulation and the magnetic network

The discovery of the chromospheric network in Ca^+K spectroheliograms (the K-line of Ca^+ at 393.4 nm) dates back to Deslandres (1899). Such a spectroheliogram is shown in Figure 6. Leighton *et al.* (1962) and Simon and Leighton (1964) performed a comparative study between magnetograms, spectroheliograms, and Dopplergrams, which revealed a strong correlation between the chromospheric network, the magnetic field distribution of the quiet Sun and supergranulation. For this reason, both magnetograms and spectroheliograms are used to trace supergranulation (e.g., Lisle *et al.*, 2000; Del Moro *et al.*, 2007). It should be kept in mind, however, that the dynamical interactions between magnetic fields and supergranulation are actually not well understood theoretically. This problem will be discussed at length in Section 8.

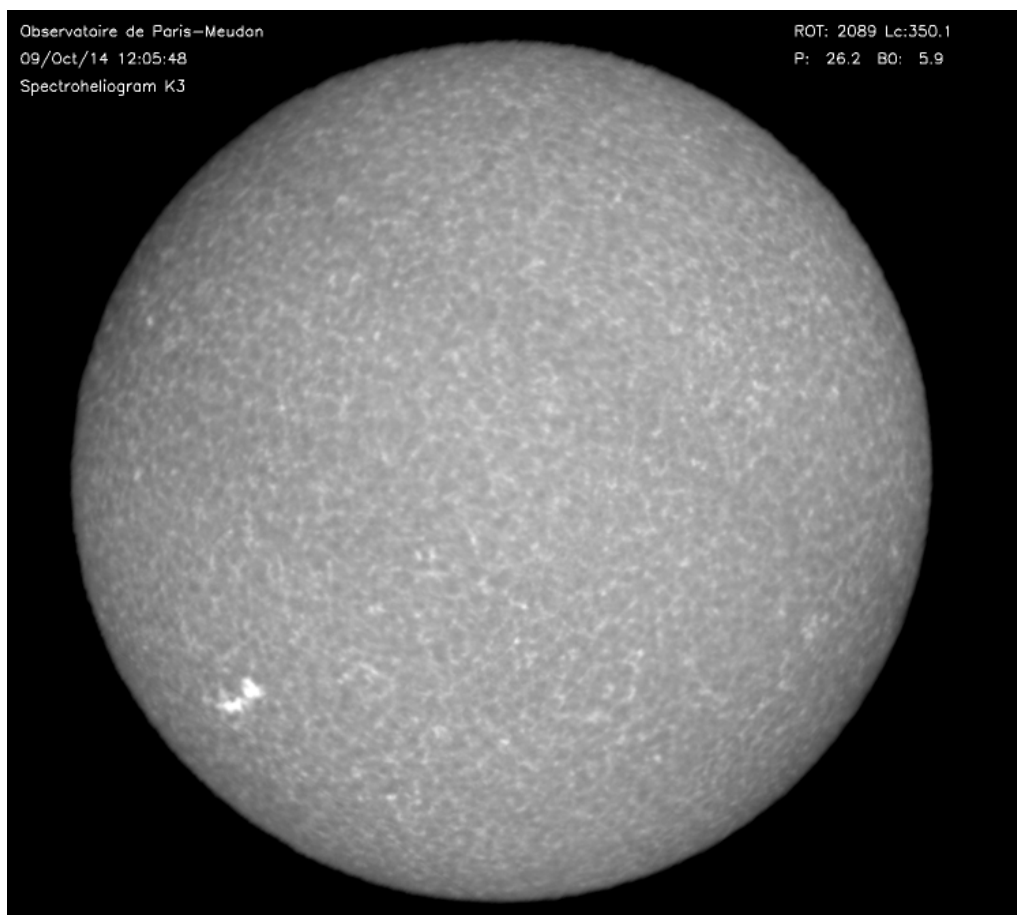


Figure 6: A view of the chromospheric network at the $\text{Ca}^+\text{K3}$ line at 393.37 nm (from Meudon Observatory).

The magnetic network refers to a distribution of magnetic field concentrations (associated with bright points in spectroheliograms) with typical field strengths of the order of 1 kG (see reviews by Solanki, 1993; de Wijn *et al.*, 2009), primarily located on the boundaries of supergranules (Simon *et al.*, 1988), in downflow areas. Several differences between supergranulation and the magnetic network have been noticed, including a 2% relative difference in the rotation rate of the two patterns (see Snodgrass and Ulrich (1990) and Section 4.5 above). The magnetic network is

not regularly distributed on the boundaries of supergranulation cells but rather concentrates into localised structures (see Figure 7). Estimates for the lifetime and size of supergranules inferred from magnetograms or spectroheliograms are significantly smaller than those based on direct velocimetric measurements (Wang and Zirin, 1989; Schrijver *et al.*, 1997; Hagenaar *et al.*, 1997). For instance, Hagenaar *et al.* (1997), using correlations of maps of the chromospheric network, obtained a typical size of 16 Mm. As far as the horizontal velocities are concerned, the tracking of magnetic network elements gives values around 350 m s^{-1} , close to the estimates derived from granule tracking (Lisle *et al.*, 2000). Krijger and Roudier (2003) found that the chromospheric network is well reproduced by letting magnetic elements that are emerging be passively advected by the surface (supergranulation) flow field.

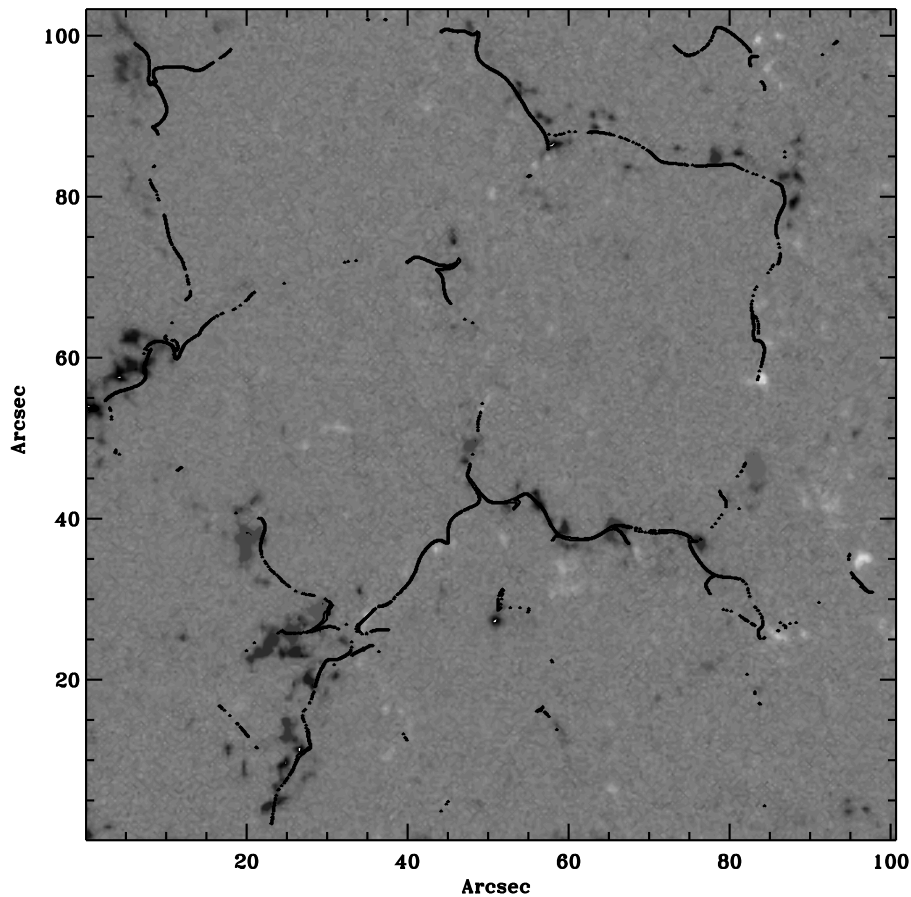


Figure 7: Magnetic field distribution (grey scale levels) on the supergranulation boundaries. The black dots show the final positions of floating corks that have been advected by the velocity field computed from the average motion of granules. The distribution of corks very neatly matches that of the magnetic field. (from Roudier *et al.*, 2009).

These results suggest that the formation of the magnetic network is in some way related to the supergranulation flow. It is however probably too simplistic and misleading to make a one-to-one correspondence between the single scale of supergranulation and the network distribution of magnetic bright points. Several studies with the Swedish Solar Telescope at La Palma obser-

vatory indicate that strong correlations between flows at scales comparable to or smaller than mesoscales (i.e., significantly smaller than supergranulation) and intense magnetic elements exist (Domínguez Cerdeña, 2003; Domínguez Cerdeña *et al.*, 2003). A recent study by Roudier *et al.* (2009), combining spectropolarimetric and photometric Hinode measurements, also demonstrated a very clear correlation between the motions at mesoscales and those of the magnetic network (see also de Wijn and Müller, 2009).

4.6.2 Internetwork fields

One of the major advances on solar magnetism in the last ten years has been the detection of quiet Sun magnetic fields at scales much smaller than that of granulation (e.g., Domínguez Cerdeña *et al.*, 2003; Berger *et al.*, 2004; Trujillo Bueno *et al.*, 2004; Rouppe van der Voort *et al.*, 2005; Lites *et al.*, 2008). The ubiquity of these fields and their energetics suggest that the dynamics of internetwork fields could also be an important piece of the supergranulation puzzle (see also Section 4.6.5 below). It is therefore useful to recall their main properties before discussing the physics of supergranulation in the next sections. Note that the following summary is not meant to be exhaustive. For a dedicated review, we refer the reader to the recent work of de Wijn *et al.* (2009).

Internetwork fields refer to mixed-polarity fields that populate the interior of supergranules. Their strength is on average thought to be much weaker than that of network fields, but magnetic bright points are also observed in the internetwork, (e.g., Muller, 1983; Nisenson *et al.*, 2003; de Wijn *et al.*, 2005; Lites *et al.*, 2008). Besides, network and internetwork fields are known to be in permanent interaction (e.g., Martin, 1988). In the light of nowadays high-resolution observations, the historical dichotomy between network and internetwork fields appears to be rather blurred (this point will be further discussed in Section 8.1).

Internetwork magnetism was originally discovered by Livingston and Harvey (1971, 1975) and subsequently studied by many authors (e.g., Martin, 1988; Keller *et al.*, 1994; Lin, 1995) at resolutions not exceeding 1" (730 km). Observations with the solar telescope at La Palma observatory revealed the existence of such fields at scales comparable and even smaller than the granulation scale (Domínguez Cerdeña *et al.*, 2003; Roudier and Muller, 2004; Rouppe van der Voort *et al.*, 2005). Recent studies based on Hinode observations (Orozco Suárez *et al.*, 2007; Lites *et al.*, 2008) reported magnetic field variations at scales comparable to or smaller than 100 km.

The strength of internetwork fields, their distribution at granulation and subgranulation scales and their preferred orientation are still a matter of debate. Almost every possible value in the 5–500 G range can be found in literature for the typical field strengths within the internetwork (Martin, 1988; Keller *et al.*, 1994; Lin, 1995; Domínguez Cerdeña *et al.*, 2003; Trujillo Bueno *et al.*, 2004; Lites *et al.*, 2008). This wide dispersion is explained by several factors. The most important one is certainly that Zeeman spectropolarimetry, one of the most frequently used tools to study solar magnetism, is affected by cancellation effects when the magnetic field reverses sign at scales smaller than the instrument resolution (Trujillo Bueno *et al.*, 2004; de Wijn *et al.*, 2009). Hence, very small-scale fields still partially escape detection via this method. Recent Zeeman spectropolarimetry estimates of the average field strength based on Hinode observations (Lites *et al.*, 2008) are 11 G for longitudinal fields and 60 G for transverse fields (horizontal fields at disc centre), but wide excursions from these average values are detected and the observed signatures may also be compatible with stronger, less space-filling magnetic fields. On the side of Hanle spectropolarimetry, Trujillo Bueno *et al.* (2004) report an average field strength of 130 G, with stronger fields in the intergranular lanes and much weaker fields in the bright centres of granules.

The previously mentioned Zeeman estimates seem to indicate that internetwork fields have a tendency to be horizontal (Orozco Suárez *et al.*, 2007; Bommier *et al.*, 2007; Lites *et al.*, 2008), sometimes even bridging over granules, but other studies have come to the opposite conclusion

that internetwork fields are mostly isotropic (Martínez González *et al.*, 2008; Asensio Ramos, 2009; Bommier *et al.*, 2009). Using Zeeman and Hanle diagnostics in a complementary way, López Ariste *et al.* (2010) very recently came to the conclusion that internetwork fields are mostly isotropic and highly disordered, with a typical magnetic energy containing scale of 10 km.

4.6.3 The magnetic power spectrum of the quiet photosphere

The scale-by-scale distribution of magnetic energy and the power spectrum of magnetic fields in the quiet photosphere are other important quantities to look at, as they may give us some clues on the type of MHD physics at work in the subgranulation to supergranulation range. Based on various types of analysis (structure statistics, wavelets, etc.), several authors have notably argued that solar magnetic fields, from the global solar scales to the smallest scales available to observations, may have a fractal or multifractal structure (Lawrence *et al.*, 1995; Komm, 1995; Nesme-Ribes *et al.*, 1996; Meunier, 1999; Janßen *et al.*, 2003; Stenflo and Holzreuter, 2002, 2003a,b; Abramenko, 2005).

Explicit studies of the power spectrum of the quiet Sun are currently limited to the range 1–100 Mm and to the line-of-sight component of the magnetic field. Most spectra available in literature have been obtained from either ground-based observations or SOHO/MDI magnetograms. We have been unable to find any study of the magnetic power spectrum of the quiet Sun covering scales well below 1 Mm, at which internetwork fields can now be detected with Hinode.

At scales below 10 Mm, the magnetic power spectrum of the quiet photosphere has been found to be rather flat and decreasing with decreasing scales. Scalings in that mesoscale interval range from k^{-1} to $k^{-1.4}$ (Lee *et al.*, 1997; Abramenko *et al.*, 2001; Harvey *et al.*, 2007; McAteer *et al.*, 2009; Longcope and Parnell, 2009). At scales larger than 10 Mm, a slightly positive flat slope $\sim k^{1.3} - k^0$ has been reported by several authors (Lee *et al.*, 1997; Abramenko *et al.*, 2001; Longcope and Parnell, 2009).

4.6.4 Supergranulation and flows in active regions

Proceeding along the description of the interactions between supergranulation and magnetic fields, one may also consider the properties of surface flows at scales comparable to supergranulation within active regions and in the vicinity of sunspots. The reason for this is twofold. First, we may wonder how the supergranulation pattern evolves locally during the formation or decay of an active region. Second, the properties of flows around sunspots may give us some hints of the effect of strong magnetic flux concentrations on the flow dynamics in the quiet photosphere.

As far as the first point is concerned, the information is fairly scarce at the moment. Rieutord *et al.* (2010) recently reported the disappearance of the supergranulation spectral peak in the kinetic energy power spectrum of solar convection during the emergence of two magnetic pores. While the pores (of a size comparable to that of a granule) are emerging, the supergranulation flow becomes very weak just like if the surrounding magnetic flux associated with the pores had a significant impact on the flow. A related observation by Hindman *et al.* (2009) shows that the fairly regular tiling of the surface of the quiet Sun associated with supergranulation is somewhat disorganised and washed away within magnetic active regions.

On the second point, many studies in the past have focused on the detection and characterisation of intrinsic flows associated with sunspot regions (see Solanki, 2003 and Thomas and Weiss, 2008 for exhaustive descriptions of sunspot structure and dynamics) and significant observational progress has been made on this problem in recent years thanks to local helioseismology (Lindsey *et al.*, 1996; Gizon *et al.*, 2000; Zhao *et al.*, 2001; Haber *et al.*, 2001; Braun and Lindsey, 2003; Haber *et al.*, 2004; Zhao *et al.*, 2004, 2009; Hindman *et al.*, 2009). The general picture that has progressively emerged is the following (see Hindman *et al.*, 2009, and Figure 8): an annular outflow called the moat flow (Sheeley Jr, 1969) is observed at the surface, close to the sunspot. There is a corresponding return

flow at depths smaller than 2 Mm, so the moat circulation is fairly shallow. In contrast, further away from the sunspot umbra, larger-scale circulations characterised by a surface inflow and a deep (> 10 Mm) outflow are inferred from helioseismic inversions.

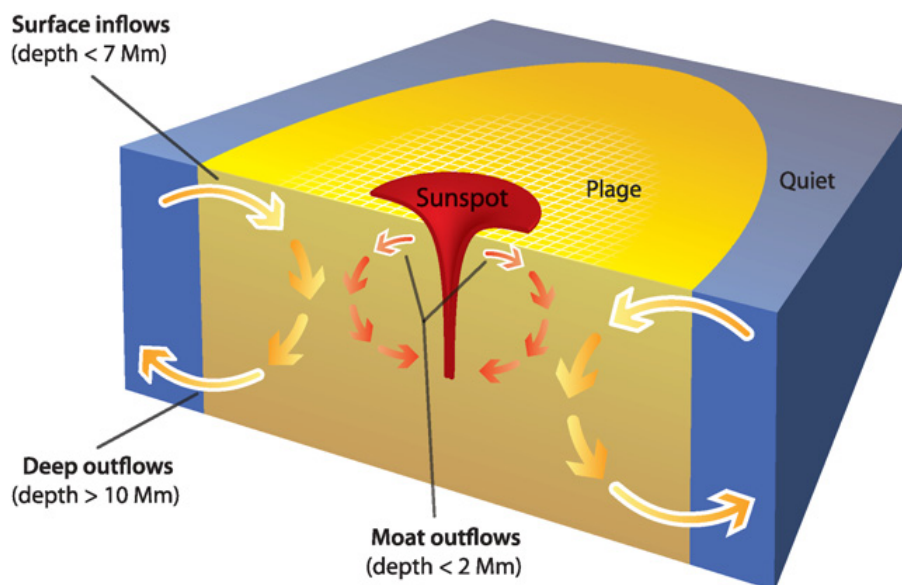


Figure 8: Structure of flows surrounding a sunspot, as inferred from helioseismology (from Hindman *et al.*, 2009).

Several authors studied the structure of the moat flow using Doppler signal (Sheeley Jr and Bhatnagar, 1971; Sheeley Jr, 1972), by tracking surface features, such as granules (Muller and Mena, 1987; Shine *et al.*, 1987) or small-scale magnetic elements (Sheeley Jr, 1972; Harvey and Harvey, 1973; Hagenaar and Shine, 2005), or using helioseismology (Gizon *et al.*, 2000). One of the conclusions of these studies is that the outflow has properties similar to those of supergranulation (see notably Brickhouse and Labonte, 1988), albeit with a larger velocity $\sim 1 \text{ km s}^{-1}$. It is however unclear whether or not this flow has anything to do with the regular supergranulation, as the outflow is centred on a strong field region in that case whereas it is the supergranulation inflow vertices that coincide with magnetic flux concentrations in the quiet Sun. As far as supergranulation is concerned, nevertheless, the lesson to be learned from helioseismology of sunspot regions is that magnetoconvection in strong fields has the naturally ability to produce a variety of coherent outflows and inflows at various horizontal and vertical scales in the vicinity of regions of strong magnetic flux. This phenomenology may be worth exploring further in the somewhat scaled-down system consisting of the supergranulation flow and local flux concentrations associated with the magnetic network in the quiet Sun (see Section 8.2 in this review).

4.6.5 Supergranulation variations over the solar cycle

In view of the association between supergranulation and the magnetic network, it is finally natural to wonder if and how the size of supergranules varies with solar activity.

Singh and Bappu (1981), studying spectroheliograms spanning a period of seven solar maxima, found a decrease of the typical size of the chromospheric network between the maxima and the minima of the cycle. Their results are in line with those of Kariyappa and Sivaraman (1994), Berrilli *et al.* (1999) and Raju and Singh (2002), but appear to be at odds with those of Wang (1988) and

Münzer *et al.* (1989), who both reported an increase of network cell sizes in regions of stronger magnetic activity, and with those of Meunier (2003), who found from MDI magnetograms spanning the first half of Cycle 23 an increase of the size of magnetic elements at supergranulation-like scales with solar activity (note that Berrilli *et al.*, 1999 also used data obtained at the beginning of Cycle 23 close to the activity minimum). These somehow contradicting results show that magnetic tracers must be used with care for this kind of measurements. The results are indeed sensitive to the thresholds used to identify the various field components (e.g., network or internetwork). Disentangling all these effects is not an easy task.

Recent studies have thus attempted to use proxies independent of magnetic tracers of supergranulation to measure its size, notably velocity features like positive divergences. DeRosa and Toomre (2004), using two data sets obtained at periods of different levels of magnetic activity, found smaller supergranulation cell sizes in the period of high activity. A similar conclusion was reached by Meunier *et al.* (2008). Meunier *et al.* (2007a) found a decrease of the typical cell sizes with increasing field strength within supergranules, but noted that larger supergranulation cells were associated with stronger network fields at their boundaries. Hence, it seems that a negative or a positive correlation can be obtained, depending on whether the level of magnetic activity is defined with respect to internetwork or network fields. Meunier *et al.* (2007a) also reported the absence of large supergranulation cells for supergranules with large internetwork magnetic field strengths, indicating that internetwork fields do have a dynamical influence on supergranules. We refer the reader to Meunier *et al.* (2007a) for a more exhaustive discussion of the previous results and of the possible shortcomings and biases of these various studies.

Finally, on the helioseismic side, the dispersion relation for the supergranulation oscillations found by Gizon *et al.* (2003) appears to be only weakly dependent on the phase of the solar cycle (Gizon and Duvall Jr, 2004). However, the same authors reported a decrease in the lifetime and power anisotropy of the pattern from solar minimum to solar maximum.

4.7 Conclusions

Since the launch of SOHO and observations with the MDI instrument, the interest in supergranulation has been renewed. Most of its main observational properties, like its size, lifetime and the strength of the associated flows are now well determined. However, other aspects of supergranulation dynamics, like the vertical dependence of the flow, the vertical component of the velocity at the edge of supergranules and the connections between supergranulation and magnetic fields are still only very partially constrained by observations. They all require further investigations.

As far as velocity measurements are concerned, we may anticipate progress in the near future on the question of the depth of supergranulation thanks to local helioseismology applied to higher-resolution observations. However, characterising vertical flows at the supergranulation scale is a more complex task since such flows are faint and very localised in space. Improving the diagnostics of the latitudinal dependence of the supergranulation pattern may also prove useful, in particular to help understand if subsurface shear plays a significant role in shaping the supergranulation flow.

Another point worth studying in more detail is the distribution of kinetic energy at scales between supergranulation and the Sun's radius. This has already been attempted using supergranules as passive tracers of larger-scale velocity patterns (Švanda *et al.*, 2006, 2008). Even more accurate studies of this kind could become feasible soon by using tracking techniques applied to images obtained with wide-field cameras imaging the full solar disc with sub-granulation resolution.

The case of the interactions with magnetic fields deserves a lot of further attention on the observational side in our view. It is now well established that flows at scales larger than granulation advect internetwork fields and tend to concentrate magnetic elements into the network, along the boundaries of supergranules. This process is essentially kinematic, in the sense that the magnetic field only has a very weak feedback on the flow. But what we observe ultimately is probably a

nonlinear statistically steady magnetised state, in which the magnetic field provides significant feedback on the flow. Hence, it would be useful to have more quantitative observational results on the relations between the properties of supergranules and the surrounding magnetic fields (internal and boundary flux, filling factors, strength, size) to characterise this feedback more precisely (we refer the reader to Section 8 for an exhaustive discussion on supergranulation and MHD). Most importantly, a precise determination of the magnetic energy spectrum of the quiet Sun over a very wide range of scales would be extremely precious to understand the nature of MHD interactions between supergranulation, network and internetwork fields. Finally, it would also be interesting to have more documented observational examples of the interactions of supergranulation with magnetic regions of various strengths (active regions, polar regions) to gain some insight into the dynamical processes at work in the problem. This latter point is important from the perspective of the global solar dynamo problem, as it would help better constrain the transport of magnetic field by turbulent diffusion at the surface of the Sun.

5 Theoretical Models of Supergranulation

We now turn to the description of existing theoretical models of supergranulation. These models are basically of two types: those that postulate that supergranulation has a convective origin (i.e., it is driven by thermal buoyancy), and those that do not. In order to set the stage for upcoming discussions, we start with a brief description of the rotating MHD Rayleigh–Bénard problem (Section 5.1), which provides the simplest mathematical description of rotating magnetoconvection in a fluid. We then review various thermal convection models of supergranulation (Section 5.2) and discuss other possible physical mechanisms involving collective “turbulent” dynamics of smaller-scale convection (Section 5.3). A few concluding remarks follow.

Before we start, it is perhaps useful to mention that most of these models are unfortunately only very qualitative, in the sense that they either rely on extremely simplified theoretical frameworks (like linear or weakly nonlinear theory in two dimensions, or simple energetic arguments) or on simple dynamical toy models designed after phenomenological considerations. The looseness of theoretical models, combined with the incompleteness of observational constraints and shortcomings of numerical simulations, has made it difficult to either validate or invalidate any theoretical argument so far. What numerical simulations tell us and how the theoretical models described below fit with numerical results and observations will be discussed in detail in Section 6.

5.1 The rotating MHD Rayleigh–Bénard convection problem

5.1.1 Formulation

The simplest formulation of the problem of thermal convection of a fluid is called the Rayleigh–Bénard problem. It describes convection of a liquid enclosed between two differentially heated horizontal plates, each held at a fixed temperature. The mathematical model is derived under the Boussinesq approximation, which amounts to assuming that the flow is highly subsonic and that density perturbations $\delta\rho$ to a uniform and constant background density ρ_o are negligible everywhere except in the buoyancy term $\delta\rho\vec{g}$, where $\vec{g} = -g\vec{e}_z$ stands for the gravity (Chandrasekhar, 1961). The equilibrium background state is a linear temperature profile with temperature decreasing from the bottom to the top of the layer. This case is in many respects different and simpler than the strongly stratified SCZ case, which treatment requires using more general compressible fluid and energy equations than those given below (Nordlund, 1982), but is sufficient to discuss many of the important physical (Section 5.2) and numerical (Section 6.1) issues pertaining to supergranulation.

Anticipating upcoming discussions on the origin of supergranulation, we extend the simplest hydrodynamic formulation of the Rayleigh–Bénard problem to the case of an electrically conducting liquid threaded by a mean vertical magnetic field denoted by $\vec{B}_o = B_o\vec{e}_z$ and rotating around a vertical axis, with a rotation rate $\vec{\Omega} = \Omega\vec{e}_z$. This set-up is shown on Figure 9.

In nondimensional form, the equations for momentum and energy conservation, the induction equation, the equations for mass conservation and magnetic field solenoidality read

$$\begin{aligned}
 \frac{\partial \vec{u}}{\partial \tau} + \vec{u} \cdot \vec{\nabla} \vec{u} + \sqrt{Ta} Pr \vec{e}_z \times \vec{u} &= -\vec{\nabla} p + Ra Pr \theta \vec{e}_z + Q \frac{Pr^2}{Pm} (\vec{\nabla} \times \vec{B}) \times \vec{B} + Pr \Delta \vec{u}, \\
 \frac{\partial \theta}{\partial \tau} + \vec{u} \cdot \vec{\nabla} \theta - u_z &= \Delta \theta, \\
 \frac{\partial \vec{B}}{\partial \tau} + \vec{u} \cdot \vec{\nabla} \vec{B} &= \vec{B} \cdot \vec{\nabla} \vec{u} + \frac{Pr}{Pm} \Delta \vec{B}, \\
 \vec{\nabla} \cdot \vec{u} = 0, \quad \vec{\nabla} \cdot \vec{B} &= 0,
 \end{aligned} \tag{2}$$

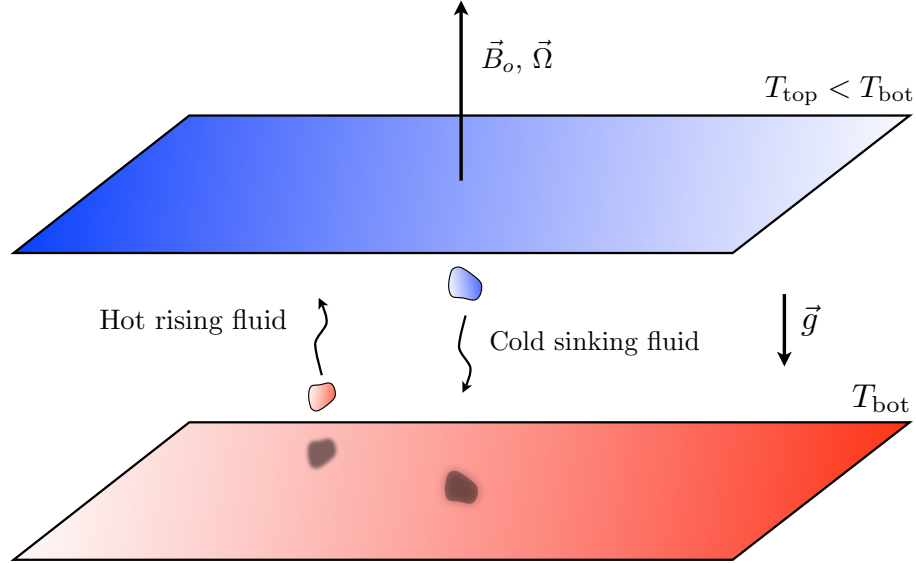


Figure 9: The rotating MHD Rayleigh–Bénard convection problem.

where the momentum equation has been written in the rotating frame, lengths are measured in terms of the thickness of the convection layer d , times are defined with respect to the thermal diffusion time $\tau_\kappa = d^2/\kappa$ (κ is the thermal diffusivity), the total magnetic field \vec{B} is expressed in terms of the Alfvén speed $V_A = B_o/\sqrt{\rho_o\mu_o}$, and temperature deviations θ to the initial linear temperature profile are measured in terms of the background temperature difference $\Delta T = T_{\text{top}} - T_{\text{bot}}$ between the two horizontal plates enclosing the fluid in the vertical direction. Nondimensional velocity and pressure fluctuations are denoted by \vec{u} and p , respectively. This set of equations must be complemented by appropriate boundary conditions, most commonly fixed temperature or fixed thermal flux conditions on the temperature, no-slip or stress-free conditions on velocity perturbations, and perfectly conducting or insulating boundaries for the magnetic field.

Several important numbers appear in the equations above, starting with the *Rayleigh number*

$$Ra = \frac{\alpha|\Delta T|gd^3}{\nu\kappa} = |N^2|\tau_\nu\tau_\kappa, \quad (3)$$

where α is the thermal expansion coefficient of the fluid defined according to $\delta\rho/\rho_o = -\alpha\theta$. Here, $N^2 = \alpha\Delta Tg/d < 0$ is the square of the Brunt–Väisälä frequency (negative for a convectively unstable layer) and $\tau_\nu = d^2/\nu$ is the viscous diffusion time, so the Rayleigh number measures the relative effects of the convection “engine”, buoyancy, and of the “brakes”, namely viscous friction and heat diffusion. The second important parameter above is the *Chandrasekhar number*

$$Q = \frac{B_o^2d^2}{\rho_o\mu_o\nu\eta} = \frac{\tau_\nu\tau_\eta}{\tau_A^2}, \quad (4)$$

which is a measure of the relative importance of magnetic tension ($\tau_A = d/V_A$ is the Alfvén crossing time) on the flow in comparison to magnetic diffusion (η is the magnetic diffusivity, $\tau_\eta = d^2/\eta$ is

the typical magnetic diffusion time) and viscous friction. The relative importance of the Coriolis force in comparison to viscous friction is measured by the *Taylor number*,

$$Ta = \frac{4\Omega^2 d^4}{\nu^2} = (2\Omega)^2 \tau_\nu^2. \quad (5)$$

Finally, $Pr = \nu/\kappa$ and $Pm = \nu/\eta$, where η is the magnetic diffusivity, stand for the *thermal* and *magnetic Prandtl numbers* (see Section 2.2).

5.1.2 Linear instability and the solar regime

In the simplest non-rotating hydrodynamic case ($Ta = Q = 0$, no induction), when the Rayleigh number is less than a critical value Ra_{crit} that depends on the particular choice of boundary conditions, diffusive processes dominate over buoyancy: the hydrostatic solution is stable, i.e., any velocity or temperature perturbations decays. For $Ra > Ra_{\text{crit}}$, convection sets in as a linear instability and perturbations grow exponentially in the form of convection rolls or hexagons with a horizontal spatial periodicity comparable to the convective layer depth d in most cases. The effects of magnetic fields and rotation on the linear stability analysis are discussed in the next paragraphs.

It should be noted that Ra , Q , and Ta are all extremely large numbers in the Sun, if they are computed from microscopic transport coefficients (Section 2.2). So, in principle, there is no reason why solar convection should be close to the instability threshold. However, theoretical studies of large-scale convection (such as supergranulation) commonly assume that viscous, thermal, and magnetic diffusion at such scales are determined by turbulent transport, not microscopic transport. This leads to much larger transport coefficients (which can be estimated, for instance, using the typical scale and velocity of the granulation pattern) and much smaller “effective” Ra , Q , and Ta , so the “large-scale” system is generally considered not too far away from criticality. Making this (strong) mean-field assumption serves to legitimate using the standard toolkits of linear and weakly nonlinear analysis to understand the large-scale behaviour of solar convection.

5.2 Convective origin of supergranulation

Following its discovery in the 1950s and further studies in the 1960s, supergranulation was quickly considered to have a convective origin, very much like the solar granulation. Since then, many theoretical models relying on the basic phenomenology of thermal convection sketched in Section 5.1.2 have been devised to explain the apparently discrete-scales regime of the dynamics of the solar surface (namely the scales of granulation and supergranulation, but also that of mesogranulation, discussed in Section 3.2).

5.2.1 Multiple mode convection

The simplest model for the emergence of a set of special scales is that of multiple steady linear or weakly nonlinearly interacting modes of thermal convection forced at different depths. The first theoretical argument of this kind is due to [Simon and Leighton \(1964\)](#), who suggested that supergranulation-scale motions corresponded to simple convection cells driven at the depth of He^{++} recombination and just advecting granulation-scale convection. [Schwarzschild \(1975\)](#) invoked an opacity break, He^+ and H^+ recombinations as the drivers of supergranulation-scale convection. [Simon and Weiss \(1968\)](#) and [Vickers \(1971\)](#), on the other hand, suggested that deep convection in the Sun had a multilayered structure composed of deep, giant cell circulations extending from the bottom of the convection zone to 40 Mm deep, topped by a shallower circulation pattern corresponding to supergranulation. In this second theory, recombination is not a necessary ingredient. [Bogart et al. \(1980\)](#) attempted to match a linear combination of convective eigenmodes to the solar

convective flux but did not find that supergranulation came out as a preferred scale of convection in this quasilinear framework.

[Antia *et al.* \(1981\)](#) argued that turbulent viscosity and diffusivity should be taken into account in linear calculations, as they alter the growth and scales of the most unstable modes of convection. In their linear calculation with microscopic viscosity and thermal diffusivity coefficients replaced by their turbulent counterparts, granulation, and supergranulation show up as the two most unstable harmonics of convection. Calibrating the amplitudes of a linear superposition of convective modes to match mixing-length estimates of the solar convective flux in the spirit of [Bogart *et al.* \(1980\)](#), [Antia and Chitre \(1993\)](#) further argued that they could reproduce the main characteristics of the power spectrum of solar surface convection.

[Gierasch \(1985\)](#) devised a one-dimensional energy model for the upper solar convection zone from which he argued that turbulent dissipation takes place and deposits thermal energy at preferred depths, thereby intensifying convection at granulation and supergranulation scales. On this subject, we also mention the work of [Wolff \(1995\)](#), who calculated that the damping of r -modes in the Sun should preferentially deposit heat 50 Mm below the surface as a result of the ionisation profile in the upper solar convection zone. This process might in turn result in convective intensification at similar horizontal scales.

5.2.2 Effects of temperature boundary conditions

An interesting theoretical suggestion on the problem of supergranulation was made by [Van der Borgh \(1974\)](#), who considered the case of steady finite-amplitude thermal convection cells in the presence of fixed heat flux boundary conditions imposed at the top and bottom of the layer. He showed that the convection pattern in this framework has much smaller temperature fluctuations than in the standard Rayleigh–Bénard model with fixed temperature boundary conditions. This makes this case quite interesting for the supergranulation problem, considering that intensity fluctuations at supergranulation scales are rather elusive (see Section 4.3).

Even more interestingly, fixed heat flux boundary conditions naturally favour marginally stable convection cells with infinite horizontal extent compared to the layer depth, or convection cells with a very large but finite horizontal extent when a weak modulation of the heat flux is allowed for ([Sparrow *et al.*, 1964](#); [Hurle *et al.*, 1967](#); [Van der Borgh, 1974](#); [Busse and Riahi, 1978](#); [Chapman and Proctor, 1980](#); [Depassier and Spiegel, 1981](#)). This case is therefore very different from the standard Rayleigh–Bénard case with fixed temperature boundary conditions, which gives rise to cells with aspect ratio of order unity. In this framework, there is no need to invoke deep convection to produce supergranulation-scale convection.

This idea was carried on with the addition of a uniform vertical magnetic field threading the convective layer. Contrary to the hydrodynamic case described above, where zero-wavenumber solutions are preferred linearly (albeit with a zero growth-rate), convection cells with a long but finite horizontal extent dominate in the magnetised case, provided that the magnetic field exceeds some threshold amplitude. The horizontal scale of the convection pattern in the model is subsequently directly dependent on the magnetic field strength. [Murphy \(1977\)](#) was the first to suggest that this model might be relevant to supergranulation. The linear problem in the Boussinesq approximation was solved by [Edwards \(1990\)](#). [Rincon and Rieutord \(2003\)](#) further solved the fully compressible linear problem numerically and revisited it in the context of supergranulation. Using typical solar values as an input for their model parameters (density scale height, turbulent viscosity etc.) they showed that the magnetic field strength (measured in the nondimensional equations by the Chandrasekhar number Q) required for compressible magnetoconvection with fixed heat flux to produce supergranulation-scale convection was of the order 100 G.

5.2.3 Oscillatory convection and the role of dissipative processes

The discovery by Gizon *et al.* (2003) that supergranulation has wave-like properties (Section 4.5) opened some new perspectives for theoretical speculation. In particular, it offered an opportunity to revive the interest for several important theoretical findings pertaining to the issue of oscillatory convection, which we now attempt to describe.

The existence of time-dependent oscillatory modes of thermal convection has been known for a long time (Chandrasekhar, 1961 provides an exhaustive presentation of linear theory on this topic). In many cases, such a behaviour requires the presence of a restoring force acting on the convective motions driven by buoyancy. It can be provided by Coriolis effects (rotation) or magnetic field tension for instance. The existence of oscillatory solutions is also known to depend very strongly on how various dissipative processes (viscous friction, thermal diffusion, and ohmic diffusion) compete in the flow. This is usually measured or parametrised in terms of the thermal Prandtl number $Pr = \nu/\kappa$, where ν is the kinematic viscosity and κ is the thermal diffusivity, the magnetic Prandtl number $Pm = \nu/\eta$, where η is the magnetic diffusivity, and the “third” Prandtl number⁷ $\zeta = \eta/\kappa = Pr/Pm$. In the Sun, $Pr \sim 10^{-4} - 10^{-10}$, $Pm \sim 10^{-2} - 10^{-5}$ (see Section 2.2), and $\zeta \ll 1$ at the photosphere.

5.2.4 Oscillatory convection, rotation, and shear

As mentioned in Section 4.5, the supergranulation flow seems to be weakly influenced by the global solar rotation. In the presence of a vertical rotation vector, overstable oscillatory convection is preferred to steady convection provided that Pr is small (Chandrasekhar, 1961). In more physical terms, an oscillation is only possible if inertial motions are not significantly damped viscously on the thermalization timescale of rising and sinking convective blobs.

Busse (2004, 2007) suggested on the basis of a local Cartesian analysis that the drift of supergranulation could be a signature of weakly nonlinear thermal convection rotating about an inclined axis and found a phase velocity consistent with the data of Gizon *et al.* (2003), assuming an eddy viscosity prescription consistent with solar estimates (based on the typical sizes and velocity of granulation). Earlier work on the linear stability of a rotating *spherical* Boussinesq fluid layer heated by internal heat sources showed that the most rapidly growing perturbations are oscillatory and form a prograde drifting pattern of convection cells at low Prandtl number in high Taylor number regimes corresponding physically to large rotation (Zhang and Busse, 1987).

A directly related issue is that of the influence of *differential rotation* on supergranulation. Green and Kosovichev (2006) considered the possible role of the solar subsurface shear layer (Schou *et al.*, 1998) by looking at the effect of a vertical shear flow on the onset of convection in a strongly stratified Cartesian layer using linear theory. They found that convective modes in the non-sheared problem become travelling when a weak shear is added. Some previous work found that this behaviour is possible either at low Pr (Kropp and Busse, 1991) or if some form of symmetry breaking is present in the equations (Matthews and Cox, 1997). Since linear shear alone cannot do the job, it is likely that density stratification plays an important role in obtaining the result. Green and Kosovichev (2006) also report that the derived phase speeds for their travelling pattern are significantly smaller than those inferred from observations by Gizon *et al.* (2003).

Note that the relative orientations and amplitudes of rotation, shear, and gravity are fundamental parameters in the sheared rotating convection problem. It should therefore be kept in mind that the results (e.g., the pattern phase velocity and wavelength) of local Cartesian theoretical models of supergranulation incorporating solar-like rotation effects are expected to depend on latitude, as the orientation of the rotation vector changes from horizontal at the equator to vertical at the

⁷ The Roberts number $q = 1/\zeta$ is also used in the context of convection in planetary cores. In the Earth’s core, $q \ll 1$, see, e.g., Zhang and Jones (1996).

pole, and the subsurface rotational velocity gradient varies with latitude in the Sun. We recall that there is as yet no conclusive observational evidence for a latitudinal dependence of the scales of supergranulation (see Section 4.5), so it is unclear if local models of sheared rotating convection can help solve the problem quantitatively. Global spherical models do not necessarily suffer from this problem, as they predict global modes with a well-defined phase velocity.

5.2.5 Oscillatory convection and magnetic fields

Magnetoconvection in a uniform vertical magnetic field is also known to preferentially take on the form of time-oscillations at onset provided that $\zeta \ll 1$ (e.g., Chandrasekhar, 1961; Proctor and Weiss, 1982), a process referred to as magnetic overstability. Oscillatory magnetoconvection is also known to occur for non-vertical magnetic fields (e.g., Matthews *et al.*, 1992; Hurlburt *et al.*, 1996; Thompson, 2005, and references therein). Physically, field lines can only be bent significantly by convective motions and act as a spring if they do not slip too much through the moving fluid, which requires, in this context, that the magnetic diffusivity of the fluid be small enough in comparison to its thermal diffusivity. Since $\zeta \ll 1$ in the quiet photosphere, oscillatory magnetoconvection represents a possible option to explain the wavy behaviour of supergranulation. On this topic, Green and Kosovichev (2007) recently built on the work of Green and Kosovichev (2006) and considered the linear theory of sheared magnetoconvection in a uniform horizontal (toroidal) field shaped by the subsurface shear layer. They report that the phase speed of the travelling waves increases in comparison to the hydrodynamic case studied by Green and Kosovichev (2006) and argue that the actual phase speed measured by Gizon *et al.* (2003) can be obtained for a uniform horizontal field of 300 G.

5.2.6 Other effects

Finally, it is known theoretically and experimentally that even in the absence of any effect such as magnetic couplings, rotation or shear, the value of the thermal Prandtl number can significantly affect the scales and time evolution of convection, both in the linear and nonlinear regimes. Its value notably controls the threshold of secondary oscillatory instabilities of convection rolls (Busse, 1972). At very low Prandtl numbers, Thual (1992) showed that a very rich dynamical behaviour resulting from the interactions between the primary convection mode and the secondary oscillatory instability takes place close to the convection threshold. This includes travelling and standing wave convection.

Most theoretical studies of supergranulation to date have been either ideal (no dissipation) or for $Pr \sim Pm \sim 1$. For this reason, some important physical effects relevant to supergranulation-scale convection may well have been overlooked until now.

5.2.7 Shortcomings of simple convection models

The previous models are interesting in many respects but it should be kept in mind that they all have very important shortcomings. First, they rely on linear or weakly nonlinear calculations, which is hard to justify considering that the actual Reynolds number in the solar photosphere is over 10^{10} and that power spectra of solar surface flows show that the dynamics is spread over many scales. A classical mean-field argument is that small-scale turbulence gives rise to effective turbulent transport coefficients, justifying that the large-scale dynamics be computed from linear or weakly nonlinear theory. Even if it is physically appealing, this argument still lacks firm theoretical foundations. Assuming that turbulent diffusion can be parametrised by using the same formal expression as microscopic diffusion is a strong assumption, and so is the neglect of direct nonlocal, nonlinear energy transfers between disparate scales. Dedicated numerical simulations

of this problem are therefore more than ever required to justify or to discard using this kind of assumptions.

Models with poor thermally conducting boundaries have the interesting feature of producing fairly shallow convection cells, with a large horizontal extent in comparison to their vertical extent. If it is confirmed that supergranulation is indeed a shallow flow (Section 4.4), investigating the theoretical basis of this assumption may prove useful to understand the origins of supergranulation. Of course, the main problem is that it remains to be demonstrated that fixed heat flux boundaries represent a good approximation of the effect of granulation-scale convection on larger-scale motions beneath the solar surface.

Finally, magnetoconvection models all assume the presence of a uniform field (either horizontal or vertical) threading the convective layer, which is certainly an oversimplified zeroth-order prescription for the magnetic field geometry in the quiet Sun. Numerical modelling probably provides the only way to incorporate more complex magnetic field geometries, time-evolution and dynamical feedback in supergranulation models.

5.3 Large-scale instabilities and collective interactions

Besides thermal convection scenarios, a few other theoretical arguments have been put forward to explain the origin of the solar supergranulation. These ideas are all based on the possible collective effects of small-scale structures such as granules, which might lead to a large-scale instability injecting energy into the supergranulation range of scales.

5.3.1 Rip currents and large-scale instabilities

The first work along this line of thought was published by Cloutman (1979). He proposed to explain the origin of supergranulation using the physical picture of rip currents on the beaches of oceans: the repeated breaking of waves on beaches induces currents (rip currents) flowing parallel to the coast line. On the Sun, he identified breakers with the rising flows of granules breaking into the stably stratified upper photosphere.

The rip current model provides an illustration of the suggestion of Rieutord *et al.* (2000) that the collective interaction of solar granules may give rise to a large-scale instability driving supergranulation flows. The idea finds its root in theoretical work on energy localisation processes in nonlinear lattices (Dauxois and Peyrard, 1993) and large-scale instabilities (“negative eddy viscosity instabilities”) of periodic flows, such as the Kolmogorov flow (Meshalkin and Sinai, 1961; Sivashinsky and Yakhot, 1985) or the decorated hexagonal flow (Gama *et al.*, 1994). Asymptotic theory on simple prescribed vortical flows can be performed under the assumption of scale separation (Dubrulle and Frisch, 1991) between the basic periodic flow and the large-scale instability mode. In such theories, the sign and amplitudes of the turbulent viscosities is found to be a function of the Reynolds number. For instance, an asymptotic theory based on a large aspect ratio expansion was developed by Newell *et al.* (1990) for thermal convection. In this problem, large-scale instabilities take on the form of a slow, long-wavelength modulation of convection roll patterns. Their evolution is governed by a phase diffusion equation with tensorial viscosity. In the case of negative effective parallel diffusion (with respect to the rolls orientation), the Eckhaus instability sets in, while the zigzag instability is preferred in the case of negative effective perpendicular diffusion.

5.3.2 Plume interactions

Another way of explaining the origin of supergranulation assumes that the pattern results from the collective interaction of plumes. The word plume usually refers to buoyantly driven rising or

sinking flows. Plumes can be either laminar or turbulent, however the turbulent ones have by far received most of the attention because of their numerous applications (see [Turner, 1986](#)).

The first numerical simulations of compressible convection at high enough Reynolds numbers (e.g., [Stein and Nordlund, 1989a](#); [Rast and Toomre, 1993](#)) quite clearly showed the importance of vigorous sinking plumes. These results prompted [Rieutord and Zahn \(1995\)](#) to study in some details the fate of these downdrafts. Unlike the downflows computed in early simulations, solar plumes are turbulent structures, which entrain the surrounding fluid (see [Figure 1](#)). As [Rieutord and Zahn \(1995\)](#) pointed it out, the mutual entrainment and merging of these plumes naturally leads to an increase of the horizontal scale as one proceeds deeper.

In this context, toy models have been elaborated to investigate the properties of “ n -body” dynamical advection-interactions between plumes. For instance, [Rast \(2003b\)](#) developed a model in which a two-dimensional flow described by a collection of individual divergent horizontal flows (“fountains”) mimicking granules is evolved under a simple set of rules governing the merging of individual elements into larger fountains and their repulsion⁸. For some parameters typical of the solar granulation (individual velocities and radius of the fountains notably), he argued that the clustering scales of the flow after a long evolution of the system resembled that of mesogranulation and supergranulation. A similar model incorporating simplified magnetic field dynamics was designed by [Crouch *et al.* \(2007\)](#). They observed some magnetic field organisation and polarity enhancement at scales similar to that of supergranulation in the course of the evolution of the model. The main caveat of these toy models is of course that they do not rely on the exact dynamical physical equations.

The previous concepts and models are appealing but theoretical and numerical support has been lacking so far to weigh their relevance to the supergranulation problem. In particular, analytical developments for fluid problems have been restricted to low Reynolds numbers and very simple analytical flow models. It is unclear if and how some quantitative progress can be made along these lines. Future high-resolution numerical simulations may offer some insight into the nonlinear dynamics at work at supergranulation scales but, as will be shown in [Section 6](#), they have not yet given us any indication that large-scale instabilities or nonlinear granulation dynamics can generate a supergranulation flow. In particular, all hydrodynamic simulations so far tend to show that plume merging is a self-similar process that does not naturally produce a flow at well-defined scale that could be identified with supergranulation.

5.4 Conclusions

In the previous paragraphs, we have reviewed the current state of affairs on the theoretical understanding of supergranulation. As cautioned already in the introduction, a breadth of simple models and ideas has been suggested over the years, but the theoretical landscape is extremely fuzzy. A shared property of all models is the looseness of the approximations on which they rely (e.g., linear theory with turbulent viscosity parametrisation, or hand-waving physical arguments on the nature of dynamical interactions between granules and their potential large-scale instabilities). Consequently, completely distinct theoretical arguments can easily be tuned to produce results that are all broadly consistent with observations. This degeneracy makes it impossible to discriminate between the various scenarios.

This issue is of course not specific to the supergranulation problem. The theoretical approach to the global solar dynamo, for instance, is more or less affected by the same syndrome. Escaping this difficult situation probably requires a significant improvement of the numerical modelling of supergranulation-scale convection. The status of this specific field is reviewed in detail in the next section.

⁸ Note that a previous work of [Simon *et al.* \(1991\)](#) already used a purely kinematic model to model mesogranular flows and exploding granules.

6 Numerical Modelling

Our understanding of turbulent convection in general and turbulent convection at the solar surface in particular has improved significantly with the advent of large-scale computing resources. As far as supergranulation is concerned, even though numerical modelling has been and is still confronted with several major computing limitations, it is now on the verge of making very interesting progress towards discriminating between various physical scenarios and ideas such as those presented in Section 5. In this section, we review the evolution of numerical simulations of solar surface convection over the last thirty years and how they have helped us make progress on the specific problem of supergranulation. We notably discuss the advantages and limitations of the various types of numerical models used to study solar surface convection, in order to identify what numerical simulations have really told us (or not told us) on the problem of supergranulation and to provide the reader with a (hopefully) clear understanding of the current important modelling issues.

The section starts with two introductory paragraphs on the numerical simulation of turbulent thermal convection in the Rayleigh–Bénard framework (Section 6.1) and in the solar context (Section 6.2). We then recall the main results obtained from granulation-scale simulations (6.3), before describing in detail the history and current status of “large-scale” hydrodynamic and MHD simulations (6.4) aiming at understanding the dynamics at scales comparable to that of supergranulation.

6.1 Numerical simulations of turbulent Rayleigh–Bénard convection

Even if the hydrodynamic non-rotating Rayleigh–Bénard problem (presented in Section 5.1) is much simpler than the solar convection problem, its numerical modelling in highly nonlinear regimes still represents a major challenge of nowadays fluid dynamics. It is therefore worth recalling the main issues and numerical requirements for this problem before discussing the solar case.

6.1.1 Rayleigh–Bénard and Navier–Stokes

In the non-rotating hydrodynamic case ($Ta = Q = 0$, no induction), the Boussinesq equations (2) are very similar to the forced Navier–Stokes equations, except that the forcing term is not an external body force but is determined self-consistently from the time-evolution of the temperature fluctuations. Based on both experimental and numerical evidence at order one Prandtl number, several authors (Rincon, 2006; Lohse and Xia, 2010) have argued that the basic phenomenology of Rayleigh–Bénard turbulence at scales below the typical Bolgiano injection scale (see Section 2.2) should be similar to that of Navier–Stokes turbulence in the inertial-range (i.e., Kolmogorov turbulence plus possible intermittency corrections). Hence, at a very good first approximation, the numerical issues and requirements to simulate the Rayleigh–Bénard problem at very high Rayleigh numbers are the same as those pertaining to the simulation of forced Navier–Stokes turbulence at high Reynolds numbers.

6.1.2 State-of-the-art modelling

The performances of turbulent convection simulations are often measured by the ratio of the imposed Rayleigh number to its critical value Ra/Ra_{crit} as the larger this quantity is, the more turbulent is the flow (the larger the Reynolds number). The highest values attained so far in simulations of the Rayleigh–Bénard problem are approximately $Ra/Ra_{\text{crit}} \sim 10^{11}$ (Verzicco and Camussi, 2003; Amati *et al.*, 2005), but most “routine” simulations of the problem are in the much softer range $Ra/Ra_{\text{crit}} \sim 10^5 - 10^7$. Achieving highly turbulent regimes first requires using high-order numerical methods such as spectral methods (Camuto *et al.*, 2006), which provide very good

numerical accuracy and constitute an ideal tool to resolve all the dynamics from the injection to the dissipation range of incompressible turbulence. The second price to pay is to use very high spatial resolutions to discretize the problem (currently, high resolutions mean $\sim 512^3$ to $\sim 1000^3$) on a non-uniform grid (to resolve boundary layers). This in turn imposes correspondingly small time steps, so the integration times of very high Rayleigh number convection are limited to a few turbulent turnover times, possibly not enough to resolve some of the long-time, large-scale, mean-field dynamics.

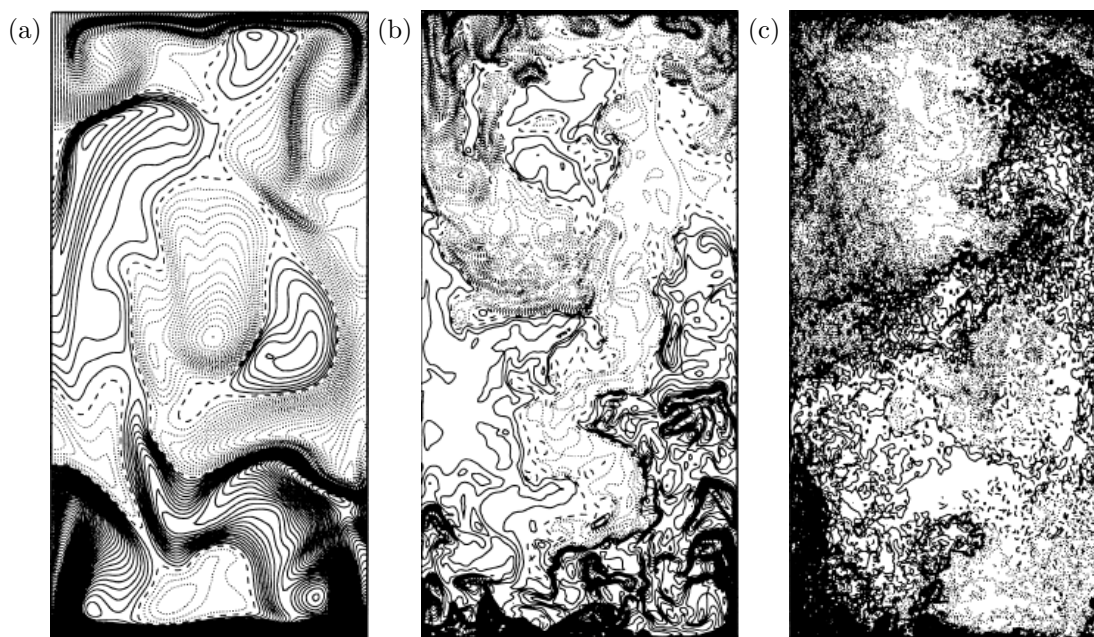


Figure 10: Snapshots of temperature fluctuations in a vertical plane, from numerical simulations of Rayleigh–Bénard convection in a slender cylindrical cell at $Pr = 0.7$ and Rayleigh-numbers (a) 2×10^7 , (b) 2×10^9 , and (c) 2×10^{11} (from Verzicco and Camussi, 2003).

Moreover, simulations at very high Rayleigh numbers are restricted to fairly low aspect ratio domains (the ratio between the horizontal and vertical extents of the domain), typically $1/2$ or 1 , so they do not as yet allow to probe the very large-scale dynamics of turbulent convection. Finally, they are limited to Prandtl numbers of order unity, so it is currently not possible to investigate the effect of scale separation between the various dissipation scales of the problem while preserving the highly nonlinear character of the simulations. An example of such a high-performance simulation is provided by Figure 10, which shows temperature snapshots in vertical planes of simulations of turbulent Rayleigh–Bénard convection in a slender cylindrical cell at $Pr = 0.7$. Two very important features can be seen on the figure:

- there is a very marked evolution of the pattern from moderate to very large Ra , showing that an asymptotic large Ra behaviour has not yet been attained in spite of the very high numerical resolution used,
- one notices the emergence of two half-cell circulations in the highest Ra regime, revealing that some large-scale coherent dynamics naturally emerges from the small-scale turbulent disorder as one goes to very strongly nonlinear regimes. How this kind of dynamics changes as a larger aspect ratio is allowed for is not understood at the moment. This point will be discussed in more detail in Section 6.4.3 in the context of supergranulation-scale simulations.

Hence, we conclude this paragraph by emphasising that even the most advanced numerical simulations to date of the simplest turbulent convection problem at hand do not yet allow to study fully comprehensively the high Rayleigh number asymptotic behaviour of convection and the large-scale dynamical evolution of the system.

6.2 Numerical simulations of solar convection

After this presentation of the state-of-the-art numerical modelling of Rayleigh–Bénard convection, we now come back to the more specific problem of the numerical simulation of solar convection. The first direct numerical simulations of astrophysical convection date back from the 1970s. In the solar context, an early noteworthy study is the one of [Graham \(1975\)](#) who revealed an asymmetry of up and downflows in two-dimensional simulations of compressible convection in a stratified medium (i.e., not in the Boussinesq approximation), as observed for granulation. The Rayleigh number was just ten times supercritical in this simulation. A similar numerical model was devised by [Chan *et al.* \(1982\)](#). [Massaquer and Zahn \(1980\)](#) used a truncated numerical model of convection to study this physical effect specific to compressible convection, which is now referred to as buoyancy braking. These early contributions, however, did not provide a fully realistic framework to understand the complexity of solar surface convection. The first attempts to incorporate some specificities of surface convection in stellar environments, like radiative transfer, are due to [Nordlund \(1982\)](#). Since then, astrophysical convection simulations have split into two families that define the main trends in the field nowadays.

A short remark is in order regarding the following “classification”. Any numerical simulation of solar convection corresponds to a specific physical set-up tailored for the purpose of studying specific physical processes. In general, a given set-up resembles one of the two families of models described below but any mix between the two is obviously possible in practice.

6.2.1 Idealised simulations

The first family of numerical models is in the spirit of the original experiments by [Graham \(1975\)](#) and can be referred to as “idealised” simulations. These simulations rely on simple models of stratified atmospheres such as polytropes and implement the standard incompressible or compressible fluid dynamics equations, including viscosity, thermal, and magnetic diffusivities in a bounded domain with idealised boundary conditions. For this purpose, they often make use of numerical spectral methods (see Section 6.1 above), which are extremely well-suited for the numerical simulation of incompressible homogeneous turbulence ([Vincent and Meneguzzi, 1991](#); [Ishihara *et al.*, 2009](#)) but face some important problems when it comes to the simulation of stratified compressible flows. For instance, they cannot capture shocks easily and one is confronted with the problem of projecting the inhomogeneous stratified direction on a spectral basis. For this reason, the vertical direction is often treated using high-order finite differences or compact finite differences with spectral-like precision (e.g., [Rincon *et al.*, 2005](#)). A spectral decomposition onto Chebyshev polynomials can nevertheless be used in this context for largely subsonic flows or if the equations are solved in the anelastic approximation ([Clune *et al.*, 1999](#)).

6.2.2 Realistic simulations

The second family of models, which started to flourish in the solar and stellar communities after the pioneering contribution of [Nordlund \(1982\)](#), is now commonly referred to as “realistic” numerical simulations. These simulations attempt to take into account simultaneously the flow dynamics and other important physical processes of particular importance in the solar context, most notably radiative transfer, solar-like density stratifications, and realistic equations of state including Helium and Hydrogen ionizations. Unlike idealised simulations, they usually ignore the physical plasma

viscosity and rely on numerical viscosity to avoid numerical blow-up. These features, coupled to the use of handmade boundary conditions, makes this kind of simulations more versatile and allows to simulate compressible stratified flows at the solar surface in a more straightforward way. Indeed, as a result of including the physics of radiative transfer, the output of these simulations can be directly compared with solar observations.

There is of course a price to pay for this versatility. The first is enhanced grid dissipation (e.g., numerical viscosity): at equal resolution, the turbulent dynamics is usually much more vigorous in the idealised set-ups. This might not be crucial in some specific cases but, as has been already briefly mentioned in Section 6.1, probing the large-scale dynamics may require achieving extremely nonlinear regimes. The second is that “realistic simulations” could be in the wrong regime, simply because they do not take into account rigorously the disparity of time and length scales of dissipative processes. This remark particularly applies to the simulation of solar MHD problems. In recent years, direct numerical simulations have shown that the dependence of the statistical properties of various turbulent MHD flows on dissipative processes can be particularly important. This has been shown for instance in the context of the fluctuation dynamo (Schekochihin *et al.*, 2007), which might be responsible for the generation of internetwork fields (Vögler and Schüssler, 2007; Pietarila Graham *et al.*, 2009), and for the problem of angular momentum transport mediated by magneto-rotational turbulence in accretion discs (Lesur and Longaretti, 2007; Fromang *et al.*, 2007). This point will be discussed further in Section 8.2 in the context of solar convection.

6.2.3 Current limitations

Finally, it is perhaps worth recalling that the finite capacities of computers make it completely impossible for any type of simulation, even today, to approach flow regimes characteristic of the solar surface and to span all the range of time and spatial scales involved in this highly nonlinear problem. It should therefore be constantly kept in mind when studying the results of numerical simulations of solar convection (and more generally of astrophysical turbulence) that neither of these types of models is perfect and that we are not actually “simulating the Sun” but a fairly quiet toy model of it. In particular, all simulations of solar convection to date are much less nonlinear than the Rayleigh–Bénard simulations presented in Section 6.1, which as we have seen are not themselves asymptotic in several respects either.

6.3 Simulations at granulation scales

6.3.1 Stratified convection and flows

The first realistic three-dimensional simulation of solar surface convection by Nordlund (1982) mentioned earlier was followed by an improved version at higher resolution (Stein and Nordlund, 1989b). These studies were primarily devoted to studying and understanding the thermal structure and observational properties of granulation. Amongst other observations, Stein and Nordlund (1989b) noticed that convective plumes in a stratified atmosphere merged into larger plumes at larger depth, producing increasingly large convective patterns deeper and deeper. Their results also demonstrated the influence of stratification on the horizontal extent of granules and on the typical plasma velocity within granules. All these results were later confirmed by Stein and Nordlund (1998) thanks to much higher resolution simulations.

On the front of idealised simulations, Chan *et al.* (1982) and Hurlburt *et al.* (1984), using 2D numerical simulations of stratified convection at Rayleigh numbers up to 1000 times supercritical and Chan and Sofia (1989, 1996) and Cattaneo *et al.* (1991), using 3D idealised simulations in strongly stratified atmospheres, confirmed and refined the results of Graham (1975) and Massaguer and Zahn (1980). All the results of the early idealised simulations (some of them being fairly strongly stratified) are qualitatively in line with those of Stein and Nordlund (1989b) as far as

the deep, large-scale dynamics is concerned. This suggests that a detailed modelling of physical processes such as radiative transfer is not required to understand the turbulent dynamics and scale-interactions in solar convection⁹. On the other hand, the surface features of granulation-scale convection are much better understood with realistic simulations, which are precisely tailored to this specific purpose.

Readers interested in the particular problem of granulation-scale convection will find much more detailed information in the recent review by Nordlund *et al.* (2009). The important point to remember from this paragraph, as far as the topic of this review is concerned, is that both types of simulations predict strong asymmetries between up and downflows and the formation of larger-scale convection at greater depth as a result of the imposed density stratification. Such results provide a numerical confirmation of the qualitative arguments put forward in the discussion of Section 2.2 on the scales of solar convection.

6.3.2 Main successes and caveats

Granulation is currently the best understood observational feature of solar convection, thanks mostly to the increasingly accurate simulations described above. Realistic simulations have in particular been extremely good at capturing the surface physics of radiative transfer and the thermodynamics (Stein and Nordlund, 1998), which is crucial to understand the strongly thermally diffusive nature of granules (as shown in Section 2.2, the thermal dissipation scale is similar to the granulation scale in the photosphere). The mild Péclet number regime typical of the solar granules is in this respect very helpful to numericists, as it allows for a proper numerical resolution of heat transfer processes at the granular scale.

However, the simulated granules drastically differ from the solar ones with respect to at least one important parameter, namely the Reynolds number. Because of the limited number of available grid points, the Reynolds number of a simulated granule is presently a few hundreds, while real granules have Reynolds numbers larger than 10^{10} . This does not seem to affect the thermal physics too much: the remarkable fit of simulated and observed absorption lines (Asplund *et al.*, 2009) demonstrates that this physics is indeed correctly captured. But research on fluid turbulence and Rayleigh–Bénard convection, as shown in Section 6.1, tells us that mild Reynolds number regimes are definitely not asymptotic with respect to the dynamics, most importantly the large-scale parts of it.

Overall, it therefore remains to be demonstrated whether or not large-scale simulations (reviewed in the next paragraph) based on the current generation of numerical models of granulation incorporate enough nonlinearity to make it possible to probe the actual dynamics at supergranulation scales.

6.4 Large-scale simulations

6.4.1 Introduction

All simulations of the 1980s and 1990s could only address either granulation-scale dynamical issues or global convection dynamics (giant cells and larger). Only in the last ten years did it become possible to start probing the dynamics at scales larger than individual granules. It is interesting in retrospect to recall (as a short anecdotal digression) the following optimistic citation, extracted

⁹ Stratified simulations with a bottom wall tend to exhibit more small-scale turbulent activity in deep layers than their open-wall counterparts, though (see Figure 12). This behaviour may be related to the enhanced shear and recirculations generated at the bottom wall, or with the fact that most of these simulations use a constant dynamical viscosity which, combined with density stratification, enhances the local Reynolds number as one moves deeper down.

from a paper by Nordlund (1985): “There is a need for numerical simulations at the scale of supergranulation [...] This is probably feasible with present day computers and numerical methods.”

Various objectives motivate large-scale simulations of stellar convection. They serve to understand the global deep dynamics of spherical stellar envelopes, such as differential rotation, meridional circulation, giant cells, angular momentum transport (see Miesch (2005) for an exhaustive review), to characterise the distribution and generation of global-scale stellar magnetic fields in the presence of turbulent convection, but are also developed to study the dynamics at intermediate scales, such as sunspot scales (Heinemann *et al.*, 2007; Rempel *et al.*, 2009) or supergranules.

In our view, one of the most important limitations that numericists face today when it comes to simulating the Sun's supergranulation is the following. Two different geometrical approaches are possible: local Cartesian simulations (taking a small patch of the solar surface) and global simulations in a spherical shell. In the local approach, the box size of the largest simulations to date (i.e., the *largest* scale of the simulation) is roughly comparable to the scale of supergranulation. Furthermore, such a configuration can only be achieved if the resolution of the turbulent processes at vigorous convective scales comparable to or smaller than the scale of granulation is sacrificed. Note also that the dynamics at supergranulation scales is tightly constrained by (periodic) lateral boundary conditions in this kind of set-up. In the global spherical approach, in contrast, the *smallest* scales of the most recent simulations are comparable to the scale of supergranulation, which means that the “supergranulation” dynamics is strongly dissipative, in sharp contrast with the solar case (as mentioned in Section 4.2, the turbulent spectrum of solar surface convection reveals that supergranulation is located at the large-scale edge of the injection range of turbulence, not in the dissipation range). In this second approach, the vigorous dynamics at granulation scales can simply not be included at the moment.

To summarise, the specific limitations of each type of simulations do not yet allow us to investigate the nonlinear dynamics and transfers of energy taking place at supergranulation scales fully consistently. These simulations nevertheless already provide us with useful informations on the large-scale dynamics of convection and magnetic dynamics in the quiet Sun.

6.4.2 Global spherical simulations

Global spherical simulations of turbulent convection appeared thirty years ago. Gilman (1975) devised the first numerical model of 2D Boussinesq convection in a spherical shell and used it to study the influence of rotation on convection, the problem of large-scale circulations in the solar convection zone and that of the interactions between supergranulation and rotation (e.g., Gilman and Foukal, 1979). Gilman and Glatzmaier (1981) and Glatzmaier (1984, 1985) extended this work to the anelastic approximation, while Valdetaro and Meneguzzi (1991) devised a fully compressible model. As a result of computer limitations at that time, these simulations were restricted to fairly laminar regimes and very large solar scales. Most simulations in spherical geometry use the expansions of the fields on spherical harmonics up to a given resolution L_{\max} (the ℓ order of the smallest scale spherical harmonic). In those terms, the resolution of the early simulations was approximately $L_{\max} = 32$. In solar units, this means that the smallest resolved horizontal scale in these simulations is

$$\lambda = \frac{2\pi R_{\odot}}{L_{\max}} \simeq 130 \text{ Mm},$$

much larger than the scale of supergranulation (36 Mm, corresponding to the spherical harmonic $\ell = 120$, see Section 4.2).

In recent years, one of the most popular codes for high-resolution three-dimensional spherical simulations of stellar convection has been the ASH (Anelastic Spherical Harmonics) code (Clune *et al.*, 1999). An interesting attempt to study supergranulation with ASH is that by DeRosa (2001),

DeRosa and Toomre (2001) and DeRosa *et al.* (2002), who carried out “idealised” three-dimensional hydrodynamic simulations in thin spherical shells with a horizontal resolution of $L_{\max} = 340$, corresponding to a smallest resolved horizontal scale of 13 Mm. Their simulations exhibit structures at scales comparable to that of supergranulation (see Figure 11). However, the physical origin of these structures is rather uncertain because the grid scale (13 Mm) is not small compared to the supergranulation scale. It is also difficult to spot why supergranulation scales would play a special role (except for being in the dissipative range) in their set-up. Finally, as mentioned earlier, the granulation dynamics, which dominates the power spectrum of solar surface convection, is not included in the model. The conclusions of this precise set of simulations are therefore unfortunately limited, but the next generations of experiments of this kind may enable significant progress on the problem.

New simulations of solar-like convective shells by Miesch *et al.* (2008) at higher spherical harmonics resolution ($L_{\max} = 682$) have recently revealed the presence of intense cyclonic downdrafts at scales comparable to those of giant cells, a very likely reminiscence of the interactions between large-scale convection and rotation described in Section 4.5. Looking at the spectrum of these simulations though, it is clear that supergranulation scales are still located in the dissipative range even at such high resolutions. This raises the concern that global simulations may not provide the most straightforward route to understand supergranulation-scale dynamics.

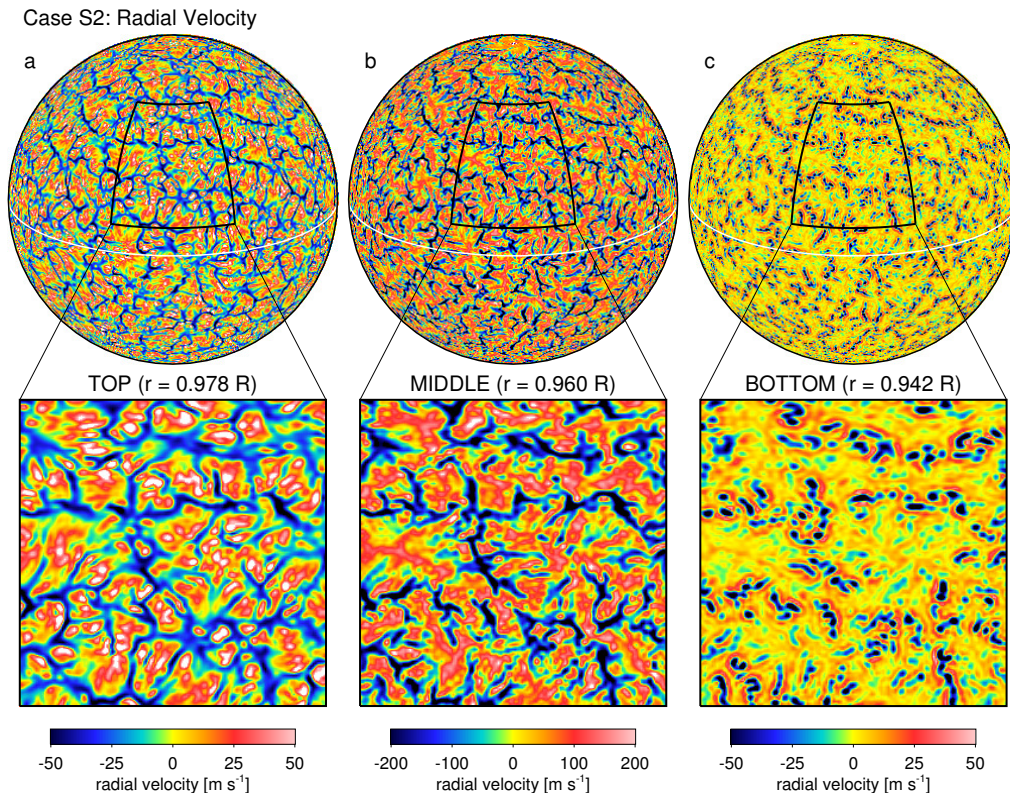


Figure 11: Radial velocity snapshots at various depths in global simulations of convection in shallow spherical shells, down to supergranulation scales (from DeRosa *et al.*, 2002).

6.4.3 Local hydrodynamic Cartesian simulations: mesoscale dynamics

The problem can also be approached by the other end, i.e., by devising models in which supergranulation scales correspond to the largest scales of the numerical domain and are consequently much larger than the actual resolution of the simulations. The general philosophy of these models is to attempt to solve for the entire nonlinear dynamics from subgranulation scales (typically 10 to 100 km with present day computers) to supergranulation scales. Computing limitations then impose that we sacrifice the global physics at scales much larger than supergranulation. Since the subgranulation to supergranulation range is expected to be fairly insensitive to curvature effects, a reasonable assumption is to perform such simulations in Cartesian geometry. As mentioned earlier, this kind of set-up is also currently subject to resolution issues: if a fair amount of the available numerical resolution is devoted to the description of turbulent dynamics in the granulation range, then the dynamics at supergranulation scales is necessarily confined to the largest scales of the numerical domain and necessarily feels the artificial lateral boundary conditions (usually taken periodic).

Proceeding along these lines, Cattaneo *et al.* (2001) attempted to study the dynamics up to “mesoscales” (to be defined below). They performed three-dimensional idealised turbulent convection simulations in the Boussinesq approximation with an aspect ratio (the ratio between the largest horizontal and vertical scales in the numerical domain) up to 20 for a Rayleigh number 5×10^5 (roughly 1000 times supercritical). Note that their simulations are actually dynamo ones (see Section 6.4.6 below) but for the purpose of the discussion, we only discuss the hydrodynamic aspects of their results in this paragraph. Cattaneo *et al.* (2001) did not find any trace of a supergranulation-like pattern in their simulations but reported the existence of a slowly evolving granule-advecting velocity field at a scale five times larger than the scale of granulation¹⁰, corresponding to a “mesogranulation”. The typical correlation time at this mesoscale is much longer than the typical turbulent turnover time at granulation scales and the energy at this scale is also much larger than that contained in the superficial granulation-scale motions. The authors suggested that the process might result from dynamical interactions at smaller scales, in the spirit of the theoretical concepts presented in Section 5.3. They also pointed out that the physical process responsible for the formation of these scales does not require that density stratification be taken into account (since it is not included in the Boussinesq approximation). The formation of mesoscale structures in large aspect ratio simulations of turbulent Boussinesq convection was subsequently confirmed by several studies (Hartlep *et al.*, 2003; Parodi *et al.*, 2004; von Hardenberg *et al.*, 2008).

The next three-dimensional experiment in the series was done by Rieutord *et al.* (2002). They performed a “realistic” hydrodynamic simulation of turbulent convection at aspect ratio 10. They did observe a growth of the typical size of convective structures with depth but did not find any evidence for the formation of dynamical scales larger than that of granulation at the surface. They pointed out that the turbulence was not very vigorous in this kind of simulations, which might explain why no supergranulation-scale dynamics is present. Another possibility is that the numerical domain was not wide or deep enough to accommodate this kind of large-scale dynamics. An important point to note is that their simulation, unlike that of Cattaneo *et al.* (2001), was designed with an open bottom boundary condition and a strongly stratified atmosphere¹¹.

¹⁰ Idealised simulations evolve nondimensional equations such as (2), so their results are not given in solar units. However, even in this kind of idealised simulations, granulation-like cells clearly appear in a thin thermal boundary layer at the upper boundary (Figure 12 provides horizontal temperature maps extracted from a similar simulation exhibiting this phenomenon). This simple observation usually serves to “calibrate” the size of the dynamical structures present in the simulations with respect to the size of granules.

¹¹ Amongst the significant differences between idealised simulations and the realistic ones, Nordlund *et al.* (1994) pointed out that using “wall-type” boundary conditions, as is standard in idealised simulations, can alter significantly the shape of the convective pattern. Indeed, this type of boundary conditions allows for a return flow after plumes smash down onto the bottom wall, which of course does not occur in the Sun until the very deep layers of the solar convection zone are reached by descending plumes. Nordlund *et al.* (1994) suggested to use stronger stratifications

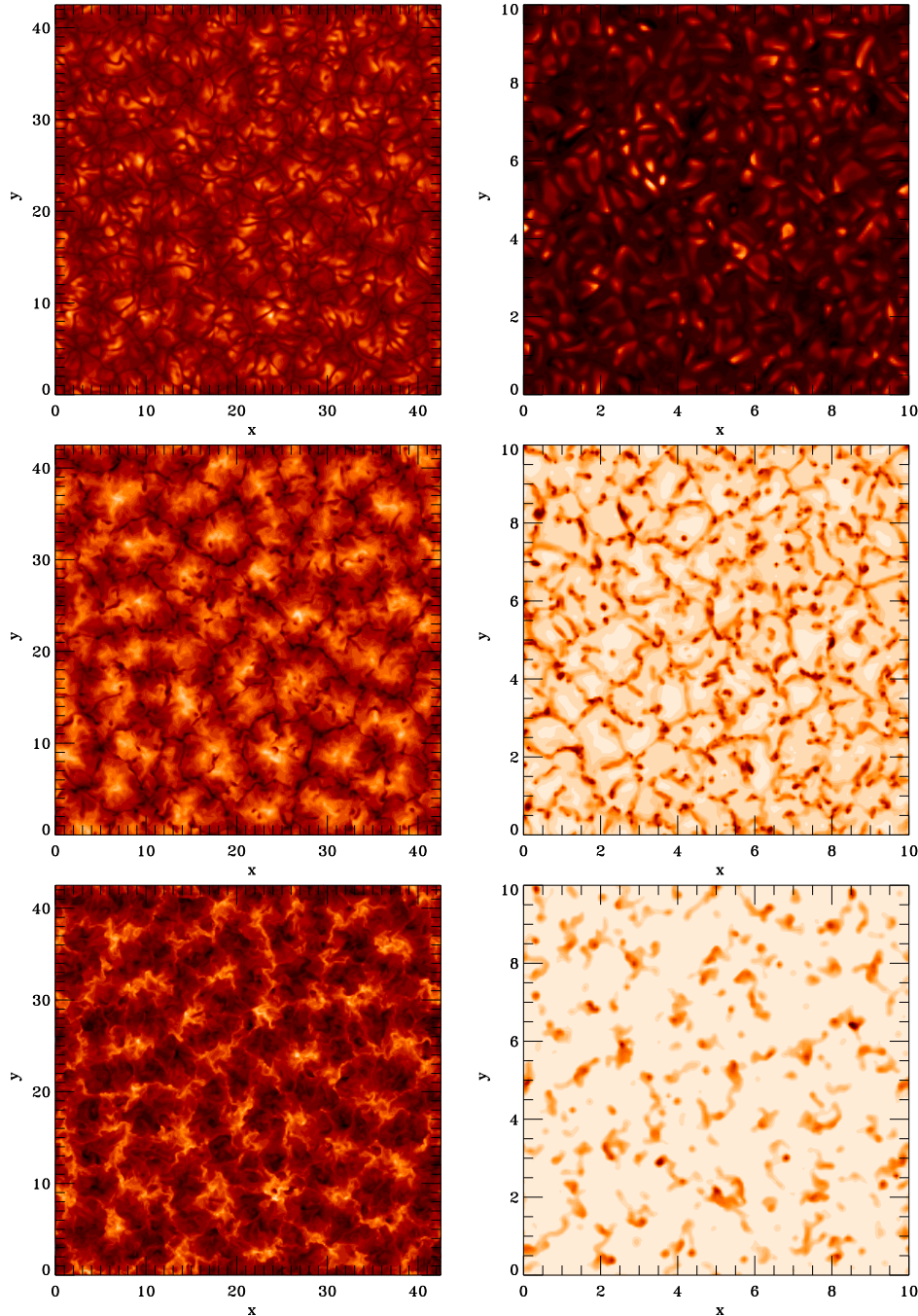


Figure 12: Comparison between horizontal temperature maps in an idealised simulation of large-scale compressible convection in a stratified polytropic atmosphere (left, aspect ratio 42, see Rincon *et al.*, 2005 for details) and horizontal temperature maps in a realistic simulation of large-scale solar-like convection (right, aspect ratio 10, see Rieutord *et al.*, 2002 for details). *Top:* $z = 0.99 d$ (left) and at optical depth $\tau = 1$ (right), respectively (surface). *Middle:* half-depth of the numerical domain. *Bottom:* bottom of the numerical domain. The emergence of the granulation pattern in the surface layers is clearly visible in both types of simulations, on top of a larger-scale mesoscale dynamics extending down to deeper layers.

Motivated by these various results, Rincon *et al.* (2005) extended three-dimensional local hydrodynamic simulations to a very wide aspect ratio ~ 42 , using a fully compressible polytropic set-up with modest density stratification, Rayleigh numbers comparable to those of Cattaneo *et al.* (2001) and wall-type boundary conditions at the top and bottom of the numerical domain. They did not find any trace of a “supergranulation bump” in the large-scale end of the velocity power spectrum either, even though their set-up allowed for such scales, but confirmed the existence of long-lived and very powerful mesoscale flows with a horizontal scale also five times larger than that of granules in idealised simulations. The temperature pattern associated with these flows is clearly visible on the left side of Figure 12. They further showed that the horizontal scale of this flow increases slowly throughout the simulation, on timescales comparable or larger than the vertical thermal diffusion timescale. This slow evolution raises the issue of the thermal relaxation of all large-scale simulations to date.

Another result of the study by Rincon *et al.* (2005) is that, from the strict scale-by-scale energetics point of view, these flows are effectively driven by thermal buoyancy. During the early linear regime, basic linear stability tells us (rightly) that the growth of the convective eigenmode takes place at scales comparable to the vertical scale of the system. But, once in the nonlinear regime, the injection of energy continuously shifts to larger horizontal scales than in the linear regime. This result therefore suggests that the mesoscale flow is not directly driven by nonlinear interactions amongst smaller scales, but that nonlinearity plays a central role in the process of scale selection, possibly by controlling the strength of turbulent transport processes acting on the large-scale dynamics.

Mesoscale circulations very likely correspond to the thermal winds observed in all laboratory experiments on convection (e.g., Krishnamurti and Howard, 1981; Sano *et al.*, 1989; Niemela *et al.*, 2001; Xi *et al.*, 2004, and references therein). The phenomenology of this process has been shown to be very subtle, as several authors argue that the flow results from a nonlinear clustering process (Xi *et al.*, 2004; Parodi *et al.*, 2004) of distinct buoyant plumes. Whether or not this kind of circulations exist in the Sun and what would be their typical scale in the solar context remains an open question.

6.4.4 State-of-the-art local hydrodynamic Cartesian simulations

The most recent numerical efforts to date, as far as local hydrodynamic Cartesian simulations are concerned, are those by Ustyugov (2008) and Stein *et al.* (2009a). The latter ran a realistic simulation in a 96 Mm wide and 20 Mm deep three-dimensional numerical box (see also Benson *et al.*, 2006 and Georgobiani *et al.*, 2007 for detailed reports on simulations of half this size) and found a monotonic smooth increase of the size of convective structures with depth, in agreement with the results presented in Section 6.3, and no or very little power enhancement at supergranulation scales in the surface power spectrum. They subsequently argued, similarly to Spruit *et al.* (1990), that there was no reason why a particular scale should pop-up in the continuum of scales present in the simulation (see Nordlund *et al.*, 2009 and Georgobiani *et al.*, 2007 for representations of the power spectra of the simulations). Ustyugov (2008) performed a similar experiment in a 60 Mm wide and 20 Mm deep three-dimensional box, using a subgrid scale model to emulate the unresolved small-scale dynamics. He reported similar results, namely a gradual monotonic increase of the convection scale with depth.

It is worth pointing out that the ionisation states of Helium and Hydrogen are part of the model of Stein *et al.* (2009a), which allowed them to test for the first time the first theoretical explanation for the origin of the supergranulation (Simon and Leighton, 1964) presented in Section 5.2.

in simulations in closed domains to attenuate this effect. Finally, upflows seem to play a much more important role in the process of vertical heat transport in idealised simulations than in realistic ones (Stein and Nordlund, 1994). This may have some important consequences regarding the most energetic scales of the flows, which correspond to the mesoscales in idealised simulations.

Considering the gradual large-scale decrease of energy in the power spectrum of their simulations, one may conclude that the existence of recombination layers of ionised elements does not have any noticeable impact on the surface flows. This is probably the most important conclusion relative to the supergranulation puzzle that can be drawn from these simulations.

6.4.5 Local hydrodynamic Cartesian simulations with rotation

Only a few local simulations have addressed the issue of the interactions between supergranulation and rotation. Hathaway (1982) made an early attempt at simulating this problem in the Boussinesq approximation, using a numerical box elongated in the horizontal direction (to the best of our knowledge, this is the first local numerical simulation of thermal convection at large aspect ratio, $A = 10$). He made the interesting observation that mean flows are generated in the presence of a tilted rotation axis and generate a subsurface shear layer (differential rotation). Since then, this kind of effects has been studied in a lot of details with local simulations at much higher numerical resolution (e.g., Brummell *et al.*, 1996, 1998; Käpylä *et al.*, 2004; Brandenburg, 2007). The focus of these papers is not specifically on the supergranulation problem but Brandenburg (2007) suggested that the travelling-wave properties of supergranulation could be due to the radial subsurface shear (see also the paper by Green and Kosovichev, 2006 mentioned in Section 5). In a more dedicated study of this kind, Egorov *et al.* (2004) reported a good agreement between the divergence-vorticity correlations obtained from simulations of rotating convection and those inferred from observations of the supergranulation flow field (discussed in Section 4.5).

6.4.6 Local MHD Cartesian simulations

Several local simulations have been devoted to the study of MHD convection at scales larger than granulation and notably to the process of network formation. As they are the most relevant for the problem of supergranulation-scale MHD, we restrict attention to three-dimensional simulations performed over the last ten years. An important distinction is in order here between two types of simulations. The first kind includes magnetoconvection simulations in an imposed mean magnetic field or with a magnetic flux introduced “by hand” at the beginning of the run. The second kind are turbulent dynamo simulations, in which the magnetic field is spontaneously generated by the turbulent convection flow starting from an infinitesimal seed field. These two types of simulations may produce qualitatively different results, as the dynamical feedback and induction terms in the equations behave in a different way for these various configurations.

One of the first of these “large-scale” MHD numerical experiments was carried out by Tao *et al.* (1998). They performed idealised simulations of strongly stratified magnetoconvection in strong imposed magnetic fields (large Q) for various aspect ratios up to $A = 8$. In the simulations with largest aspect ratio (equivalently largest horizontal extent in their set-up), they observed that magnetic fields tended to separate from the convective motions (flux separation). Strong-field magnetoconvection simulations are not directly relevant to the formation of the quiet Sun network though, but their phenomenology presents some interesting similarities with umbral dot or dark nuclei formation in sunspots and plage dynamics. Weiss *et al.* (2002) extended this work to much weaker field regimes and found that magnetic flux tended to organise into a network at scales larger than granulation, much like in the quiet Sun. The scale at which this “network” forms in their simulations seems to correspond to that of the mesoscale circulations observed in all idealised simulations (Section 6.4.3).

Large-scale simulations of Boussinesq MHD convection in more turbulent regimes were performed by Cattaneo (1999), Emonet and Cattaneo (2001) and Cattaneo *et al.* (2003). In the absence of a mean field threading the layer (the dynamo set-up mentioned at the beginning of the paragraph), they found that small-scale disordered magnetic fields generated by turbulent dynamo action organise into larger-scale “mesoscale” magnetic structures. In the opposite limit

of a strong mean field, they found that the dominant scales of turbulent convection are tightly constrained and reduced by magnetic tension. On this topic, we also mention the work of [Bushby and Houghton \(2005\)](#), [Bushby *et al.* \(2008\)](#) and [Stein and Nordlund \(2006\)](#), who investigated the formation process of magnetic ribbons and point-like flux concentrations using mesoscale simulations (accommodating for just a few granules). The first group followed the idealised approach of simulations of three-dimensional compressible magnetoconvection in weak field regimes and the second group a realistic approach, starting their simulation with a uniform horizontal magnetic field. Another noteworthy effort towards an improved modelling of MHD convection at scales larger than granulation is by [Vögler and Schüssler \(2007\)](#), who studied the generation and distribution of magnetic fields by the fluctuation dynamo process using realistic numerical simulations at moderate aspect ratio.

The specific problem of supergranulation-scale MHD was only attacked in recent years. [Ustyugov \(2006, 2007, 2009\)](#) performed several realistic magnetoconvection simulations in an imposed 50 G vertical field, the largest of these simulations being for a 20 Mm deep and 60 Mm wide box. He observed the formation of a magnetic network at scales in the meso-supergranulation range, with magnetic elements being either point-like or organised in flux sheets or magnetic ribbons. Some snapshots of his simulations are reproduced in [Figure 13](#).

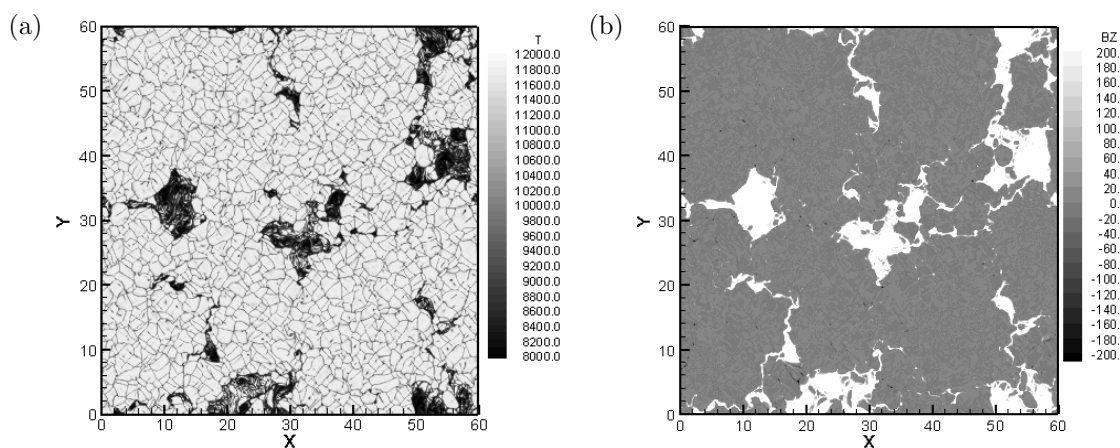


Figure 13: Horizontal maps of (a) temperature and (b) vertical magnetic field fluctuations in the surface layers of local realistic simulations of large-scale MHD convection (from [Ustyugov, 2009](#)).

Another very recent attempt is by [Stein *et al.* \(2009b\)](#), who performed a set of MHD simulations in 20 Mm deep and 48 Mm wide box in which a magnetic field is introduced initially at the bottom of the numerical domain in the form of a uniform horizontal flux. Even though the time extent of their simulations is just comparable with the supergranulation timescale, their results show that the sweeping of magnetic field elements at the boundaries of supergranular-like structures leads to the formation of a magnetic network, very much like in the simulations of [Ustyugov \(2009\)](#).

6.5 Conclusions

The numerical study of supergranulation has become a very active topic in the last decade, as simulations presented in [Section 6.4](#) attest. [Table 1](#) provides a list of the most important numerical efforts dedicated to this problem so far.

The most recent large-scale three-dimensional models represent numerical *tours de force* and are increasingly successful at reproducing observational features of solar surface magnetoconvection

Table 1: Numerical simulations dedicated to the study of mesogranulation to supergranulation scale dynamics. The “Type” entry specifies whether the simulations are idealised (I) Boussinesq (Bouss.), anelastic (Anel.) or polytropic (Poly.) simulations or realistic (R) simulations (Section 6.2). The box size and duration of simulations in Mm and solar hours (sh) or days are given for qualitative comparative purposes only, as these quantities are actual input parameters of the realistic simulations (and of the global simulations by DeRosa *et al.*, 2002) but not of idealised simulations (only the aspect ratio and density stratification are). For local idealised simulations, the size and duration of the simulation in solar units is estimated empirically by setting the horizontal size of the “granules” visible in the upper 10% surface layers of the simulations to 1 Mm, their vertical extent to 150 km (the width of the entropy jump in realistic simulations; see, e.g., Stein and Nordlund, 1998) and the typical turnover time of the mesoscale cells described in Section 6.4.4 to 1 h (see corresponding discussions in Section 6.4.3).

Reference	Type	MHD	Resolution	Box size (Mm ³)	Duration
Cattaneo <i>et al.</i> (2001)	I-Bouss.	Yes	1024 ² × 96	~ 30 × 30 × 1.5	~ 35 sh
DeRosa <i>et al.</i> (2002)	I-Anel.	No	1024 × 512 × 128	4400 × 4400 × 56	80 d
Miesch <i>et al.</i> (2008)	I-Anel.	No	2048 × 1024 × 257	4400 × 4400 × 190	560 d
Rieutord <i>et al.</i> (2002)	R	No	315 ² × 82	30 × 30 × 3.2	7 sh
Rincon <i>et al.</i> (2005)	I-Poly.	No	1024 ² × 82	~ 64 × 64 × 1.5	~ 15 sh
Ustyugov (2008)	R	No	600 ² × 168	60 × 60 × 20	24 sh
Ustyugov (2009)	R	Yes	600 ² × 204	60 × 60 × 20	24 sh
Stein <i>et al.</i> (2009a)	R	No	1000 ² × 500	96 × 96 × 20	64 sh
Stein <i>et al.</i> (2009b)	R	Yes	500 ² × 500	48 × 48 × 20	48 sh

in the granulation to supergranulation range. One of their main achievements has been the test of standard helioseismic diagnostic tools with numerical data sets: the results compare reasonably well with those extracted from real data (e.g., Georgobiani *et al.*, 2007; Couvidat and Birch, 2009). Another important point on the topic of “virtual observations” is that large-scale simulations have helped validate granule-tracking techniques to reconstruct velocity fields at the solar surface (Rieutord *et al.*, 2001).

On the specific problem of the origin of supergranulation, an important result is that the supergranulation scale does not seem to emerge as a particular scale in purely hydrodynamic simulations incorporating the ionisation of Hydrogen and Helium, which tends to disprove the “classical” Simon and Leighton (1964) supergranulation theory. Finally, it is encouraging for the future that the most recent MHD simulations to date (Ustyugov, 2009; Stein *et al.*, 2009b) start to be large enough for meaningful numerical studies of the process of network formation and supergranulation-scale MHD to be possible.

It is fair to say, however, that even the most advanced and impressive numerical efforts to date can only be considered as preliminary with respect to the supergranulation puzzle. As shown in Section 4.2, recent observations indicate that the supergranulation scale is an undeniable feature of the horizontal velocity power spectrum of solar surface convection, whatever method is used to compute the spectrum. This observation has not been reproduced by any numerical simulation so far. The superrotation rate of supergranules is another open question that no simulation can address at the moment. Finally, the interactions between supergranulation, the magnetic network, and internetwork fields are still poorly understood.

7 Summary of Current Knowledge and Issues

This long tour of the main observational, theoretical and numerical results on the problem of supergranulation being completed, we are now in a position to provide hurried (as well as less hurried) readers with a synthetic presentation of what has been learned so far on the supergranulation phenomenon and what are the current issues. The presentation of a more personal outlook and suggestions for future research is deferred to Section 8.

7.1 Observations

The Sun's supergranulation is a large-scale coherent pattern detected in the surface layers of the quiet Sun. The *impression* given by observations is that it is simply superimposed on a stochastic, highly nonlinear background smaller-scale flow pattern, the granulation. Characterising the supergranulation velocity pattern requires monitoring solar surface flows over long times, over wide fields of views, or over a large set of independent observations. The properties of the supergranulation velocity field can be summarised as follows.

- The *length scale* of the supergranulation flow, as given by the kinetic energy power spectrum of the horizontal component of solar surface flows, is in the range of 20–70 Mm with a preferred scale of 36 Mm (Section 4.2.1). These results come from both Dopplergrams (Hathaway *et al.*, 2000) and from granule tracking in wide-field high resolution image series (Rieutord *et al.*, 2008). The size of the field must be sufficiently large to secure the statistical convergence of the results.
- The typical *size* of supergranules, defined as coherent diverging flow cells at the solar surface, is in the range 10–30 Mm (Hirzberger *et al.*, 2008). The derived average size is sensitive to the method used to identify supergranules.
- The *kinetic energy excess* associated with *supergranulation* in the power spectrum of solar surface flows lies *on the large-scale side of the injection range of photospheric turbulence* located at the granulation scale (Section 4.2.1 and Figure 4).
- The most recent estimate of the *lifetime* of supergranules, based on the largest sample of supergranules collected so far, is 1.6 ± 0.7 d (Hirzberger *et al.*, 2008). The dispersion in the measurements of supergranules lifetimes is also fairly large (Section 4.2.2).
- Rms *horizontal velocities* at supergranulation scale are of the order of 350 m s^{-1} , while rms *vertical velocities* are around 30 m s^{-1} (Hathaway *et al.*, 2002). As velocities depend on the scales considered, the relation between amplitude and scale, namely the power spectrum, provides the most suitable observable to estimate the amplitude of the supergranulation velocity field (Section 4.2.3).
- Local helioseismology indicates that supergranules are *shallow structures* (Section 4.4), possibly not deeper than 5 Mm (Sekii *et al.*, 2007). The mean vertical profile of the supergranulation flow is not very well constrained at the moment. More precise determinations are definitely called for.

Note that the foregoing determinations are not independent of each other, because velocity scales can be derived from the combination of length and time scales. Namely, 30 Mm divided by 1.7 d gives 205 m s^{-1} , which is in reasonable agreement with direct measurements of supergranulation-scale velocities. In our view, the computation of the power spectra of solar surface flows provides one of the most robust methods to make progress on the determination of these various quantities

in the future. Most notably, an accurate determination of the *vertical velocity spectrum* of vertical velocities in the supergranulation range is still lacking.

Besides this set of typical scales associated with the supergranulation velocity pattern, several other observational signatures and properties of supergranulation have been studied.

- *Horizontal intensity fluctuations* at supergranulation scales are very faint (Section 4.3). The latest studies indicate that supergranules are slightly warmer at their centre. The temperature drop is less than 3 K (Meunier *et al.*, 2007b; Goldbaum *et al.*, 2009).
- Supergranulation is affected by the *global solar rotation* (Section 4.5). Locally, supergranules are anticyclonic structures (Gizon and Duvall Jr, 2003), their mean vertical vorticity is negative in the northern hemisphere and positive in the southern one. The supergranulation pattern has been observed to propagate anisotropically in the prograde direction (Gizon *et al.*, 2003).
- Supergranulation has *dynamical interactions* with the *magnetic fields* of the quiet Sun. Most notably, supergranules are strongly correlated with the magnetic network (Section 4.6). Correlations between the size of supergranules and the strength of network and internetwork fields have been evidenced recently (Meunier *et al.*, 2007a). The solar-cycle dependence of the pattern remains uncertain though, as various papers have been giving contradicting results.

The bounds on intensity variations seem to be well established now. The proper rotation of supergranules, as measured by their local mean vertical vorticity, is also well constrained by local helioseismology. On the other hand, we believe that more work is required to quantitatively constrain the interaction of supergranules with magnetic fields. A determination of the *magnetic energy spectrum* of the quiet Sun over a wide range of scales would be extremely useful to put constraints on the physical processes at the origin of the network and internetwork fields and on their interactions with supergranulation (see Section 8 below).

Figure 14 is an attempt to depict the standard view of the supergranulation phenomenon, as constrained by the observations summarised above.

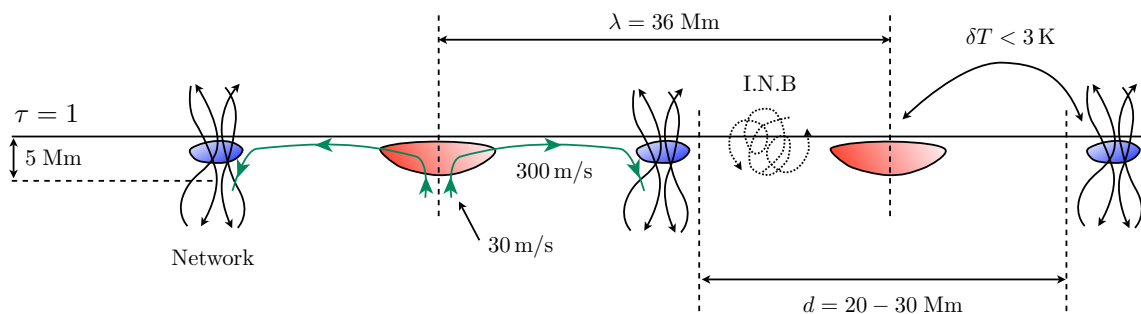


Figure 14: A schematic view of the supergranulation phenomenon, as constrained by observations. λ is the scale where the horizontal kinetic energy spectral density is maximum. d is the diameter of “coherent structures” (supergranules). The red and blue patches depict the warm and cold regions of the flow. I.N.B denotes the internetwork magnetic field. Note that the indicated internetwork and network fields geometries roughly correspond to the standard historical picture of quiet Sun magnetic fields and their relation to supergranulation (Section 4.6). As discussed in Sections 4.6.2 and 8, this picture must be significantly nuanced in reality, as the dichotomy between network and internetwork fields is probably not quite as clear as indicated in this drawing.

7.2 Theory

Two major types of physical scenarios have been suggested to explain the origin of supergranulation.

- *Thermal convection scenarios*, in which buoyancy is the main driver of the supergranulation flow (Section 5.2). Various effects (magnetic fields, shear, rotation, effective boundary conditions) have been explored within the framework of linear and weakly nonlinear theory to explain the size of the supergranulation pattern, its weak thermal signature, its oscillations and propagation.
- *Collective interaction scenarios*, whereby supergranulation emerges as a large-scale coherent pattern triggered by nonlinear interactions of vigorous smaller-scale structures like granulation (see Rieutord *et al.*, 2000 and Section 5.3). These scenarios have mostly been explored quantitatively through “toy model” simulations (Rast, 2003b; Crouch *et al.*, 2007) that do not incorporate the full complexity of dynamical MHD equations. In our view, direct numerical simulations provide the most promising way of making progress on this side in the future.

A shared property of all models is the looseness of the approximations on which they rely (e.g., linear theory with turbulent viscosity parametrisation, or purely phenomenological arguments on the nature of dynamical interactions between granules and their potential large-scale instabilities). Completely distinct theoretical arguments can easily be tuned to produce results that are all broadly consistent with observations. This degeneracy makes it impossible to discriminate between various scenarios and to come up with a proper theoretical explanation for the origin of supergranulation that could be unambiguously validated by observations.

Finally, it is possible but certainly not obvious that supergranulation can be explained quantitatively by a simple mathematical theoretical model. In any case, one of the most urgent tasks to overcome some of the previously mentioned shortcomings is to figure out if the basic assumptions and arguments on which current theoretical models rely (linear theory, effective boundary conditions, convection in uniform magnetic fields, etc.) are justified, and to test them quantitatively with the help of large-scale numerical simulations.

7.3 Numerical simulations

The complexity and nonlinearity of the physical environment of supergranulation is extraordinary: vigorous turbulent small-scale flows in a strongly stratified atmosphere, ionisation physics, rotation, shear, and tortuous magnetic fields geometries at all observable scales may all have something to do with the supergranulation phenomenon. As argued several times in this review, numerical simulations have a unique potential for approaching this complexity. They have now become an unavoidable tool to uncover the real nature of supergranulation and to test the various qualitative theoretical pictures described in Section 5.

Numerical simulations dedicated to the supergranulation problem are still in their infancy though, mostly because they remain awfully expensive in terms of computing time. The latest generation of numerical experiments, summarised in Table 1, barely accommodates for the scale of supergranulation. The main results obtained so far are summarised below.

- *Global spherical simulations* (DeRosa *et al.*, 2002) exhibit a supergranulation-like pattern, but the scale of this pattern is dangerously close to the grid scale of the simulations (Section 6.4.2).
- In *local large-scale idealised simulations* (Cattaneo *et al.*, 2001; Rincon *et al.*, 2005), two patterns can be singled out of the continuum of turbulent scales: a granulation pattern forming in the upper thermal boundary layer, and a larger-scale, extremely energetic mesoscale pattern,

which extends through the whole convective layer (Figure 12). Whether or not this pattern has anything to do with supergranulation or with the hypothetical solar mesogranulation is not understood (see Section 6.4.3 for an in-depth discussion).

- *Local large-scale realistic simulations of hydrodynamic convection* (Stein *et al.*, 2009a) do not exhibit any significant energy excess at supergranulation scales in spite of the presence of Hydrogen and Helium ionizations in the model (Section 6.4.4). This result therefore tends to disprove the “classical” Simon and Leighton (1964) supergranulation theory.
- *Local large-scale realistic simulations of MHD convection* reveal the formation of a magnetic network at scales ranging from mesoscales to supergranulation scales (Section 6.4.6). What sets the scale of this network and the emergence of supergranulation as a special scale in these simulations has not been investigated yet, but a recent study (Ustyugov, 2009) suggests that strong magnetic flux concentrations play a significant role in the scale-selection process.

Numericists will have to address several important issues in the forthcoming years. One of the main problems is that all dedicated simulations to date are still fairly dissipative (much more than the Rayleigh–Bénard simulations described in Section 6.1, for instance). Local large-scale simulations, for instance, barely accommodate 10 grid points within a granule. This kind of resolution is not sufficient to capture all the dynamics of solar surface flows, as the viscous and magnetic dissipation scales are both much smaller than 100 km (Section 2.2) at the solar surface. As mentioned in Sections 6.2 and 6.5, resolving dissipation scales properly has recently turned out to be essential to make progress on several turbulent MHD problems, such as magnetic field generation (dynamo action) by non-helical turbulent velocity fields. A related point is that uncovering the full dynamical physics of large scales and avoiding spurious finite-box effects requires both very large numerical domains and large integration times of the simulations, which is not ensured in today’s experiments. This point is easily illustrated by the supergranulation-scale dichotomy between global and local simulations discussed in Section 6.4.

Overall, the current computing limitations are such that numerical simulations are still far away from the parameter regime typical of the Sun. Hence, one cannot exclude that all simulations to date miss some critical multiscale dynamical phenomena, either purely hydrodynamic or MHD. Large-scale simulations are also currently too expensive for any decent scan of the parameter space of the problem to be possible. However, it is fair to say that the perspective of petaflop computations holds the promise of significant numerical breakthroughs in a ten-years future.

8 Discussion and Outlook

Arriving at the end of this review, we cannot escape the conclusion that the solution to the supergranulation puzzle is not as yet conspicuous. However, the combination of observational and numerical results indicates that a likely key to solve the problem is to understand the large-scale interactions between magnetic fields and velocity fields in the quiet Sun. In order to stimulate future work and discussions, we would like to conclude this work by dwelling on the suggestion that *supergranulation is a feature of statistically steady saturated turbulent MHD convection in an extended domain*.

We start with a few contextual comments that motivate this suggestion (Section 8.1) and then explore the main features and critical points of such a scenario (Section 8.2). We finally propose a set of numerical and observational studies whose results would significantly help make progress on the understanding of large-scale MHD turbulence in the quiet Sun (Section 8.3).

8.1 Preliminary comments

8.1.1 The large-scale tail of the kinetic power spectrum

The energetic signature of supergranulation lies in the 10–100 Mm range of the horizontal kinetic energy spectrum of solar surface convection, i.e., in the large-scale tail of the spectrum extending beyond the injection range (see Figure 4 and Figure 22 in Nordlund *et al.*, 2009 for instance). Both observationally and numerically derived kinetic energy spectra show us that there is some kinetic energy in that range, even though it lies beyond the typical injection scale¹². But, in all hydrodynamic simulations of supergranulation-scale convection to date, the kinetic energy of the flow in that range has been observed to be a monotonically decreasing, quasi-self-similar function of the horizontal scale. In the solar photosphere, estimates for the associated typical horizontal velocities range from 1–2 km s⁻¹ at granulation scale to 50–100 m s⁻¹ at 100 Mm.

These results suggest two conclusions. First, horizontal flows are naturally generated at all scales in the 10–100 Mm range by an essentially hydrodynamic process. Second, supergranulation scales do not appear to be singled out by that process, to the best of today's knowledge. Hence, even though we cannot yet rule out that a purely hydrodynamic process would make supergranulation a special scale, we should consider alternative scenarios. The suggestion that supergranulation could be a large-scale dynamical feature of MHD turbulence in the quiet photosphere is particularly appealing in this respect. It is notably supported by recent observations of the disappearance of the spectral bump of supergranulation during the emergence of a pore (Rieutord *et al.*, 2010).

8.1.2 Supergranulation, network and internetwork fields

Supergranulation and the magnetic network are strongly correlated observationally (see Simon and Leighton, 1964, and Section 4.6). The process of magnetic network formation has often been described in simple kinematic terms by assuming that small-scale magnetic fields are locally intensified and stochastically advected to larger scales, being eventually concentrated at the boundaries of a preexisting supergranulation flow field. Here, we would like to take on a somewhat more dynamical and less causal point of view, by simply suggesting that *the magnetic network and supergranulation may originate in a coupled, undistinguishable dynamical way*. This suggestion notably echoes the conclusions of Crouch *et al.* (2007), who describe supergranulation as an “emergent length scale” based on the results of numerical *n*-body toy models mimicking MHD effects.

¹² This is not actually specific of thermal convection. Decaying homogeneous turbulence experiments, for instance, exhibit decreasing large-scale kinetic energy spectra – Saffman–Birkhoff or Batchelor spectra (see, e.g., Davidson, 2004, Chap. 6).

Also, even though internetwork and network fields have been historically separated into two families based on their different strength, distribution, and orientation properties, there is no a priori reason to believe that their dynamics are physically disconnected, so we wish to keep both types of fields in the following discussion of the dynamics at large scales (see also Section 4.6.2 and the findings of Meunier *et al.*, 2007a regarding the correlation between internetwork field strengths and supergranulation scales). From an MHD turbulence perspective, they can all be considered as part of a continuous hierarchy of magnetic structures whose energy distribution and geometrical properties vary with scale in some yet to be understood way (for a similar argument, see Stenflo and Holzreuter, 2003a). Note that this statement is not quite as extreme as saying that the structure of the magnetic field is self-similar (Section 4.6.3).

8.2 Nonlinear MHD at large scales

Understanding the dynamical interactions of network and internetwork magnetic fields with large-scale flows is a difficult task, as the physical origin of these fields is itself rather uncertain. They may result from the emergence of magnetic fields generated far into the SCZ, or from small-scale turbulent dynamo action in the surface layers (Durney *et al.*, 1993; Petrovay and Szakaly, 1993; Cattaneo, 1999; Vögler and Schüssler, 2007; Danilovic *et al.*, 2010; Pietarila Graham *et al.*, 2010), or from some reprocessing of the field of decaying active regions (Spruit *et al.*, 1987), or from a mixture of all these processes.

8.2.1 Comparing energy spectra

Clues on the possible relationship and dynamical interactions between the large-scale dynamics of solar surface flows and magnetic fields may be obtained by analysing the combined shapes of the kinetic $E(k)$ and magnetic $E_M(k)$ power spectra

$$\left\langle \frac{1}{2}v^2 \right\rangle = \int_0^\infty E(k)dk, \quad \left\langle \frac{B^2}{2\rho\mu_0} \right\rangle = \int_0^\infty E_M(k)dk, \quad (6)$$

and that of other spectral quantities, such as the cross-spectrum between velocity and magnetic field or the magnetic tension spectrum. As mentioned in Section 4.6.3, our knowledge of $E_M(k)$ is rather crude. We know that it is a growing function of scale at least in the 1–10 Mm range where $E(k)$ is decreasing. A tentative comparison between available spectra obtained by various authors indicates that the spectral energy density of the vertical magnetic field¹³ is an order of magnitude smaller than the spectral energy density of horizontal motions at 10 Mm and is comparable to that of vertical motions at the same scale. This suggests that $E(k)$ and $E_M(k)$ cross at some large scale (as defined in k -space) around which magnetic effects become comparable to hydrodynamic effects (buoyancy, pressure, etc.), implying that *the large-scale distribution of magnetic energy is not simply slaved to that of kinetic energy* but affects it in some way.

8.2.2 Breaking the large-scale similarity of solar surface flows

We may subsequently wonder what should be the visible physical consequences of the large-scale dynamical interactions between the flow and the magnetic field and what the spectral crossover scale is. In the absence of any available major observational or theoretical constraint, we shall discuss the simple and possibly naive idea that the spectral crossover scale in the photospheric layers of the quiet Sun lies somewhere in the network-supergranulation range, implying that supergranulation would be a dynamical MHD scale. This suggestion is illustrated in Figure 15,

¹³ Available magnetic power spectra are derived from polarimetric measurements which mostly track the vertical component of the magnetic field at disc centre.

which depicts a possible spectral-space distribution of magnetic and kinetic energy in the quiet Sun, from the largest scales of interest in the context of this paper to the smallest dissipative scale (see legend for detailed warnings regarding the interpretation of the figure). Such a configuration breaks the self-similarity of the large-scale tail of the velocity power spectrum, as the crossover between the magnetic and kinetic power spectra now represents a special scale in terms of energetics. This represents an important change compared to the purely hydrodynamic view presented in Section 8.1.1.

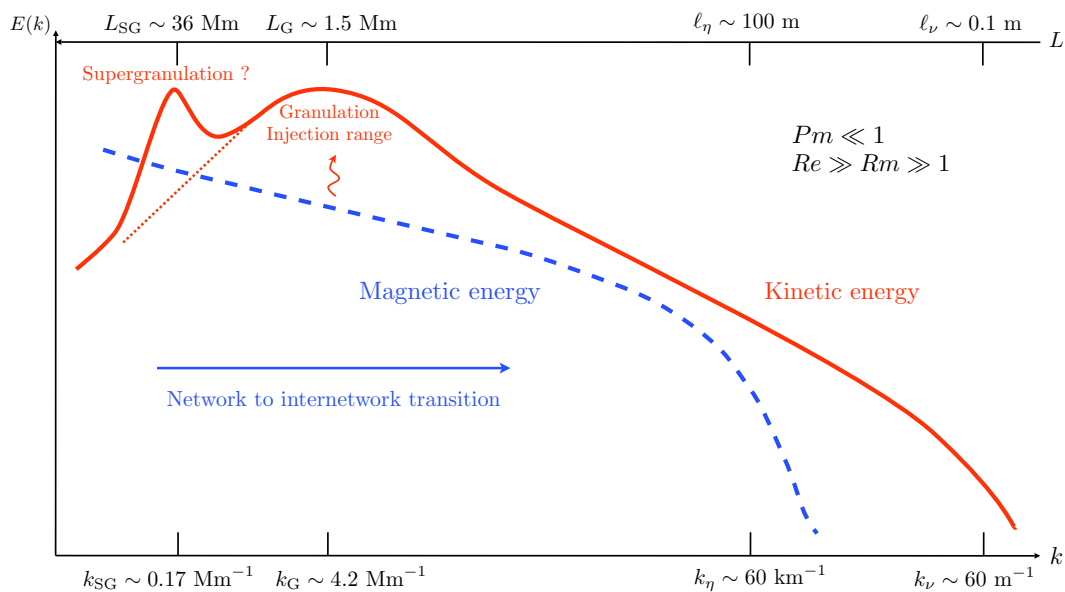


Figure 15: A tentative log-log spectral-space description of nonlinear MHD turbulence in the quiet photosphere. The kinetic energy spectrum is represented by a full red line and the magnetic energy spectrum by a dashed blue line ($k = 2\pi/L$). The thin dotted red line is representative of the results of state-of-the-art hydrodynamic simulations of supergranulation-scale convection (Stein *et al.*, 2009a). The ordering of the small-scale cutoffs results from $Pm \ll 1$ (see Section 2.2). A rather flat spectral slope for the magnetic spectrum has been represented in the range of scales smaller than 10 Mm in accordance with the data of Lee *et al.* (1997); Abramenko *et al.* (2001), and Harvey *et al.* (2007). The shape of the small-scale part of the spectrum below 0.5–1 Mm and of the large-scale part of the spectrum beyond 10 Mm are very speculative (Section 4.6.3), as we do not know what kind of MHD processes are at work in these ranges of scales. As indicated in the text, the field geometry and most energetic scales at subgranulation scales are still controversial issues (e.g., López Ariste *et al.*, 2010) and the field production mechanism itself is a matter of debate (Vögler and Schüssler, 2007). Finally, the relative amplitude of the magnetic and kinetic energy spectra is somewhat arbitrary but has been calibrated so as to comply with the argument developed in the text.

Without yet going into the details of dynamical magnetic feedback, note that the previous suggestion is simply that MHD turbulence in extended domains (in comparison to the typical injection scale of the turbulence) exhibits dynamical magnetic effects specifically enabled by the large extent of the domain. These nonlinearities very likely add up to more familiar MHD nonlinearities (quenching of specific flow scales, density evacuation) affecting scales in between the injection and dissipation scales of the turbulence (see, for instance, Schekochihin *et al.*, 2004 for a detailed account of saturation in turbulent dynamo simulations at large to moderate Pm). In this context, supergranulation would probably be better interpreted as a by-product of the nonlinear saturation of MHD turbulence in the quiet Sun, not as its main cause.

8.2.3 Dynamical magnetic feedback: a tricky question

The main theoretical challenges to enforce the credibility of this scenario are to understand physically how the magnetic field feeds back on the large-scale flow and how the magnetic and kinetic power spectra form consistently. These two questions are currently almost completely open.

The most intuitive feedback mechanism that can be thought of in the light of our current knowledge of the dynamics of the quiet photosphere is that a large-scale distribution of strong magnetic flux tubes emerging from smaller-scale dynamics (like for instance in the n -body model of Crouch *et al.*, 2007) collectively reinforces the flow at supergranulation scales, very much like strong sunspot fields support circulations towards the umbra in the far field (see Section 4.6.4, Figure 8 and Wang, 1988 for a similar suggestion). This picture qualitatively complies with the remark of Ustyugov (2009) that strong magnetic flux concentrations seem to play an important role in the scale-selection process in simulations of network formation. A very interesting physical and mathematical argument along this line was made by Longcope *et al.* (2003), whose calculations suggest that the dynamical feedback of a distribution of magnetic fibrils embedded into the solar plasma physically translates into a large-scale viscoelasticity of the plasma. We note that a central question in this problem is to determine whether one should expect a depletion or an increase in the kinetic energy at the supergranulation scale, as a result of the magnetic feedback.

Yet another possible magnetic feedback mechanism is through the interactions between magnetic fields and radiation¹⁴. Observations, theory, and simulations all suggest that magnetic concentrations tend to depress the opacity surfaces of the photosphere, which in turn is thought to channel radiation outwards (Spruit, 1976; Vögler, 2005). Strong magnetic concentrations at network scales may thereby alter the convection process at supergranulation scale and consequently single this scale out in the energy spectrum.

Overall, we note that the difficulty to understand the physical nature of dynamical magnetic feedback in this problem is in no way an exception. Nonlinear MHD phenomena are notorious for defying simple handwaving arguments. For instance, current observations seem to rule out the possibility of a simple scale-by-scale equipartition of magnetic and kinetic energy down to the smallest observable scales. The most advanced simulations of the small-scale solar surface dynamo (Vögler and Schüssler, 2007) cannot answer the question of nonlinear dynamo saturation in a definite, asymptotic way as yet¹⁵. Finally, the scale-locality of dynamical interactions is not guaranteed in nonlinear MHD flows, including the small-scale dynamo (Schekochihin *et al.*, 2004; Yousef *et al.*, 2007), so the simple observation of an equipartition of energy at some scale is probably not sufficient to understand the physics of magnetic feedback fully consistently.

8.2.4 Comments on the equipartition argument

Equipartition has been discussed at length in the context of supergranulation (e.g., Parker, 1963; Simon and Leighton, 1964; Clark and Johnson, 1967; Simon and Weiss, 1968; Frazier, 1970; Parker, 1974; Frazier, 1976). The main concern with the argument has been that many flux concentrations in the network are known to exceed kG strengths and are therefore well above equipartition with the supergranulation flow field. Indeed, using the typical value for the velocity field at supergranulation scales given in Section 4.2.3 and an order of magnitude estimate for the plasma density in the first 1 Mm below $\tau = 1$, we see that for the kinetic and magnetic energy densities to be comparable in

¹⁴ We are grateful to one of the referees for pointing this out to us.

¹⁵ All such simulations (Cattaneo, 1999; Vögler and Schüssler, 2007) are for $Pm \sim 1$ or larger and asymptotically not large Re . How saturation takes place and whether equipartition should be expected in both ($Pm \gg 1, \gg Re \gg 1$) and ($Pm \ll 1, Re \gg \gg 1$) limits is unknown (Schekochihin *et al.*, 2004; Yousef *et al.*, 2007; Schekochihin *et al.*, 2007; Tilgner and Brandenburg, 2008; Cattaneo and Tobias, 2009), so it is currently very difficult and potentially risky to predict how and at which level of magnetic energy the putative solar surface dynamo saturates.

the supergranulation peak range, an rms magnetic field strength of 100 G is required:

$$E_{\text{kin}} = 45 \left(\frac{\rho}{10^{-3} \text{ kg m}^{-3}} \right) \left(\frac{V}{300 \text{ m s}^{-1}} \right)^2 \text{ J m}^{-3}, \quad (7)$$

$$E_{\text{mag}} = 40 \left(\frac{B}{100 \text{ G}} \right)^2 \text{ J m}^{-3}. \quad (8)$$

Hence, the magnetic energy density of strong network elements appears to be roughly 100 times larger than that of the supergranulation flow.

This result mostly suggests that supergranulation-scale motions cannot themselves generate these flux tubes. Partial evacuation of density and vigorous localized motions such as granulation-scale motions seem to be required to obtain superequipartition fields (Webb and Roberts, 1978; Spruit, 1979; Spruit and Zweibel, 1979; Unno and Ando, 1979; Proctor, 1983; Hughes and Proctor, 1988; Bushby *et al.*, 2008). This does not imply, however, that the supergranulation and network scales are not selected by nonlinear magnetic feedback processes. Actually, the existence of localized magnetic concentrations exceeding equipartition with the supergranulation flow certainly hints that magnetic effects cannot be bypassed to explain the dynamics of supergranulation.

Note finally that the energetics of the field is not the only important parameter of the problem. The curvature of magnetic field lines (the variation of the field along itself) is equally important to understand their dynamical role. In this respect, strong but straight localized flux tubes may not be particularly effective at interacting with the flow in comparison to weaker but significantly more tangled fields. Understanding the effective large-scale magnetic response at the surface of the quiet Sun therefore very likely requires considering the integrated dynamical contribution of the whole multiscale distribution of surface fields instead of the simple magnetic pressure estimate of individual magnetic elements populating the magnetic network.

8.3 Suggestions for future research

The previous discussion on turbulent MHD processes at the surface of the quiet Sun underlines that *future progress on the supergranulation problem is probably conditioned to further research on the dynamics of turbulent solar magnetism*. In the course of the argument, a number of key open questions naturally arose.

- What is the magnetic power spectrum of the quiet Sun in the six decades spanning the 100 m – 100 Mm range?
- How does the multiscale magnetic field distribution of the quiet Sun originate?
- How does the dynamical magnetic feedback operate, and at which scales?

Some of these questions are already at least partially answerable with nowadays observational and numerical facilities, or they will become so in the near future.

From the observational point of view, we emphasise the need for a statistical description of solar surface MHD turbulence, as opposed to a description in terms of individual “structures” such as flux tubes or magnetic “elements”. The distributions and geometries of magnetic and velocity fields in the quiet photosphere appear to be so different that their large-scale interactions can probably only be understood in statistical terms. A determination of the magnetic energy spectrum of the quiet Sun over a very wide range of scales would notably be extremely useful to understand the physics of MHD turbulence in the quiet Sun and to put constraints on the physical processes at the origin of network and internetwork fields – and consequently on the supergranulation problem.

Our theoretical and numerical understanding of supergranulation-scale MHD convection is scarce. We do have numerical (Ustyugov, 2009; Stein *et al.*, 2009b) hints that advection of weak, small-scale fields and their subsequent clustering can lead to the formation of increasingly energetic magnetic features distributed on larger scales. This phenomenology was already discussed many years ago by Parker (1963) and is included in the n -body model of Crouch *et al.* 2007. But is it possible to gain a better understanding of this process, starting from the MHD equations?

An essential issue from the point of view of large-scale MHD turbulence is to decipher the preliminary stages of production of quiet Sun magnetic fields up to supergranulation scales. A possible theoretical approach to this problem would be to study the large-scale structure of magnetic eigenmodes in simplified models of turbulent dynamo action, such as the Kraichnan–Kazantsev model (Kazantsev, 1968; Kraichnan, 1968). Such an approach has recently been taken on from a generic perspective by Malyshkin and Boldyrev (2009). Another interesting exercise would be to study the outcome of turbulent induction by a high Rm compressible flow in an extended domain threaded by a weak uniform mean field. This process is distinct from the fluctuation dynamo and could be responsible for the generation of a small-scale magnetic imprint of the global solar dynamo (e.g., Brandenburg and Subramanian, 2005). In the incompressible limit, it produces a simple k^{-1} magnetic energy spectrum (Ruzmaikin and Shukurov, 1982; Schekochihin *et al.*, 2007), not that far from the solar magnetic power spectrum in the 1–10 Mm range (Section 4.6.2).

Finally, in order to explain why the supergranulation scale appears to be special in the quiet photosphere, one needs to better understand the statistically steady state of turbulent MHD convection in this region. The main problem is that we do not currently know what simple nonhelical incompressible low Pm MHD turbulence looks like in dynamical regimes – even in small spatial domains – both when the magnetic field is produced by local turbulent dynamo action (e.g., Cattaneo, 1999; Schekochihin *et al.*, 2004, 2007; Vögler and Schüssler, 2007) and in the presence of a net magnetic flux (Cattaneo *et al.*, 2003; Stein *et al.*, 2009b; Ustyugov, 2009). Addressing this question in the context of supergranulation-scale simulations therefore represents a daunting task. On this side, we currently have no choice but to perform mildly nonlinear simulations in $Pm \sim 1$ regimes with imposed magnetic flux. To gain some insight into the highly nonlinear behaviour of turbulent MHD flows, these efforts should be complemented by dynamical simulations of specific MHD processes, such as the small-scale dynamo, in smaller domains but more extreme parameter regimes (higher Re and Rm , low Pm). By combining both approaches, it may eventually be possible to understand nonlinear MHD physics at supergranulation scales.

The general message that we tried to convey in this section is that the supergranulation puzzle may turn out to be a very challenging MHD turbulence problem, the solution to which will certainly require simultaneous progress on MHD theory and observational and numerical solar physics. This dual fundamental physics and astrophysics perspective of the supergranulation problem, we believe, makes it a particularly exciting challenge for the future.

9 Acknowledgements

We wish to thank our many collaborators and colleagues who have contributed in various ways to trigger and sustain our interest in the supergranulation problem over the years. We are particularly grateful to Thierry Roudier, François Lignières and Nadège Meunier for sharing their insights into solar convection and magnetism with us and for their reading of the manuscript. We also thank Laurent Gizon for providing us with some information on local helioseismology techniques.

References

- Abramenko, V., Yurchyshyn, V., Wang, H. and Goode, P.R., 2001, “Magnetic Power Spectra Derived from Ground and Space Measurements of the Solar Magnetic Fields”, *Solar Phys.*, **201**, 225–240. [DOI], [ADS] (Cited on pages 26 and 57.)
- Abramenko, V.I., 2005, “Multifractal Analysis Of Solar Magnetograms”, *Solar Phys.*, **228**, 29–42. [DOI], [ADS] (Cited on page 26.)
- Amati, G., Koal, K., Massaioli, F., Sreenivasan, K.R. and Verzicco, R., 2005, “Turbulent thermal convection at high Rayleigh numbers for a Boussinesq fluid of constant Prandtl number”, *Phys. Fluids*, **17**(12), 121701. [DOI], [ADS] (Cited on page 38.)
- Antia, H.M. and Chitre, S.M., 1993, “Discrete cellular scales of solar convection”, *Solar Phys.*, **145**, 227–239. [DOI], [ADS] (Cited on page 33.)
- Antia, H.M., Chitre, S.M. and Pandey, S.K., 1981, “Granulation and supergranulation as convective modes in the solar envelope”, *Solar Phys.*, **70**, 67–91. [DOI], [ADS] (Cited on page 33.)
- Asensio Ramos, A., 2009, “Evidence for Quasi-Isotropic Magnetic Fields from Hinode Quiet-Sun Observations”, *Astrophys. J.*, **701**, 1032–1043. [DOI], [ADS] (Cited on page 26.)
- Asplund, M., Grevesse, N., Sauval, A.J. and Scott, P., 2009, “The Chemical Composition of the Sun”, *Annu. Rev. Astron. Astrophys.*, **47**, 481–522. [DOI], [ADS] (Cited on page 42.)
- Beck, J.G. and Schou, J., 2000, “Supergranulation rotation”, *Solar Phys.*, **193**, 333–343. [ADS] (Cited on page 22.)
- Beckers, J.M., 1968, “Photospheric Brightness Differences Associated with the Solar Supergranulation”, *Solar Phys.*, **5**, 309–322. [DOI], [ADS] (Cited on page 18.)
- Benson, D., Stein, R. and Nordlund, Å., 2006, “Supergranulation Scale Convection Simulations”, in *Solar MHD Theory and Observations: A High Spatial Resolution Perspective*, (Eds.) Leibacher, J., Stein, R.F., Uitenbrock, H., Proceedings of the conference held 18–22 July, 2005, at the National Solar Observatory, Sacramento Peak, Sunspot, New Mexico, USA, vol. 354 of ASP Conference Series, p. 92, Astronomical Society of the Pacific, San Francisco. [ADS] (Cited on page 47.)
- Berger, T.E., Rouppe van der Voort, L.H.M., Löfdahl, M.G., Carlsson, M., Fossum, A., Hansteen, V.H., Marthinussen, E., Title, A. and Scharmer, G., 2004, “Solar magnetic elements at 0".1 resolution. General appearance and magnetic structure”, *Astron. Astrophys.*, **428**, 613–628. [DOI], [ADS] (Cited on page 25.)
- Berrilli, F., Florio, A. and Ermolli, I., 1998, “On the Geometrical Properties of the Chromospheric Network”, *Solar Phys.*, **180**, 29–45. [ADS] (Cited on page 17.)
- Berrilli, F., Ermolli, I., Florio, A. and Pietropaolo, E., 1999, “Average properties and temporal variations of the geometry of solar network cells”, *Astron. Astrophys.*, **344**, 965–972. [ADS] (Cited on pages 27 and 28.)
- Berrilli, F., Del Moro, D., Consolini, G., Pietropaolo, E., Duvall Jr, T.L. and Kosovichev, A.G., 2004, “Structure Properties of Supergranulation and Granulation”, *Solar Phys.*, **221**, 33–45. [DOI], [ADS] (Cited on page 17.)
- Bogart, R.S., Gierasch, P.J. and MacAuslan, J.M., 1980, “Linear modes of convection in the solar envelope”, *Astrophys. J.*, **236**, 285–293. [DOI], [ADS] (Cited on pages 32 and 33.)

- Bolgiano, J., R., 1959, “Turbulent Spectra in a Stably Stratified Atmosphere”, *J. Geophys. Res.*, **64**, 2226–2229. [DOI], [ADS] (Cited on page 7.)
- Bommier, V., Landi Degl’Innocenti, E., Landolfi, M. and Molodij, G., 2007, “UNNOFIT inversion of spectro-polarimetric maps observed with THEMIS”, *Astron. Astrophys.*, **464**, 323–339. [DOI], [ADS] (Cited on page 25.)
- Bommier, V., Martínez González, M., Bianda, M., Frisch, H., Asensio Ramos, A., Gelly, B. and Landi Degl’Innocenti, E., 2009, “The quiet Sun magnetic field observed with ZIMPOL on THEMIS. I. The probability density function”, *Astron. Astrophys.*, **506**, 1415–1428. [DOI], [ADS] (Cited on page 26.)
- Brandenburg, A., 2007, “Near-surface shear layer dynamics”, in *Convection in Astrophysics*, (Eds.) Kupka, F., Roxburgh, I., Lam Chan, K., Prague, Czech Republic, August 21–25, 2006, vol. 239 of IAU Symposia, pp. 457–466, Cambridge University Press, Cambridge. [DOI], [ADS] (Cited on page 48.)
- Brandenburg, A. and Subramanian, K., 2005, “Astrophysical magnetic fields and nonlinear dynamo theory”, *Phys. Rep.*, **417**, 1–209. [DOI], [ADS] (Cited on page 60.)
- Braun, D.C. and Lindsey, C., 2003, “Helioseismic imaging of the farside and the interior”, in *Local and Global Helioseismology: The Present and Future*, (Ed.) Sawaya-Lacoste, H., Proceedings of SOHO 12/GONG+ 2002, 27 October–1 November 2002, Big Bear Lake, California, U.S.A., vol. SP-517 of ESA Conference Proceedings, pp. 15–22, ESA Publications Division, Noordwijk. [ADS] (Cited on pages 20 and 26.)
- Brickhouse, N.S. and Labonte, B.J., 1988, “Mass and energy flow near sunspots. I. Observations of moat properties”, *Solar Phys.*, **115**, 43–60. [DOI], [ADS] (Cited on page 27.)
- Brummell, N.H., Hurlburt, N.E. and Toomre, J., 1996, “Turbulent Compressible Convection with Rotation. I. Flow Structure and Evolution”, *Astrophys. J.*, **473**, 494–513. [DOI], [ADS] (Cited on page 48.)
- Brummell, N.H., Hurlburt, N.E. and Toomre, J., 1998, “Turbulent Compressible Convection with Rotation. II. Mean Flows and Differential Rotation”, *Astrophys. J.*, **493**, 955–969. [DOI], [ADS] (Cited on page 48.)
- Bushby, P.J. and Houghton, S.M., 2005, “Spatially intermittent fields in photospheric magnetoconvection”, *Mon. Not. R. Astron. Soc.*, **362**, 313–320. [DOI], [ADS] (Cited on page 49.)
- Bushby, P.J., Houghton, S.M., Proctor, M.R.E. and Weiss, N.O., 2008, “Convective intensification of magnetic fields in the quiet Sun”, *Mon. Not. R. Astron. Soc.*, **387**, 698–706. [DOI], [ADS], [arXiv:0804.1238] (Cited on pages 49 and 59.)
- Busse, F.H., 1972, “The oscillatory instability of convection rolls in a low Prandtl number fluid”, *J. Fluid Mech.*, **52**, 97–112. [DOI], [ADS] (Cited on page 35.)
- Busse, F.H., 2004, “On thermal convection in slowly rotating systems”, *Chaos*, **14**, 803–808. [DOI], [ADS] (Cited on page 34.)
- Busse, F.H., 2007, “Convection in the Presence of an Inclined Axis of Rotation with Applications to the Sun”, *Solar Phys.*, **245**, 27–36. [DOI], [ADS] (Cited on page 34.)
- Busse, F.H. and Riahi, N., 1978, “Nonlinear convection in a layer with nearly insulating boundaries”, *J. Fluid Mech.*, **86**, 243–256. [ADS] (Cited on page 33.)

- Canuto, C., Hussaini, M.Y., Quarteroni, A. and Zang, T.A., 2006, *Spectral Methods: Fundamentals in Single Domains*, Scientific Computation, Springer, Berlin; New York. [Google Books] (Cited on page 38.)
- Cattaneo, F., 1999, “On the Origin of Magnetic Fields in the Quiet Photosphere”, *Astrophys. J. Lett.*, **515**, L39–L42. [DOI], [ADS] (Cited on pages 48, 56, 58, and 60.)
- Cattaneo, F. and Tobias, S.M., 2009, “Dynamo properties of the turbulent velocity field of a saturated dynamo”, *J. Fluid Mech.*, **621**, 205–214. [DOI], [ADS] (Cited on page 58.)
- Cattaneo, F., Brummell, N.H., Toomre, J., Malagoli, A. and Hurlburt, N.E., 1991, “Turbulent compressible convection”, *Astrophys. J.*, **370**, 282–294. [DOI], [ADS] (Cited on page 41.)
- Cattaneo, F., Lenz, D. and Weiss, N., 2001, “On the Origin of the Solar Mesogranulation”, *Astrophys. J. Lett.*, **563**, L91–L94. [DOI], [ADS] (Cited on pages 45, 47, 50, and 53.)
- Cattaneo, F., Emonet, T. and Weiss, N., 2003, “On the Interaction between Convection and Magnetic Fields”, *Astrophys. J.*, **588**, 1183–1198. [DOI], [ADS] (Cited on pages 48 and 60.)
- Chan, K.L. and Sofia, S., 1989, “Turbulent compressible convection in a deep atmosphere. IV. Results of three-dimensional computations”, *Astrophys. J.*, **336**, 1022–1040. [DOI], [ADS] (Cited on page 41.)
- Chan, K.L. and Sofia, S., 1996, “Turbulent compressible convection in a deep atmosphere. V. Higher order statistical moments for a deeper case”, *Astrophys. J.*, **466**, 372. [DOI], [ADS] (Cited on page 41.)
- Chan, K.L., Sofia, S. and Wolff, C.L., 1982, “Turbulent compressible convection in a deep atmosphere. I. Preliminary two-dimensional results”, *Astrophys. J.*, **263**, 935–943. [DOI], [ADS] (Cited on pages 40 and 41.)
- Chandrasekhar, S., 1961, *Hydrodynamic and Hydromagnetic Stability*, International Series of Monographs on Physics, Clarendon Press, Oxford. [ADS], [Google Books] (Cited on pages 30, 34, and 35.)
- Chapman, C.J. and Proctor, M.R.E., 1980, “Nonlinear Rayleigh-Bénard convection between poorly conducting boundaries”, *J. Fluid Mech.*, **101**, 759–782. [DOI], [ADS] (Cited on page 33.)
- Chillá, F., Ciliberto, S., Innocenti, C. and Pampaloni, E., 1993, “Boundary layer and scaling properties in turbulent thermal convection”, *Nuovo Cimento D*, **15**, 1229–1249. [DOI], [ADS] (Cited on page 7.)
- Chou, D.-Y., Labonte, B.J., Braun, D.C. and Duvall Jr, T.L., 1991, “Power spectra of solar convection”, *Astrophys. J.*, **372**, 314–320. [DOI], [ADS] (Cited on page 11.)
- Chou, D.-Y., Chen, C.-S., Ou, K.-T. and Wang, C.-C., 1992, “Power spectra of median- and small-scale solar convection”, *Astrophys. J.*, **396**, 333–339. [DOI], [ADS] (Cited on page 11.)
- Clark, A.J. and Johnson, H.K., 1967, “Magnetic-Field Accumulation in Supergranules”, *Solar Phys.*, **2**, 433–440. [DOI], [ADS] (Cited on page 58.)
- Cloutman, L.D., 1979, “The Supergranulation: Solar Rip Currents?”, *Astron. Astrophys.*, **74**, L1–L3. [ADS] (Cited on page 36.)
- Clune, T.C., Elliott, J.R., Miesch, M.S., Toomre, J. and Glatzmaier, G.A., 1999, “Computational aspects of a code to study rotating turbulent convection in spherical shells”, *Parallel Comput.*, **25**, 361–380. [DOI] (Cited on pages 40 and 43.)

- Clyne, J., Mininni, P., Norton, A. and Rast, M.P., 2007, “Interactive desktop analysis of high resolution simulations: application to turbulent plume dynamics and current sheet formation”, *New J. Phys.*, **9**, 301. [DOI], [ADS]. URL (accessed 25 January 2010): <http://stacks.iop.org/1367-2630/9/301> (Cited on page 8.)
- Couvidat, S. and Birch, A.C., 2009, “Helioseismic Travel-Time Definitions and Sensitivity to Horizontal Flows Obtained from Simulations of Solar Convection”, *Solar Phys.*, **257**, 217–235. [DOI], [ADS] (Cited on page 50.)
- Crouch, A.D., Charbonneau, P. and Thibault, K., 2007, “Supergranulation as an Emergent Length Scale”, *Astrophys. J.*, **662**, 715–729. [DOI], [ADS] (Cited on pages 37, 53, 55, 58, and 60.)
- Danilovic, S., Schüssler, M. and Solanki, S.K., 2010, “Probing quiet Sun magnetism using MURaM simulations and Hinode/SP results: support for a local dynamo”, *Astron. Astrophys.*, **513**, A1. [DOI], [arXiv:1001.2183] (Cited on page 56.)
- Dauxois, T. and Peyrard, M., 1993, “Energy localization in nonlinear lattices”, *Phys. Rev. Lett.*, **70**, 3935–3938. [DOI], [ADS] (Cited on page 36.)
- Davidson, P.A., 2004, *Turbulence: An Introduction for Scientists and Engineers*, Oxford University Press, Oxford; New York. [ADS], [Google Books] (Cited on page 55.)
- de Wijn, A.G. and Müller, D., 2009, “On the relationship between magnetic field and mesogranulation”, in *The Second Hinode Science Meeting: Beyond Discovery-Toward Understanding*, (Eds.) Lites, B., Cheung, M., Magara, T., Mariska, J., Reeves, K., Proceedings of a meeting held 29 September – 3 October 2008, at the NCAR, Boulder, Colorado, USA, vol. 425 of ASP Conference Series, p. 211, Astronomical Society of the Pacific, San Francisco. [ADS], [arXiv:0902.1967] (Cited on page 25.)
- de Wijn, A.G., Rutten, R.J., Haverkamp, E.M.W.P. and Sütterlin, P., 2005, “DOT tomography of the solar atmosphere. IV. Magnetic patches in internetwork areas”, *Astron. Astrophys.*, **441**, 1183–1190. [DOI], [ADS] (Cited on page 25.)
- de Wijn, A.G., Stenflo, J.O., Solanki, S.K. and Tsuneta, S., 2009, “Small-Scale Solar Magnetic Fields”, *Space Sci. Rev.*, **144**, 275–315. [DOI], [ADS] (Cited on pages 23 and 25.)
- Del Moro, D., Berrilli, F., Duvall Jr, T.L. and Kosovichev, A.G., 2004, “Dynamics and Structure of Supergranulation”, *Solar Phys.*, **221**, 23–32. [DOI], [ADS] (Cited on page 17.)
- Del Moro, D., Giordano, S. and Berrilli, F., 2007, “3D photospheric velocity field of a supergranular cell”, *Astron. Astrophys.*, **472**, 599–605. [ADS] (Cited on page 23.)
- Depassier, M.C. and Spiegel, E.A., 1981, “The large-scale structure of compressible convection”, *Astron. J.*, **86**, 496–512. [DOI], [ADS] (Cited on page 33.)
- DeRosa, M.L., 2001, *Dynamics in the upper solar convection zone*, Ph.D. Thesis, University of Colorado at Boulder, Boulder. [ADS] (Cited on page 43.)
- DeRosa, M.L. and Toomre, J., 2001, “Numerical simulations of supergranular scales of convection in shallow spherical shells”, in *Helio- and Asteroseismology at the Dawn of the Millennium*, (Eds.) Wilson, A., Pallé, P.L., Proceedings of the SOHO 10/GONG 2000 Workshop: 2–6 October 2000, Instituto de Astrofísica de Canarias, Santa Cruz de Tenerife, Tenerife, Spain, vol. SP-464 of ESA Conference Proceedings, pp. 595–600, ESA Publications Division, Noordwijk. [ADS] (Cited on page 44.)

- DeRosa, M.L. and Toomre, J., 2004, “Evolution of Solar Supergranulation”, *Astrophys. J.*, **616**, 1242–1260. [DOI], [ADS] (Cited on pages 16, 17, and 28.)
- DeRosa, M.L., Duvall Jr, T.L. and Toomre, J., 2000, “Near-Surface Flow Fields Deduced Using Correlation Tracking and Time-Distance Analyses”, *Solar Phys.*, **192**, 351–361. [DOI], [ADS] (Cited on page 16.)
- DeRosa, M.L., Gilman, P.A. and Toomre, J., 2002, “Solar Multiscale Convection and Rotation Gradients Studied in Shallow Spherical Shells”, *Astrophys. J.*, **581**, 1356–1374. [DOI], [ADS] (Cited on pages 44, 50, and 53.)
- Deslandres, H., 1899, “Organisation de l’enregistrement quotidien de la Chromosphère entière du Soleil à l’observatoire de Meudon. Premières résultats”, *C. R. Acad. Sci.*, **129**, 1222–1225. Online version (accessed 31 May 2010): <http://gallica.bnf.fr/ark:/12148/bpt6k3085b.image.f1222.pagination> (Cited on page 23.)
- Deubner, F.-L., 1971, “Some Properties of Velocity Fields in the Solar Photosphere. III: Oscillatory and Supergranular Motions as a Function of Height”, *Solar Phys.*, **17**, 6–20. [DOI], [ADS] (Cited on page 20.)
- Domínguez Cerdeña, I., 2003, “Evidence of mesogranulation from magnetograms of the Sun”, *Astron. Astrophys.*, **412**, L65–L68. [DOI], [ADS] (Cited on page 25.)
- Domínguez Cerdeña, I., Sánchez Almeida, J. and Kneer, F., 2003, “Inter-network magnetic fields observed with sub-arcsec resolution”, *Astron. Astrophys.*, **407**, 741–757. [DOI], [ADS] (Cited on page 25.)
- Dubrulle, B. and Frisch, U., 1991, “Eddy viscosity of parity-invariant flow”, *Phys. Rev. A*, **43**, 5355–5364. [DOI], [ADS] (Cited on page 36.)
- Durney, B.R., De Young, D.S. and Roxburgh, I.W., 1993, “On the generation of the large-scale and turbulent magnetic fields in solar-type stars”, *Solar Phys.*, **145**, 207–225. [DOI], [ADS] (Cited on page 56.)
- Duvall Jr, T.L., 1980, “The equatorial rotation rate of the supergranulation cells”, *Solar Phys.*, **66**, 213–221. [DOI], [ADS] (Cited on pages 21 and 22.)
- Duvall Jr, T.L., 1998, “Recent Results and Theoretical Advances in Local Helioseismology”, in *Structure and Dynamics of the Interior of the Sun and Sun-like Stars*, (Eds.) Korzennik, S., Wilson, A., SOHO 6/GONG 98 Workshop, 1–4 June 1998, Boston, Massachusetts, USA, vol. SP-418 of ESA Conference Proceedings, pp. 581–585, ESA, Noordwijk (Cited on page 20.)
- Duvall Jr, T.L. and Gizon, L., 2000, “Time-distance helioseismology with f modes as a method for measurement of near-surface flows”, *Solar Phys.*, **192**, 177–191. [DOI], [ADS] (Cited on page 22.)
- Duvall Jr, T.L., Kosovichev, A.G., Scherrer, P.H., Bogart, R.S., Bush, R.I., de Forest, C., Hoeksema, J.T., Schou, J., Saba, J.L.R., Tarbell, T.D., Title, A.M., Wolfson, C.J. and Milford, P.N., 1997, “Time-distance helioseismology with the MDI instrument: initial results”, *Solar Phys.*, **170**, 63–73. [DOI], [ADS] (Cited on page 20.)
- Edwards, J.M., 1990, “On the influence of the thermal and magnetic boundary conditions on the linear theory of magnetoconvection”, *Geophys. Astrophys. Fluid Dyn.*, **55**, 1–17. [DOI], [ADS] (Cited on page 33.)

- Egorov, P., Rüdiger, G. and Ziegler, U., 2004, “Vorticity and helicity of the solar supergranulation flow-field”, *Astron. Astrophys.*, **425**, 725–728. [DOI], [ADS] (Cited on page 48.)
- Emonet, T. and Cattaneo, F., 2001, “Small-Scale Photospheric Fields: Observational Evidence and Numerical Simulations”, *Astrophys. J. Lett.*, **560**, L197–L200. [DOI], [ADS] (Cited on page 48.)
- Foukal, P. and Fowler, L., 1984, “A photometric study of heat flow at the solar photosphere”, *Astrophys. J.*, **281**, 442–454. [DOI], [ADS] (Cited on page 18.)
- Frazier, E.N., 1970, “Multi-Channel Magnetograph Observations. II. Supergranulation”, *Solar Phys.*, **14**, 89–111. [DOI], [ADS] (Cited on pages 17, 18, and 58.)
- Frazier, E.N., 1976, “The photosphere – magnetic and dynamic state”, *Philos. Trans. R. Soc. London, Ser. A*, **281**, 295–303. [DOI], [ADS] (Cited on page 58.)
- Frisch, U., 1995, *Turbulence: The Legacy of A. N. Kolmogorov*, Cambridge University Press, Cambridge; New York. [ADS], [Google Books] (Cited on page 8.)
- Fromang, S., Papaloizou, J., Lesur, G. and Heinemann, T., 2007, “MHD simulations of the magnetorotational instability in a shearing box with zero net flux. II. The effect of transport coefficients”, *Astron. Astrophys.*, **476**, 1123–1132. [DOI], [ADS] (Cited on page 41.)
- Gama, S., Vergassola, M. and Frisch, U., 1994, “Negative eddy viscosity in isotropically forced two-dimensional flow: Linear and nonlinear dynamics”, *J. Fluid Mech.*, **260**, 95–126. [DOI], [ADS] (Cited on page 36.)
- Georgobiani, D., Zhao, J., Kosovichev, A.G., Benson, D., Stein, R.F. and Nordlund, Å., 2007, “Local Helioseismology and Correlation Tracking Analysis of Surface Structures in Realistic Simulations of Solar Convection”, *Astrophys. J.*, **657**, 1157–1161. [DOI], [ADS] (Cited on pages 47 and 50.)
- Gierasch, P.J., 1985, “On the energetics of the solar supergranulation”, *Astrophys. J.*, **288**, 795–800. [DOI], [ADS] (Cited on page 33.)
- Gilman, P.A., 1975, “Linear Simulations of Boussinesq Convection in a Deep Rotating Spherical Shell”, *J. Atmos. Sci.*, **32**, 1331–1352. [DOI], [ADS] (Cited on page 43.)
- Gilman, P.A. and Foukal, P.V., 1979, “Angular velocity gradients in the solar convection zone”, *Astrophys. J.*, **229**, 1179–1185. [DOI], [ADS] (Cited on page 43.)
- Gilman, P.A. and Glatzmaier, G.A., 1981, “Compressible convection in a rotating spherical shell. I. Anelastic equations. II. A linear anelastic model. III. Analytic model for compressible vorticity waves”, *Astrophys. J. Suppl. Ser.*, **45**, 335–388. [DOI], [ADS] (Cited on page 43.)
- Ginet, G.P. and Simon, G.W., 1992, “On the evidence for mesogranules in solar power spectra”, *Astrophys. J.*, **386**, 359–363. [DOI], [ADS] (Cited on page 11.)
- Gizon, L. and Birch, A.C., 2005, “Local Helioseismology”, *Living Rev. Solar Phys.*, **2**, lrsp-2005-6. [ADS]. URL (accessed 25 January 2010): <http://livingreviews.org/lrsp-2005-6> (Cited on pages 16, 21, and 22.)
- Gizon, L. and Duvall Jr, T.L., 2003, “Supergranulation Supports Waves”, in *Local and Global Helioseismology: The Present and Future*, (Ed.) Sawaya-Lacoste, H., Proceedings of SOHO 12/GONG+ 2002, 27 October–1 November 2002, Big Bear Lake, California, U.S.A, vol. SP-517 of ESA Conference Proceedings, pp. 43–52, ESA Publications Division, Noordwijk. [ADS] (Cited on pages 21 and 52.)

- Gizon, L. and Duvall Jr, T.L., 2004, “Solar-cycle variations in the spectrum of supergranulation”, in *Multi-Wavelength Investigations of Solar Activity*, (Eds.) Stepanov, A.V., Benevolenskaya, E.E., Kosovichev, A.G., St. Petersburg, Russian Federation, June 14–19, 2004, vol. 223 of IAU Symposium, pp. 41–44, Cambridge University Press, Cambridge; New York. [ADS] (Cited on pages 22 and 28.)
- Gizon, L., Duvall Jr, T.L. and Larsen, R.M., 2000, “Seismic Tomography of the Near Solar Surface”, *J. Astrophys. Astron.*, **21**, 339–342. [ADS] (Cited on pages 26 and 27.)
- Gizon, L., Duvall Jr, T.L. and Schou, J., 2003, “Wave-like properties of solar supergranulation”, *Nature*, **421**, 43–44. [DOI], [ADS] (Cited on pages 22, 28, 34, 35, and 52.)
- Glatzmaier, G.A., 1984, “Numerical simulations of stellar convective dynamos. I. The model and method”, *J. Comput. Phys.*, **55**, 461–484. [DOI], [ADS] (Cited on page 43.)
- Glatzmaier, G.A., 1985, “Numerical simulations of stellar convective dynamos. II. Field propagation in the convection zone”, *Astrophys. J.*, **291**, 300–307. [DOI], [ADS] (Cited on page 43.)
- Goldbaum, N., Rast, M.P., Ermolli, I., Sands, J.S. and Berrilli, F., 2009, “The Intensity Profile of the Solar Supergranulation”, *Astrophys. J.*, **707**, 67–73. [DOI], [ADS] (Cited on pages 20 and 52.)
- Graham, E., 1975, “Numerical simulation of two-dimensional compressible convection”, *J. Fluid Mech.*, **70**, 689–703. [ADS] (Cited on pages 40 and 41.)
- Green, C.A. and Kosovichev, A.G., 2006, “Traveling Convective Modes in the Sun’s Subsurface Shear Layer”, *Astrophys. J. Lett.*, **641**, L77–L80. [DOI], [ADS] (Cited on pages 34, 35, and 48.)
- Green, C.A. and Kosovichev, A.G., 2007, “Magnetic Effect on Wavelike Properties of Solar Supergranulation”, *Astrophys. J. Lett.*, **665**, L75–L78. [DOI], [ADS] (Cited on page 35.)
- Haber, D.A., Hindman, B.W., Toomre, J., Bogart, R.S. and Hill, F., 2001, “Daily variations of large-scale subsurface flows and global synoptic flow maps from dense-pack ring-diagram analyses”, in *Helio- and Asteroseismology at the Dawn of the Millennium*, (Eds.) Wilson, A., Pallé, P.L., Proceedings of the SOHO 10/GONG 2000 Workshop: 2–6 October 2000, Instituto de Astrofísica de Canarias, Santa Cruz de Tenerife, Tenerife, Spain, vol. SP-464 of ESA Conference Proceedings, pp. 209–212, ESA Publications Division, Noordwijk. [ADS] (Cited on page 26.)
- Haber, D.A., Hindman, B.W., Toomre, J. and Thompson, M.J., 2004, “Organized Subsurface Flows near Active Regions”, *Solar Phys.*, **220**, 371–380. [DOI], [ADS] (Cited on page 26.)
- Hagenaar, H.J. and Shine, R.A., 2005, “Moving Magnetic Features around Sunspots”, *Astrophys. J.*, **635**, 659–669. [DOI], [ADS] (Cited on page 27.)
- Hagenaar, H.J., Schrijver, C.J. and Title, A.M., 1997, “The Distribution of Cell Sizes of the Solar Chromospheric Network”, *Astrophys. J.*, **481**, 988–995. [DOI], [ADS] (Cited on pages 17 and 24.)
- Hart, A.B., 1954, “Motions in the Sun at the photospheric level. IV. The equatorial rotation and possible velocity fields in the photosphere”, *Mon. Not. R. Astron. Soc.*, **114**, 17–38. [ADS] (Cited on pages 5, 13, and 18.)
- Hart, A.B., 1956, “Motions in the Sun at the photospheric level. VI. Large-scale motions in the equatorial region”, *Mon. Not. R. Astron. Soc.*, **116**, 38–55. [ADS] (Cited on pages 5 and 16.)

- Hartlep, T., Tilgner, A. and Busse, F.H., 2003, "Large Scale Structures in Rayleigh-Bénard Convection at High Rayleigh Numbers", *Phys. Rev. Lett.*, **91**(6), 064 501. [DOI], [ADS] (Cited on page 45.)
- Harvey, J.W., Branston, D., Henney, C.J. and Keller, C.U., 2007, "Seething Horizontal Magnetic Fields in the Quiet Solar Photosphere", *Astrophys. J. Lett.*, **659**, L177–L180. [DOI], [ADS] (Cited on pages 26 and 57.)
- Harvey, K. and Harvey, J., 1973, "Observations of Moving Magnetic Features near Sunspots", *Solar Phys.*, **28**, 61–71. [DOI], [ADS] (Cited on page 27.)
- Hathaway, D.H., 1982, "Nonlinear simulations of solar rotation effects in supergranules", *Solar Phys.*, **77**, 341–356. [DOI], [ADS] (Cited on page 48.)
- Hathaway, D.H., Beck, J.G., Bogart, R.S., Bachmann, K.T., Khatri, G., Petitto, J.M., Han, S. and Raymond, J., 2000, "The Photospheric Convection Spectrum", *Solar Phys.*, **193**, 299–312. [DOI], [ADS] (Cited on pages 11, 16, 19, and 51.)
- Hathaway, D.H., Beck, J.G., Han, S. and Raymond, J., 2002, "Radial Flows in Supergranules", *Solar Phys.*, **205**, 25–38. [ADS] (Cited on pages 16, 18, and 51.)
- Hathaway, D.H., Williams, P.E. and Cuntz, M., 2006, "Supergranule Superrotation Identified as a Projection Effect", *Astrophys. J.*, **644**, 598–602. [DOI], [ADS] (Cited on page 22.)
- Heinemann, T., Nordlund, Å., Scharmer, G.B. and Spruit, H.C., 2007, "MHD Simulations of Penumbra Fine Structure", *Astrophys. J.*, **669**, 1390–1394. [DOI], [ADS] (Cited on page 43.)
- Hindman, B.W., Haber, D.A. and Toomre, J., 2009, "Subsurface Circulations within Active Regions", *Astrophys. J.*, **698**, 1749–1760. [DOI], [ADS] (Cited on pages 26 and 27.)
- Hirzberger, J., Gizon, L., Solanki, S.K. and Duvall Jr, T.L., 2008, "Structure and Evolution of Supergranulation from Local Helioseismology", *Solar Phys.*, **251**, 417–437. [DOI], [ADS] (Cited on pages 17 and 51.)
- Hughes, D.W. and Proctor, M.R.E., 1988, "Magnetic fields in the solar convection zone: Magnetoconvection and magnetic buoyancy", *Annu. Rev. Fluid Mech.*, **20**, 187–223. [DOI], [ADS] (Cited on page 59.)
- Hurlburt, N.E., Toomre, J. and Massaguer, J.M., 1984, "Two-dimensional compressible convection extending over multiple scale heights", *Astrophys. J.*, **282**, 557–573. [DOI], [ADS] (Cited on page 41.)
- Hurlburt, N.E., Matthews, P.C. and Proctor, M.R.E., 1996, "Nonlinear Compressible Convection in Oblique Magnetic Fields", *Astrophys. J.*, **457**, 933–938. [DOI], [ADS] (Cited on page 35.)
- Hurle, D.T.J., Jakeman, E. and Pike, E.R., 1967, "On the Solution of the Bénard Problem with Boundaries of Finite Conductivity", *Proc. R. Soc. London, Ser. A*, **296**, 469–475. [ADS] (Cited on page 33.)
- Ichimoto, K., Tsuneta, S., Suematsu, Y., Shimizu, T., Otsubo, M., Kato, Y., Noguchi, M., Nakagiri, M., Tamura, T., Katsukawa, Y., Kubo, M., Sakamoto, Y., Hara, H., Minesugi, K., Ohnishi, A., Saito, H., Kawaguchi, N., Matsushita, T., Nakaoji, T., Nagae, K., Sakamoto, J., Hasuyama, Y., Mikami, I., Miyawaki, K., Sakurai, Y., Kaido, N., Horiuchi, T., Shimada, S., Inoue, T., Mitsutake, M., Yoshida, N., Takahara, O., Takeyama, N., Suzuki, M. and Abe, S., 2004, "The Solar Optical Telescope onboard the Solar-B", in *Optical, Infrared, and Millimeter Space Telescopes*,

- (Ed.) Mather, J.C., 21–25 June 2004, Glasgow, Scotland, United Kingdom, vol. 5487 of Proc. SPIE, pp. 1142–1151, SPIE, Bellingham, WA. [DOI], [ADS] (Cited on page 11.)
- Ishihara, T., Gotoh, T. and Kaneda, Y., 2009, “Study of High-Reynolds Number Isotropic Turbulence by Direct Numerical Simulation”, *Annu. Rev. Fluid Mech.*, **41**, 165–180. [DOI], [ADS] (Cited on page 40.)
- Janßen, K., Vögler, A. and Kneer, F., 2003, “On the fractal dimension of small-scale magnetic structures in the Sun”, *Astron. Astrophys.*, **409**, 1127–1134. [DOI], [ADS] (Cited on page 26.)
- Käpylä, P.J., Korpi, M.J. and Tuominen, I., 2004, “Local models of stellar convection: Reynolds stresses and turbulent heat transport”, *Astron. Astrophys.*, **422**, 793–816. [DOI], [ADS] (Cited on page 48.)
- Kariyappa, R. and Sivaraman, K.R., 1994, “Variability of the solar chromospheric network over the solar cycle”, *Solar Phys.*, **152**, 139–144. [DOI], [ADS] (Cited on page 27.)
- Kazantsev, A.P., 1968, “Enhancement of a Magnetic Field by a Conducting Fluid”, *Sov. Phys. JETP*, **26**, 1031. [ADS] (Cited on page 60.)
- Keller, C.U., Deubner, F.-L., Egger, U., Fleck, B. and Povel, H.P., 1994, “On the strength of solar intra-network fields”, *Astron. Astrophys.*, **286**, 626–634. [ADS] (Cited on page 25.)
- Komm, R., Howe, R., Hill, F., Miesch, M., Haber, D. and Hindman, B., 2007, “Divergence and Vorticity of Solar Subsurface Flows Derived from Ring-Diagram Analysis of MDI and GONG Data”, *Astrophys. J.*, **667**, 571–584. [DOI], [ADS] (Cited on page 21.)
- Komm, R.W., 1995, “Wavelet analysis of a magnetogram”, *Solar Phys.*, **157**, 45–50. [DOI], [ADS] (Cited on page 26.)
- Kraichnan, R.H., 1968, “Small-Scale Structure of a Scalar Field Convected by Turbulence”, *Phys. Fluids*, **11**, 945–953. [DOI], [ADS] (Cited on page 60.)
- Krijger, J.M. and Roudier, T., 2003, “Photospheric flows measured with TRACE II. Network formation”, *Astron. Astrophys.*, **403**, 715–723. [DOI], [ADS] (Cited on page 24.)
- Krishnamurti, R. and Howard, L.N., 1981, “Large-Scale Flow Generation in Turbulent Convection”, *Proc. Natl. Acad. Sci. USA*, **78**, 1981–1985. [DOI], [ADS] (Cited on page 47.)
- Kropp, M. and Busse, F.H., 1991, “Thermal convection in differentially rotating systems”, *Geophys. Astrophys. Fluid Dyn.*, **61**, 127–148. [DOI], [ADS] (Cited on page 34.)
- Kuhn, J.R., Armstrong, J.D., Bush, R.I. and Scherrer, P., 2000, “Rossby waves on the Sun as revealed by solar ‘hills’”, *Nature*, **405**, 544–546. [DOI], [ADS] (Cited on page 22.)
- Lawrence, J.K., Cadavid, A.C. and Ruzmaikin, A.A., 1995, “Multiplicative cascade models of multifractal solar magnetic fields”, *Phys. Rev. D*, **51**, 316–324. [DOI], [ADS] (Cited on page 26.)
- Lawrence, J.K., Cadavid, A.C. and Ruzmaikin, A., 2001, “Mesogranulation and Turbulence in Photospheric Flows”, *Solar Phys.*, **202**, 27–39. [ADS] (Cited on page 12.)
- Lee, J., Chae, J.-C., Yun, H.S. and Zirin, H., 1997, “Power Spectra of Solar Network and Non-Network Fields”, *Solar Phys.*, **171**, 269–282. [ADS] (Cited on pages 26 and 57.)
- Leighton, R.B., Noyes, R.W. and Simon, G.W., 1962, “Velocity Fields in the Solar Atmosphere. I. Preliminary Report”, *Astrophys. J.*, **135**, 474–499. [DOI], [ADS] (Cited on pages 5, 16, 17, and 23.)

- Lesur, G. and Longaretti, P.-Y., 2007, "Impact of dimensionless numbers on the efficiency of magnetorotational instability induced turbulent transport", *Mon. Not. R. Astron. Soc.*, **378**, 1471–1480. [DOI], [ADS] (Cited on page 41.)
- Lin, H., 1995, "On the Distribution of the Solar Magnetic Fields", *Astrophys. J.*, **446**, 421. [DOI], [ADS] (Cited on page 25.)
- Lin, H. and Kuhn, J.R., 1992, "Precision IR and visible solar photometry", *Solar Phys.*, **141**, 1–26. [DOI], [ADS] (Cited on page 18.)
- Lindsey, C. and Braun, D.C., 2004, "Principles of Seismic Holography for Diagnostics of the Shallow Subphotosphere", *Astrophys. J. Suppl. Ser.*, **155**, 209–225. [DOI], [ADS] (Cited on page 21.)
- Lindsey, C., Braun, D.C., Jefferies, S.M., Woodard, M.F., Fan, Y., Gu, Y. and Redfield, S., 1996, "Doppler Acoustic Diagnostics of Subsurface Solar Magnetic Structure", *Astrophys. J.*, **470**, 636–646. [DOI], [ADS] (Cited on page 26.)
- Lisle, J., DeRosa, M.L. and Toomre, J., 2000, "New Approach to Study Extended Evolution of Supergranular Flows and Their Advection of Magnetic Elements", *Solar Phys.*, **197**, 21–30. [ADS] (Cited on pages 23 and 24.)
- Lisle, J.P., Rast, M.P. and Toomre, J., 2004, "Persistent North-South Alignment of the Solar Supergranulation", *Astrophys. J.*, **608**, 1167–1174. [DOI], [ADS] (Cited on page 22.)
- Lites, B.W., Kubo, M., Socas-Navarro, H., Berger, T., Frank, Z., Shine, R., Tarbell, T., Title, A., Ichimoto, K., Katsukawa, Y., Tsuneta, S., Suematsu, Y., Shimizu, T. and Nagata, S., 2008, "The Horizontal Magnetic Flux of the Quiet-Sun Internetwork as Observed with the Hinode Spectro-Polarimeter", *Astrophys. J.*, **672**, 1237–1253. [DOI], [ADS] (Cited on page 25.)
- Livingston, W. and Harvey, J., 1971, "The Kitt Peak Magnetograph. IV: 40-Channel Probe and the Detection of Weak Photospheric Fields", in *Solar Magnetic Fields*, (Ed.) Howard, R., Paris, France, August 31–September 4, 1970, vol. 43 of IAU Symposia, pp. 51–61, Reidel, Dordrecht. [ADS] (Cited on page 25.)
- Livingston, W.C. and Harvey, J., 1975, "A New Component of Solar Magnetism - The Inner Network Fields", *Bull. Am. Astron. Soc.*, **7**, 346. [ADS] (Cited on page 25.)
- Lohse, D. and Xia, K.-Q., 2010, "Small-scale properties of turbulent Rayleigh-Bénard convection", *Annu. Rev. Fluid Mech.*, **42**, 335. [DOI], [ADS] (Cited on page 38.)
- Longcope, D.W. and Parnell, C.E., 2009, "The Number of Magnetic Null Points in the Quiet Sun Corona", *Solar Phys.*, **254**, 51–75. [DOI], [ADS] (Cited on page 26.)
- Longcope, D.W., McLeish, T.C.B. and Fisher, G.H., 2003, "A Viscoelastic Theory of Turbulent Fluid Permeated with Fibril Magnetic Fields", *Astrophys. J.*, **599**, 661–674. [DOI], [ADS] (Cited on page 58.)
- López Ariste, A., Manso Sainz, R., Asensio Ramos, A., Martínez González, M.J., Malherbe, J.M. and Gelly, B., 2010, "The nature of solar internetwork magnetic fields: constraints from Hanle and Zeeman diagnostics", unknown status (Cited on pages 26 and 57.)
- L'vov, V.S., 1991, "Spectra of velocity and temperature fluctuations with constant entropy flux of fully developed free-convective turbulence", *Phys. Rev. Lett.*, **67**, 687–690. [DOI], [ADS] (Cited on page 7.)

- Malyshkin, L. and Boldyrev, S., 2009, “Magnetic Dynamo Action in Astrophysical Turbulence”, *Astrophys. J.*, **697**, 1433–1438. [DOI], [ADS] (Cited on page 60.)
- Martin, S.F., 1988, “The identification and interaction of network, intranetwork, and ephemeral-region magnetic fields”, *Solar Phys.*, **117**, 243–259. [DOI], [ADS] (Cited on page 25.)
- Martínez González, M.J., Asensio Ramos, A., López Ariste, A. and Manso Sainz, R., 2008, “Near-IR internetwork spectro-polarimetry at different heliocentric angles”, *Astron. Astrophys.*, **479**, 229–234. [DOI], [ADS] (Cited on page 26.)
- Massager, J.M. and Zahn, J.-P., 1980, “Cellular convection in a stratified atmosphere”, *Astron. Astrophys.*, **87**, 315–327. [ADS] (Cited on pages 40 and 41.)
- Matloch, L., Cameron, R., Schmitt, D. and Schüssler, M., 2009, “Modelling of solar mesogranulation”, *Astron. Astrophys.*, **504**, 1041–1055. [DOI], [ADS] (Cited on page 12.)
- Matthews, P. and Cox, S., 1997, “Linear stability of rotating convection in an imposed shear flow”, *J. Fluid Mech.*, **350**, 271–293. [ADS] (Cited on page 34.)
- Matthews, P.C., Hurlburt, N.E., Proctor, M.R.E. and Brownjohn, D.P., 1992, “Compressible magnetoconvection in oblique fields: Linearized theory and simple nonlinear models”, *J. Fluid Mech.*, **240**, 559–569. [DOI], [ADS] (Cited on page 35.)
- McAteer, R.T.J., Gallagher, P.T. and Conlon, P.A., 2009, “Turbulence, complexity, and solar flares”, *Adv. Space Res.*, **45**, 1067–1074. [DOI], [arXiv:0909.5636] (Cited on page 26.)
- Meshalkin, L.D. and Sinai, I.G., 1961, “Investigation of the stability of a stationary solution of a system of equations for the plane movement of an incompressible viscous fluid”, *Prikl. Mat. Mekh.*, **25**(6), 1140–1143 (Cited on page 36.)
- Meunier, N., 1999, “Fractal Analysis of Michelson Doppler Imager Magnetograms: A Contribution to the Study of the Formation of Solar Active Regions”, *Astrophys. J.*, **515**, 801–811. [DOI], [ADS] (Cited on page 26.)
- Meunier, N., 2003, “Statistical properties of magnetic structures: Their dependence on scale and solar activity”, *Astron. Astrophys.*, **405**, 1107–1120. [DOI], [ADS] (Cited on page 28.)
- Meunier, N. and Roudier, T., 2007, “The superrotation of solar supergranules”, *Astron. Astrophys.*, **466**, 691–696. [ADS] (Cited on page 22.)
- Meunier, N., Roudier, T. and Tkaczuk, R., 2007a, “Are supergranule sizes anti-correlated with magnetic activity?”, *Astron. Astrophys.*, **466**, 1123–1130. [DOI], [ADS] (Cited on pages 28, 52, and 56.)
- Meunier, N., Tkaczuk, R. and Roudier, T., 2007b, “Intensity variations inside supergranules”, *Astron. Astrophys.*, **463**, 745–753. [DOI], [ADS] (Cited on pages 20 and 52.)
- Meunier, N., Tkaczuk, R., Roudier, T. and Rieutord, M., 2007c, “Velocities and divergences as a function of supergranule size”, *Astron. Astrophys.*, **461**, 1141–1147. [DOI], [ADS] (Cited on pages 16 and 22.)
- Meunier, N., Roudier, T. and Rieutord, M., 2008, “Supergranules over the solar cycle”, *Astron. Astrophys.*, **488**, 1109–1115. [DOI], [ADS] (Cited on pages 20 and 28.)
- Miesch, M.S., 2005, “Large-Scale Dynamics of the Convection Zone and Tachocline”, *Living Rev. Solar Phys.*, **2**, lrsp-2005-1. [ADS]. URL (accessed 25 January 2010): <http://www.livingreviews.org/lrsp-2005-1> (Cited on pages 7 and 43.)

- Miesch, M.S., Brun, A.S., DeRosa, M.L. and Toomre, J., 2008, "Structure and Evolution of Giant Cells in Global Models of Solar Convection", *Astrophys. J.*, **673**, 557–575. [DOI], [ADS], [arXiv:0707.1460] (Cited on pages 44 and 50.)
- Moffatt, H.K., 1961, "The amplification of a weak applied magnetic field by turbulence in fluids of moderate conductivity", *J. Fluid Mech.*, **11**, 625–635. [DOI], [ADS] (Cited on page 9.)
- Muller, R., 1983, "The dynamical behavior of facular points in the quiet photosphere", *Solar Phys.*, **85**, 113–121. [DOI], [ADS] (Cited on page 25.)
- Muller, R. and Mena, B., 1987, "Motions around a decaying sunspot", *Solar Phys.*, **112**, 295–303. [DOI], [ADS] (Cited on page 27.)
- Münzer, H., Schröter, E.H., Wöhl, H. and Hanslmeier, A., 1989, "Pole-equator-difference of the size of the chromospheric Ca II-K-network in quiet and active solar regions", *Astron. Astrophys.*, **213**, 431–435. [ADS] (Cited on page 28.)
- Murphy, J.O., 1977, "The Effect of a Magnetic Field on the Onset of Thermal Convection when Constant Flux Boundary Conditions Apply", *Proc. Astron. Soc. Australia*, **3**, 164–165. [ADS] (Cited on page 33.)
- Nesme-Ribes, E., Meunier, N. and Collin, B., 1996, "Fractal analysis of magnetic patterns from Meudon spectroheliograms", *Astron. Astrophys.*, **308**, 213–218. [ADS] (Cited on page 26.)
- Newell, A.C., Passot, T. and Souli, M., 1990, "The phase diffusion and mean drift equations for convection at finite Rayleigh numbers in large containers", *J. Fluid Mech.*, **220**, 187–252. [DOI], [ADS] (Cited on page 36.)
- Niemela, J.J., Skrbek, L., Sreenivasan, K.R. and Donnelly, R.J., 2000, "Turbulent convection at very high Rayleigh numbers", *Nature*, **404**, 837–840. [DOI], [ADS] (Cited on page 7.)
- Niemela, J.J., Skrbek, L., Sreenivasan, K.R. and Donnelly, R.J., 2001, "The wind in confined thermal convection", *J. Fluid Mech.*, **449**, 169–178. [ADS] (Cited on page 47.)
- Nisenson, P., van Ballegooijen, A.A., de Wijn, A.G. and Sütterlin, P., 2003, "Motions of Isolated G-Band Bright Points in the Solar Photosphere", *Astrophys. J.*, **587**, 458–463. [DOI], [ADS] (Cited on page 25.)
- Nordlund, A., 1982, "Numerical simulations of the solar granulation. I. Basic equations and methods", *Astron. Astrophys.*, **107**, 1–10. [ADS] (Cited on pages 30, 40, and 41.)
- Nordlund, A., 1985, "Solar convection", *Solar Phys.*, **100**, 209–235. [DOI], [ADS] (Cited on page 43.)
- Nordlund, Å., Galsgaard, K. and Stein, R.F., 1994, "Magnetconvection and magnetoturbulence", in *Solar Surface Magnetism*, (Eds.) Rutten, R.J., Schrijver, C.J., Proceedings of the NATO Advanced Research Workshop, held in Soesterberg, The Netherlands, November 1–5, 1993, vol. 433 of NATO ASI Series C, p. 471, Kluwer, Dordrecht; Boston. [ADS] (Cited on page 45.)
- Nordlund, Å., Stein, R.F. and Asplund, M., 2009, "Solar Surface Convection", *Living Rev. Solar Phys.*, **6**, lrsp-2009-2. [ADS]. URL (accessed 25 January 2010): <http://www.livingreviews.org/lrsp-2009-2> (Cited on pages 7, 11, 42, 47, and 55.)
- November, L.J., 1989, "The vertical component of the supergranular convection", *Astrophys. J.*, **344**, 494–503. [DOI], [ADS] (Cited on page 18.)

- November, L.J., 1994, “Inferring the depth extent of the horizontal supergranular flow”, *Solar Phys.*, **154**, 1–17. [DOI], [ADS] (Cited on pages 11, 18, and 20.)
- November, L.J. and Simon, G.W., 1988, “Precise proper-motion measurement of solar granulation”, *Astrophys. J.*, **333**, 427–442. [DOI], [ADS] (Cited on pages 11 and 13.)
- November, L.J., Toomre, J., Gebbie, K.B. and Simon, G.W., 1981, “The detection of mesogranulation on the Sun”, *Astrophys. J. Lett.*, **245**, L123–L126. [DOI], [ADS] (Cited on pages 11 and 18.)
- Orozco Suárez, D., Bellot Rubio, L.R., del Toro Iniesta, J.C., Tsuneta, S., Lites, B.W., Ichimoto, K., Katsukawa, Y., Nagata, S., Shimizu, T., Shine, R.A., Suematsu, Y., Tarbell, T.D. and Title, A.M., 2007, “Quiet-Sun Internetwork Magnetic Fields from the Inversion of Hinode Measurements”, *Astrophys. J. Lett.*, **670**, L61–L64. [DOI], [ADS] (Cited on page 25.)
- Parker, E.N., 1963, “Kinematical Hydromagnetic Theory and its Application to the Low Solar Photosphere”, *Astrophys. J.*, **138**, 552–575. [DOI], [ADS] (Cited on pages 58 and 60.)
- Parker, E.N., 1974, “Hydraulic Concentration of Magnetic Fields in the Solar Photosphere. I. Turbulent Pumping”, *Astrophys. J.*, **189**, 563–568. [DOI], [ADS] (Cited on page 58.)
- Parodi, A., von Hardenberg, J., Passoni, G., Provenzale, A. and Spiegel, E.A., 2004, “Clustering of Plumes in Turbulent Convection”, *Phys. Rev. Lett.*, **92**(19), 194503. [DOI], [ADS] (Cited on pages 45 and 47.)
- Petrovay, K. and Szakaly, G., 1993, “The origin of intranetwork fields: a small-scale solar dynamo”, *Astron. Astrophys.*, **274**, 543. [ADS] (Cited on page 56.)
- Pietarila Graham, J., Danilovic, S. and Schüssler, M., 2009, “Turbulent Magnetic Fields in the Quiet Sun: Implications of Hinode Observations and Small-Scale Dynamo Simulations”, *Astrophys. J.*, **693**, 1728–1735. [DOI], [ADS] (Cited on pages 9 and 41.)
- Pietarila Graham, J., Cameron, R. and Schüssler, M., 2010, “Turbulent Small-Scale Dynamo Action in Solar Surface Simulations”, *Astrophys. J.*, **714**, 1606–1616. [DOI], [ADS] (Cited on page 56.)
- Plaskett, H.H., 1916, “A Variation in the Solar Rotation”, *Astrophys. J.*, **43**, 145. [DOI], [ADS] (Cited on page 5.)
- Potts, H.E., Barrett, R.K. and Diver, D.A., 2004, “Balltracking: An highly efficient method for tracking flow fields”, *Astron. Astrophys.*, **424**, 253–262. [DOI], [ADS] (Cited on page 13.)
- Proctor, M.R.E., 1983, “Amplification of magnetic fields by compressible convection”, in *Solar and Stellar Magnetic Fields: Origins and Coronal Effects*, (Ed.) Stenflo, J.O., Zurich, Switzerland, August 2–6, 1982, vol. 102 of IAU Symposium, pp. 301–304, Reidel, Dordrecht; Boston. [ADS] (Cited on page 59.)
- Proctor, M.R.E. and Weiss, N.O., 1982, “Magnetocovection”, *Rep. Prog. Phys.*, **45**, 1317–1379. [DOI], [ADS] (Cited on page 35.)
- Raju, K.P. and Singh, J., 2002, “Dependence of Supergranular Length-Scales on Network Magnetic Fields”, *Solar Phys.*, **207**, 11–16. [ADS] (Cited on page 27.)
- Rast, M.P., 1998, “Compressible plume dynamics and stability”, *J. Fluid Mech.*, **369**, 125–149. [ADS] (Cited on page 8.)

- Rast, M.P., 2003a, “Supergranulation: new observation, possible explanation”, in *Local and Global Helioseismology: The Present and Future*, (Ed.) Sawaya-Lacoste, H., Proceedings of SOHO 12/GONG+ 2002, 27 October–1 November 2002, Big Bear Lake, California, U.S.A, vol. SP-517 of ESA Conference Proceedings, pp. 163–172, ESA Publications Division, Noordwijk. [ADS] (Cited on page 20.)
- Rast, M.P., 2003b, “The Scales of Granulation, Mesogranulation, and Supergranulation”, *Astrophys. J.*, **597**, 1200–1210. [DOI], [ADS] (Cited on pages 37 and 53.)
- Rast, M.P. and Toomre, J., 1993, “Compressible Convection with Ionization. II. Thermal Boundary-Layer Instability”, *Astrophys. J.*, **419**, 240. [DOI], [ADS] (Cited on page 37.)
- Rast, M.P., Lisle, J.P. and Toomre, J., 2004, “The Spectrum of the Solar Supergranulation: Multiple Nonwave Components”, *Astrophys. J.*, **608**, 1156–1166. [DOI], [ADS] (Cited on page 22.)
- Rempel, M., Schüssler, M., Cameron, R.H. and Knölker, M., 2009, “Penumbral Structure and Outflows in Simulated Sunspots”, *Science*, **325**, 171. [DOI], [ADS] (Cited on page 43.)
- Rieutord, M., 2008, “The solar dynamo”, *C. R. Physique*, **9**, 757–765. [DOI], [ADS] (Cited on page 9.)
- Rieutord, M. and Zahn, J.-P., 1995, “Turbulent plumes in stellar convective envelopes”, *Astron. Astrophys.*, **296**, 127–138. [ADS] (Cited on pages 7 and 37.)
- Rieutord, M., Roudier, T., Malherbe, J.M. and Rincon, F., 2000, “On mesogranulation, network formation and supergranulation”, *Astron. Astrophys.*, **357**, 1063–1072. [ADS] (Cited on pages 11, 36, and 53.)
- Rieutord, M., Roudier, T., Ludwig, H.-G., Nordlund, Å. and Stein, R., 2001, “Are granules good tracers of solar surface velocity fields?”, *Astron. Astrophys.*, **377**, L14–L17. [DOI], [ADS] (Cited on pages 13 and 50.)
- Rieutord, M., Ludwig, H.-G., Roudier, T., Nordlund, Å. and Stein, R., 2002, “A simulation of solar convection at supergranulation scale”, *Nuovo Cimento C*, **25**, 523–528. [ADS] (Cited on pages 45, 46, and 50.)
- Rieutord, M., Roudier, T., Roques, S. and Ducottet, C., 2007, “Tracking granules on the Sun's surface and reconstructing velocity fields. I. The CST algorithm”, *Astron. Astrophys.*, **471**, 687–694. [DOI], [ADS] (Cited on page 13.)
- Rieutord, M., Meunier, N., Roudier, T., Rondi, S., Beigbeder, F. and Parès, L., 2008, “Solar supergranulation revealed by granule tracking”, *Astron. Astrophys.*, **479**, L17–L20. [DOI], [ADS] (Cited on pages 13, 15, 16, 19, and 51.)
- Rieutord, M., Roudier, T., Rincon, F., Malherbe, J.-M., Meunier, N., Berger, T. and Frank, Z., 2010, “On the power spectrum of solar surface flows”, *Astron. Astrophys.*, **512**, A4. [DOI], [arXiv:0911.3319] (Cited on pages 11, 12, 13, 16, 18, 19, 20, 26, and 55.)
- Rincon, F., 2006, “Anisotropy, inhomogeneity and inertial-range scalings in turbulent convection”, *J. Fluid Mech.*, **563**, 43–69. [DOI], [ADS] (Cited on pages 7 and 38.)
- Rincon, F., 2007, “Theories of convection and the spectrum of turbulence in the solar photosphere”, in *Convection in Astrophysics*, (Eds.) Kupka, F., Roxburgh, I., Chan, K., Prague, Czech Republic, August 21–25, 2006, vol. 239 of IAU Symposium, pp. 58–63, Cambridge University Press, Cambridge. [DOI], [ADS] (Cited on page 7.)

- Rincon, F. and Rieutord, M., 2003, “Stability of a compressible fluid layer in a magnetic field: a simple model for supergranulation”, in *SF2A-2003: Scientific Highlights 2003*, (Eds.) Combes, F., Barret, D., Contini, T., Pagani, L., Semaine de l’Astrophysique Française, Bordeaux, France, June 16–20, 2003, p. 103, EDP Sciences, Les Ulis. [ADS] (Cited on page 33.)
- Rincon, F., Lignières, F. and Rieutord, M., 2005, “Mesoscale flows in large aspect ratio simulations of turbulent compressible convection”, *Astron. Astrophys.*, **430**, L57–L60. [DOI], [ADS] (Cited on pages 40, 46, 47, 50, and 53.)
- Roudier, T. and Muller, R., 2004, “Relation between families of granules, mesogranules and photospheric network”, *Astron. Astrophys.*, **419**, 757–762. [DOI], [ADS] (Cited on page 25.)
- Roudier, T., Rieutord, M., Malherbe, J.M. and Vigneau, J., 1999a, “Determination of horizontal velocity fields at the sun’s surface with high spatial and temporal resolution”, *Astron. Astrophys.*, **349**, 301–311. [ADS] (Cited on page 13.)
- Roudier, T., Rieutord, M., Malherbe, J.M. and Vigneau, J., 1999b, “Determination of horizontal velocity fields at the sun’s surface with high spatial and temporal resolution”, *Astron. Astrophys.*, **349**, 301–311. [ADS] (Cited on page 11.)
- Roudier, T., Rieutord, M., Brito, D., Rincon, F., Malherbe, J.M., Meunier, N., Berger, T. and Frank, Z., 2009, “Mesoscale dynamics on the Sun’s surface from HINODE observations”, *Astron. Astrophys.*, **495**, 945–952. [DOI], [ADS] (Cited on pages 24 and 25.)
- Roupe van der Voort, L.H.M., Hansteen, V.H., Carlsson, M., Fossum, A., Marthinussen, E., van Noort, M.J. and Berger, T.E., 2005, “Solar magnetic elements at 0.1 arcsec resolution. II. Dynamical evolution”, *Astron. Astrophys.*, **435**, 327–337. [DOI], [ADS] (Cited on page 25.)
- Ruzmaikin, A.A. and Shukurov, A.M., 1982, “Spectrum of the galactic magnetic fields”, *Astrophys. Space Sci.*, **82**, 397–407. [DOI], [ADS] (Cited on page 60.)
- Sano, M., Wu, X.Z. and Libchaber, A., 1989, “Turbulence in helium-gas free convection”, *Phys. Rev. A*, **40**, 6421–6430. [DOI], [ADS] (Cited on page 47.)
- Schekochihin, A.A., Cowley, S.C., Taylor, S.F., Maron, J.L. and McWilliams, J.C., 2004, “Simulations of the Small-Scale Turbulent Dynamo”, *Astrophys. J.*, **612**, 276–307. [DOI], [ADS] (Cited on pages 57, 58, and 60.)
- Schekochihin, A.A., Iskakov, A.B., Cowley, S.C., McWilliams, J.C., Proctor, M.R.E. and Yousef, T.A., 2007, “Fluctuation dynamo and turbulent induction at low magnetic Prandtl numbers”, *New J. Phys.*, **9**, 300. [DOI], [ADS]. URL (accessed 25 January 2010): <http://stacks.iop.org/1367-2630/9/300> (Cited on pages 9, 41, 58, and 60.)
- Schou, J., 2003, “Wavelike Properties of Solar Supergranulation Detected in Doppler Shift Data”, *Astrophys. J. Lett.*, **596**, L259–L262. [DOI], [ADS] (Cited on page 22.)
- Schou, J., Antia, H.M., Basu, S., Bogart, R.S., Bush, R.I., Chitre, S.M., Christensen-Dalsgaard, J., di Mauro, M.P., Dziembowski, W.A., Eff-Darwich, A., Gough, D.O., Haber, D.A., Hoeksema, J.T., Howe, R., Korzennik, S.G., Kosovichev, A.G., Larsen, R.M., Pijpers, F.P., Scherrer, P.H., Sekii, T., Tarbell, T.D., Title, A.M., Thompson, M.J. and Toomre, J., 1998, “Helioseismic Studies of Differential Rotation in the Solar Envelope by the Solar Oscillations Investigation Using the Michelson Doppler Imager”, *Astrophys. J.*, **505**, 390–417. [DOI], [ADS] (Cited on page 34.)

- Schrijver, C.J., Hagenaar, H.J. and Title, A.M., 1997, “On the Patterns of the Solar Granulation and Supergranulation”, *Astrophys. J.*, **475**, 328. [DOI], [ADS] (Cited on pages 17 and 24.)
- Schwarzschild, M., 1975, “On the scale of photospheric convection in red giants and supergiants”, *Astrophys. J.*, **195**, 137–144. [DOI], [ADS] (Cited on page 32.)
- Sekii, T., Kosovichev, A.G., Zhao, J., Tsuneta, S., Shibahashi, H., Berger, T.E., Ichimoto, K., Katsukawa, Y., Lites, B., Nagata, S., Shimizu, T., Shine, R.A., Suematsu, Y., Tarbell, T.D. and Title, A.M., 2007, “Initial Helioseismic Observations by Hinode/SOT”, *Publ. Astron. Soc. Japan*, **59**, 637. [ADS] (Cited on pages 20 and 51.)
- Sheeley Jr, N.R., 1969, “The Evolution of the Photospheric Network”, *Solar Phys.*, **9**, 347–357. [DOI], [ADS] (Cited on page 26.)
- Sheeley Jr, N.R., 1972, “Observations of the Horizontal Velocity Field Surrounding Sunspots”, *Solar Phys.*, **25**, 98–103. [DOI], [ADS] (Cited on page 27.)
- Sheeley Jr, N.R. and Bhatnagar, A., 1971, “Two-Dimensional Observations of the Velocity Fields in and around Sunspots”, *Solar Phys.*, **19**, 338–346. [DOI], [ADS] (Cited on page 27.)
- Shine, R.A., Title, A.M., Tarbell, T.D. and Topka, K.P., 1987, “White light sunspot observations from the Solar Optical Universal Polarimeter on Spacelab-2”, *Science*, **238**, 1264–1267. [DOI], [ADS] (Cited on page 27.)
- Shine, R.A., Simon, G.W. and Hurlburt, N.E., 2000, “Supergranule and Mesogranule Evolution”, *Solar Phys.*, **193**, 313–331. [DOI], [ADS] (Cited on page 12.)
- Simon, G.W. and Leighton, R.B., 1964, “Velocity Fields in the Solar Atmosphere. III. Large-Scale Motions, the Chromospheric Network, and Magnetic Fields”, *Astrophys. J.*, **140**, 1120–1147. [DOI], [ADS] (Cited on pages 5, 11, 16, 18, 23, 32, 47, 50, 54, 55, and 58.)
- Simon, G.W. and Weiss, N.O., 1968, “Supergranules and the Hydrogen Convection Zone”, *Z. Astrophys.*, **69**, 435. [ADS] (Cited on pages 32 and 58.)
- Simon, G.W., Title, A.M., Topka, K.P., Tarbell, T.D., Shine, R.A., Ferguson, S.H. and Zirin, H. [SOUP Team], 1988, “On the relation between photospheric flow fields and the magnetic field distribution on the solar surface”, *Astrophys. J.*, **327**, 964–967. [DOI], [ADS] (Cited on page 23.)
- Simon, G.W., Title, A.M. and Weiss, N.O., 1991, “Modeling mesogranules and exploders on the solar surface”, *Astrophys. J.*, **375**, 775–788. [DOI], [ADS] (Cited on page 37.)
- Singh, J. and Bappu, M.K.V., 1981, “A dependence on solar cycle of the size of the Ca⁺ network”, *Solar Phys.*, **71**, 161–168. [DOI], [ADS] (Cited on page 27.)
- Sivashinsky, G. and Yakhot, V., 1985, “Negative viscosity effect in large-scale flows”, *Phys. Fluids*, **28**, 1040–1042. [DOI], [ADS] (Cited on page 36.)
- Snodgrass, H.B. and Ulrich, R.K., 1990, “Rotation of Doppler features in the solar photosphere”, *Astrophys. J.*, **351**, 309–316. [DOI], [ADS] (Cited on pages 21, 22, and 23.)
- Solanki, S.K., 1993, “Small-scale solar magnetic fields: An overview”, *Space Sci. Rev.*, **63**, 1–188. [DOI], [ADS] (Cited on page 23.)
- Solanki, S.K., 2003, “Sunspots: An overview”, *Astron. Astrophys. Rev.*, **11**, 153–286. [DOI], [ADS] (Cited on page 26.)

- Sparrow, E.M., Goldstein, R.J. and Jonsson, V.K., 1964, “Thermal instability in a horizontal fluid layer: effect of boundary conditions and non-linear temperature profile”, *J. Fluid Mech.*, **18**, 513–528. [DOI], [ADS] (Cited on page 33.)
- Spruit, H.C., 1974, “A model of the solar convection zone”, *Solar Phys.*, **34**, 277–290. [DOI], [ADS] (Cited on page 9.)
- Spruit, H.C., 1976, “Pressure equilibrium and energy balance of small photospheric fluxtubes”, *Solar Phys.*, **50**, 269–295. [DOI], [ADS] (Cited on page 58.)
- Spruit, H.C., 1979, “Convective collapse of flux tubes”, *Solar Phys.*, **61**, 363–378. [DOI], [ADS] (Cited on page 59.)
- Spruit, H.C. and Zweibel, E.G., 1979, “Convective instability of thin flux tubes”, *Solar Phys.*, **62**, 15–22. [DOI], [ADS] (Cited on page 59.)
- Spruit, H.C., Title, A.M. and van Ballegoijen, A.A., 1987, “Is there a weak mixed polarity background field? Theoretical arguments”, *Solar Phys.*, **110**, 115–128. [DOI], [ADS] (Cited on page 56.)
- Spruit, H.C., Nordlund, Å. and Title, A.M., 1990, “Solar convection”, *Annu. Rev. Astron. Astrophys.*, **28**, 263–301. [DOI], [ADS] (Cited on pages 11 and 47.)
- Stein, R.F. and Nordlund, A., 1989a, “Topology of convection beneath the solar surface”, *Astrophys. J.*, **342**, L95–L98. [DOI], [ADS] (Cited on page 37.)
- Stein, R.F. and Nordlund, A., 1989b, “Topology of convection beneath the solar surface”, *Astrophys. J. Lett.*, **342**, L95–L98. [DOI], [ADS] (Cited on page 41.)
- Stein, R.F. and Nordlund, A., 1994, “Subphotospheric Convection”, in *Infrared Solar Physics*, (Eds.) Rabin, D.M., Jefferies, J.T., Lindsey, C., Tucson, AZ, USA, March 2–6, 1992, vol. 154 of IAU Symposia, p. 225, Kluwer Academic, Dordrecht; Boston. [ADS] (Cited on page 47.)
- Stein, R.F. and Nordlund, Å., 1998, “Simulations of Solar Granulation. I. General Properties”, *Astrophys. J.*, **499**, 914–933. [DOI], [ADS] (Cited on pages 41, 42, and 50.)
- Stein, R.F. and Nordlund, Å., 2006, “Solar Small-Scale Magnetoconvection”, *Astrophys. J.*, **642**, 1246–1255. [DOI], [ADS] (Cited on page 49.)
- Stein, R.F., Georgobiani, D., Schafenberger, W., Nordlund, Å. and Benson, D., 2009a, “Supergranulation Scale Convection Simulations”, in *Cool Stars, Stellar Systems and the Sun*, (Ed.) Stempels, E., Proceedings of the 15th Cambridge Workshop, St. Andrews (Scotland), 21–25 July 2008, vol. 1094 of AIP Conference Proceedings, pp. 764–767, American Institute of Physics, Melville, NY. [DOI], [ADS] (Cited on pages 47, 50, 54, and 57.)
- Stein, R.F., Lagerfjård, A., Nordlund, Å. and Georgobiani, D., 2009b, “Solar Flux Emergence Simulations”, *Solar Phys.* [DOI], [arXiv:0912.4938] (Cited on pages 49, 50, and 60.)
- Stenflo, J.O. and Holzreuter, R., 2002, “Empirical view of magnetoconvection”, in *SOLMAG 2002*, (Ed.) Sawaya-Lacoste, H., Proceedings of the Magnetic Coupling of the Solar Atmosphere Euroconference and IAU Colloquium 188, 11–15 June 2002, Santorini, Greece, vol. SP-505 of ESA Special Publication, pp. 101–104, European Space Agency, Noordwijk. [ADS] (Cited on page 26.)

- Stenflo, J.O. and Holzreuter, R., 2003a, “Distribution of Magnetic Fields at Scales Beyond the Spatial Resolution Limit”, in *Current Theoretical Models and Future High Resolution Solar Observations: Preparing for ATST*, (Eds.) Pevtsov, A.A., Uitenbroek, H., vol. 286 of ASP Conference Series, p. 169, Astronomical Society of the Pacific, San Francisco. [ADS] (Cited on pages 26 and 56.)
- Stenflo, J.O. and Holzreuter, R., 2003b, “Flux tubes or fractal distributions – on the nature of photospheric magnetic fields”, *Astron. Nachr.*, **324**, 397. [ADS] (Cited on page 26.)
- Stix, M., 2004, *The Sun: An Introduction*, Astronomy and Astrophysics Library, Springer, Berlin; New York, 2nd corr. edn. [ADS], [Google Books] (Cited on page 7.)
- Straus, T. and Bonaccini, D., 1997, “Dynamics of the solar photosphere. I. Two-dimensional spectroscopy of mesoscale phenomena”, *Astron. Astrophys.*, **324**, 704–712. [ADS] (Cited on page 11.)
- Straus, T., Deubner, F.-L. and Fleck, B., 1992, “Is mesogranulation a distinct regime of convection?”, *Astron. Astrophys.*, **256**, 652–659. [ADS] (Cited on page 11.)
- Suematsu, Y., Tsuneta, S., Ichimoto, K., Shimizu, T., Otsubo, M., Katsukawa, Y., Nakagiri, M., Noguchi, M., Tamura, T., Kato, Y., Hara, H., Kubo, M., Mikami, I., Saito, H., Matsushita, T., Kawaguchi, N., Nakaoji, T., Nagae, K., Shimada, S., Takeyama, N. and Yamamuro, T., 2008, “The Solar Optical Telescope of Solar-B (Hinode): The Optical Telescope Assembly”, *Solar Phys.*, **249**, 197–220. [DOI], [ADS] (Cited on page 11.)
- Švanda, M., Klvaňa, M. and Sobotka, M., 2006, “Large-scale horizontal flows in the solar photosphere. I. Method and tests on synthetic data”, *Astron. Astrophys.*, **458**, 301–306. [DOI], [ADS] (Cited on page 28.)
- Švanda, M., Zhao, J. and Kosovichev, A.G., 2007, “Comparison of Large-Scale Flows on the Sun Measured by Time-Distance Helioseismology and Local Correlation Tracking”, *Solar Phys.*, **241**, 27–37. [DOI], [ADS] (Cited on page 16.)
- Švanda, M., Klvaňa, M., Sobotka, M. and Bumba, V., 2008, “Large-scale horizontal flows in the solar photosphere. II. Long-term behaviour and magnetic activity response”, *Astron. Astrophys.*, **477**, 285–292. [DOI], [ADS] (Cited on page 28.)
- Tao, L., Weiss, N.O., Brownjohn, D.P. and Proctor, M.R.E., 1998, “Flux Separation in Stellar Magnetoconvection”, *Astrophys. J. Lett.*, **496**, L39. [DOI], [ADS] (Cited on page 48.)
- Thomas, J.H. and Weiss, N.O., 2008, *Sunspots and Starspots*, vol. 46 of Cambridge Astrophysics Series, Cambridge University Press, Cambridge; New York. [ADS] (Cited on page 26.)
- Thompson, S.D., 2005, “Magnetoconvection in an inclined magnetic field: linear and weakly non-linear models”, *Mon. Not. R. Astron. Soc.*, **360**, 1290–1304. [DOI], [ADS] (Cited on page 35.)
- Thual, O., 1992, “Zero-Prandtl-number convection”, *J. Fluid Mech.*, **240**, 229–258. [DOI], [ADS] (Cited on page 35.)
- Tilgner, A. and Brandenburg, A., 2008, “A growing dynamo from a saturated Roberts flow dynamo”, *Mon. Not. R. Astron. Soc.*, **391**, 1477–1481. [DOI], [ADS] (Cited on page 58.)
- Title, A.M., Tarbell, T.D., Topka, K.P., Ferguson, S.H. and Shine, R.A. [SOUP Team], 1989, “Statistical properties of solar granulation derived from the SOUP instrument on Spacelab 2”, *Astrophys. J.*, **336**, 475–494. [DOI], [ADS] (Cited on page 11.)

- Tkaczuk, R., Rieutord, M., Meunier, N. and Roudier, T., 2007, “Tracking granules on the Sun’s surface and reconstructing velocity fields. II. Error analysis”, *Astron. Astrophys.*, **471**, 695–703. [DOI], [ADS] (Cited on page 13.)
- Trujillo Bueno, J., Shchukina, N. and Asensio Ramos, A., 2004, “A substantial amount of hidden magnetic energy in the quiet Sun”, *Nature*, **430**, 326–329. [DOI], [ADS] (Cited on page 25.)
- Turner, J.S., 1986, “Turbulent entrainment: The development of the entrainment assumption, and its application to geophysical flows”, *J. Fluid Mech.*, **173**, 431–471. [DOI], [ADS] (Cited on page 37.)
- Unno, W. and Ando, H., 1979, “Instability of a thin magnetic tube in the solar atmosphere”, *Geophys. Astrophys. Fluid Dyn.*, **12**, 107–115. [DOI], [ADS] (Cited on page 59.)
- Ustyugov, S.D., 2006, “Magnetohydrodynamic Simulation of Solar Supergranulation”, in *Numerical Modeling of Space Plasma Flows*, (Eds.) Zank, G.P., Pogorelov, N.V., Proceedings of 1ST IGPP–CalSpace International Conference held 26–30 March, 2006, in Palm Springs, California, USA, vol. 359 of ASP Conference Series, pp. 226–231, Astronomical Society of the Pacific, San Francisco. [ADS], [astro-ph/0605627] (Cited on page 49.)
- Ustyugov, S.D., 2007, “Numerical Simulation of Solar Magnetoconvection with Realistic Physics”, in *Fifty Years of Romanian Astrophysics*, (Eds.) Dumitrache, C., Popescu, N.A., Suran, M.D., Mioc, V., Proceedings of the conference held in Bucharest, Romania, 27–30 September 2006, vol. 895 of AIP Conference Proceedings, pp. 109–114, American Institute of Physics, Melville, NY. [DOI], [ADS] (Cited on page 49.)
- Ustyugov, S.D., 2008, “Large Eddy Simulation of Solar Photosphere Convection with Realistic Physics”, in *Subsurface and Atmospheric Influences on Solar Activity*, (Eds.) Howe, R., Komm, R.W., Balasubramaniam, K.S., Petrie, G.J.D., Proceedings of a workshop held at the NSO/Sac, Sunspot, New Mexico, USA, 16–20 April 2007, vol. 383 of ASP Conference Series, pp. 43–48, Astronomical Society of the Pacific, San Francisco. [ADS], [arXiv:0710.3023] (Cited on pages 47 and 50.)
- Ustyugov, S.D., 2009, “Realistic Magnetohydrodynamical Simulation of Solar Local Supergranulation”, in *Solar-Stellar Dynamos as Revealed by Helio- and Asteroseismology: GONG 2008/SOHO 21*, (Eds.) Dikpati, M., Arentoft, T., González Hernández, I., Lindsey, C., Hill, F., Proceedings of a conference held 11–15 August 2008 at the HAO, Boulder, Colorado, USA, vol. 426 of ASP Conference Series, p. 427, Astronomical Society of the Pacific, San Francisco. [ADS], [arXiv:0906.5232] (Cited on pages 49, 50, 54, 58, and 60.)
- Valdettaro, L. and Meneguzzi, M., 1991, “Compressible Magnetohydrodynamics in Spherical Geometry”, in *The Sun and Cool Stars: Activity, Magnetism, Dynamos*, (Eds.) Tuominen, I., Moss, D., Rüdiger, G., Proceedings of IAU Colloquium No. 130, held in Helsinki, Finland, 17–20 July 1990, vol. 380 of Lecture Notes in Physics, p. 80, Springer, Berlin; New York. [ADS] (Cited on page 43.)
- Van der Borgh, R., 1974, “Nonlinear Thermal Convection in a Layer with Imposed Energy Flux”, *Aust. J. Phys.*, **27**, 481–493. [ADS] (Cited on page 33.)
- Verzicco, R. and Camussi, R., 2003, “Numerical experiments on strongly turbulent thermal convection in a slender cylindrical cell”, *J. Fluid Mech.*, **477**, 19–49. [DOI], [ADS] (Cited on pages 38 and 39.)
- Vickers, G.T., 1971, “On the Formation of Giant Cells and Supergranules”, *Astrophys. J.*, **163**, 363. [DOI], [ADS] (Cited on page 32.)

- Vincent, A. and Meneguzzi, M., 1991, “The spatial structure and statistical properties of homogeneous turbulence”, *J. Fluid Mech.*, **225**, 1–20. [DOI], [ADS] (Cited on page 40.)
- Vögler, A., 2005, “On the effect of photospheric magnetic fields on solar surface brightness: Results of radiative MHD simulations”, *Mem. Soc. Astron. Ital.*, **76**, 842–849. [ADS] (Cited on page 58.)
- Vögler, A. and Schüssler, M., 2007, “A solar surface dynamo”, *Astron. Astrophys.*, **465**, L43–L46. [DOI], [ADS] (Cited on pages 41, 49, 56, 57, 58, and 60.)
- von Hardenberg, J., Parodi, A., Passoni, G., Provenzale, A. and Spiegel, E.A., 2008, “Large-scale patterns in Rayleigh Bénard convection”, *Phys. Lett. A*, **372**, 2223–2229. [DOI], [ADS] (Cited on page 45.)
- Wang, H., 1988, “On the relationship between magnetic fields and supergranule velocity fields”, *Solar Phys.*, **117**, 343–358. [DOI], [ADS] (Cited on pages 27 and 58.)
- Wang, H., 1989, “Do mesogranules exist?”, *Solar Phys.*, **123**, 21–32. [DOI], [ADS] (Cited on page 11.)
- Wang, H. and Zirin, H., 1989, “Study of supergranules”, *Solar Phys.*, **120**, 1–17. [DOI], [ADS] (Cited on pages 17 and 24.)
- Webb, A.R. and Roberts, B., 1978, “Vertical motions in an intense magnetic flux tube. II: Convective instability”, *Solar Phys.*, **59**, 249–274. [DOI], [ADS] (Cited on page 59.)
- Wedemeyer-Böhm, S. and Rouppe van der Voort, L., 2009, “On the continuum intensity distribution of the solar photosphere”, *Astron. Astrophys.*, **503**, 225–239. [DOI], [ADS] (Cited on page 18.)
- Weiss, N.O., Proctor, M.R.E. and Brownjohn, D.P., 2002, “Magnetic flux separation in photospheric convection”, *Mon. Not. R. Astron. Soc.*, **337**, 293–304. [DOI], [ADS] (Cited on page 48.)
- Williams, P.E., Hathaway, D.H. and Cuntz, M., 2007, “Solar Rossby Wave ‘Hills’ Identified as Supergranules”, *Astrophys. J. Lett.*, **662**, L135–L138. [DOI], [ADS] (Cited on page 22.)
- Wolff, C., 1995, “Oscillation-convection coupling: Cause of supergranulation”, *Astrophys. J.*, **443**, 423–433. [DOI], [ADS] (Cited on page 33.)
- Woodard, M.F., 2007, “Probing Supergranular Flow in the Solar Interior”, *Astrophys. J.*, **668**, 1189–1195. [DOI], [ADS] (Cited on page 20.)
- Worden, S.P., 1975, “Infrared observations of supergranule temperature structure”, *Solar Phys.*, **45**, 521–532. [DOI], [ADS] (Cited on page 18.)
- Worden, S.P. and Simon, G.W., 1976, “A study of supergranulation using a diode array magnetograph”, *Solar Phys.*, **46**, 73–91. [DOI], [ADS] (Cited on pages 17 and 20.)
- Xi, H.-D., Lam, S. and Xia, K.-Q., 2004, “From laminar plumes to organized flows: the onset of large-scale circulation in turbulent thermal convection”, *J. Fluid Mech.*, **503**, 47–56. [DOI], [ADS] (Cited on page 47.)
- Yousef, T.A., Rincon, F. and Schekochihin, A.A., 2007, “Exact scaling laws and the local structure of isotropic magnetohydrodynamic turbulence”, *J. Fluid Mech.*, **575**, 111. [DOI], [ADS] (Cited on page 58.)
- Zhang, K. and Jones, C.A., 1996, “On Small Roberts Number Magnetoconvection in Rapidly Rotating Systems”, *Proc. R. Soc. London, Ser. A*, **452**, 981–995. [ADS] (Cited on page 34.)

- Zhang, K.-K. and Busse, F.H., 1987, “On the onset of convection in rotating spherical shells”, *Geophys. Astrophys. Fluid Dyn.*, **39**, 119–147. [DOI], [ADS] (Cited on page 34.)
- Zhao, J. and Kosovichev, A.G., 2003, “On the inference of supergranular flows by time-distance helioseismology”, in *Local and Global Helioseismology: The Present and Future*, (Ed.) Sawaya-Lacoste, H., Proceedings of SOHO 12/GONG+ 2002, 27 October–1 November 2002, Big Bear Lake, California, U.S.A, vol. SP-517 of ESA Conference Proceedings, pp. 417–420, ESA Publications Division, Noordwijk. [ADS] (Cited on page 20.)
- Zhao, J., Kosovichev, A.G. and Duvall Jr, T.L., 2001, “Investigation of Mass Flows beneath a Sunspot by Time-Distance Helioseismology”, *Astrophys. J.*, **557**, 384–388. [DOI], [ADS] (Cited on page 26.)
- Zhao, J., Kosovichev, A.G. and Duvall Jr, T.L., 2004, “On the Relationship between the Rotational Velocity and the Field Strength of Solar Magnetic Elements”, *Astrophys. J. Lett.*, **607**, L135–L138. [DOI], [ADS] (Cited on page 26.)
- Zhao, J., Kosovichev, A.G. and Sekii, T., 2009, “High-Resolution Helioseismic Imaging of Subsurface Structures and Flows of A Solar Active Region Observed by Hinode”, *Astrophys. J.*, **708**, 304–313. [DOI], [ADS], [arXiv:0911.1161] (Cited on page 26.)